12-2017

DYNAMIC ASSESSMENT OF NK CELL INTERACTIONS WITH PEDIATRIC TUMOR CELLS TO PREDICT RESPONSE TO IMMUNOTHERAPY

Arianexys Aquino Lopez

DYNAMIC ASSESSMENT OF NK CELL INTERACTIONS WITH PEDIATRIC TUMOR CELLS TO PREDICT RESPONSE TO IMMUNOTHERAPY

by

Arianexys Aquino-López, B.S.

APPROVED:

_____
Eugenie S. Kleinerman, MD
Advisory Professor

_____
Dean A. Lee, MD PhD

_____
Michael A. Curran, PhD

_____
Jordan Orange, MD PhD

_____
Kimberly Schluns, PhD

_____
Zahid H. Siddik, PhD

APPROVED:

_____

Dean, The University of Texas MD Anderson Cancer Center UTHealth Graduate School of Biomedical Sciences

DYNAMIC ASSESSMENT OF NK CELL INTERACTIONS WITH PEDIATRIC TUMOR CELLS TO PREDICT RESPONSE TO IMMUNOTHERAPY

A

DISSERTATION

Presented to the Faculty of

The University of Texas

MD Anderson Cancer Center UTHealth

Graduate School of Biomedical Sciences

in Partial Fulfillment

of the Requirements

for the Degree of

DOCTOR OF PHILOSOPHY

by

Arianexys Aquino-López, B.S.
Houston, Texas

December, 2017

Copyright

Permission was obtained from the copyright holders to use material published at:

Aquino-López A, Senyukov VV, Vlasic Z, Kleinerman ES, Lee DA: Interferon Gamma Induces Changes in Natural Killer (NK) Cell Ligand Expression and Alters NK Cell-Mediated Lysis of Pediatric Cancer Cell Lines. *Frontiers in immunology* 2017, 8:391.

Kannan GS, **Aquino-Lopez A**, Lee DA: Natural killer cells in malignant hematology: A primer for the non-immunologist. *Blood Rev* 2016.

.

Dedication

To my God.

To my devoted husband Miguel Angel, my loving parents Doris and Ediberto, and my siblings Ediberto, Yánciris and Orvill.

Acknowledgments

I would like to start by acknowledging my two mentors Dr. Eugenie S. Kleinerman and Dr. Dean Lee. Thanks Dr. Lee for giving me the opportunity to work on the exciting field of NK cell immunotherapy, and thanks for all your guidance and mentorship. Thanks to Dr. Kleinerman for kindly agreeing to be my mentor and for welcoming me into the Kleinerman lab family. I feel more than blessed for having two wonderful mentors as role models. Thanks to my advisory committee members Dr. Michael A. Curran, Dr. Jordan Orange, Dr. Kimberly Schluns and Dr. Zahid Siddik for their contributions during my training. Thanks to the Lee and Kleinerman lab members for training me on laboratory techniques, and giving me input on my project. Special thanks to Vladimir Senyukov for introducing me to CyTOF, Jennifer Foltz for allowing me to be a collaborator, Claudia Alvarez for her guidance on matrigel experiments, and Yuanzheng Yang for his patience training me on animal work. Thanks to Jolie Schafer for collaborating with the mass cytometry data from patient samples. Thanks to my two gifted summer students Zlatko Vlasic and Michael Smith for their work and contributions. Thanks to our collaborators Gabrielle Romain and Navin Varadarajan from the University of Houston, for the assistance with Timelapse experiments. Thanks to Duncan H. Mak for his assistance with the mass cytometry samples at the Flow Core. Thanks to the personnel from the U54 MD/PhD Program, especially Dr. Ilka Rios for her guidance and support. Thanks to Dr. Paloma Monroig and Dr. Rocío Rivera, my MD/PhD colleagues, for all the guidance and support through this journey. Thanks also to the UTHealth MD/PhD program for welcoming us UPR students as part of their family. Thanks to the Association of Minority Biomedical Researchers (AMBR) and GSBS Community Outreach for allowing me to

serve Houston's community and our GSBS community. I would also like to acknowledge the support from the American Legion Auxiliary Fellowship in Cancer Research, the George M. Stancel, PhD Fellowship in Biomedical Sciences and the U54 Grant.

Thanks to my St. Vincent de Paul Church community for their support and prayers. Thanks to my husband Miguel Angel, for all his patience and support through every step of my career. Thanks to my parents Doris and Ediberto, my godparents Sandra and Miguel, my in-laws Diana and Miguel, my siblings Ediberto, Yánciris and Orvill, and my brothers and sisters in-law, for all the unconditional love and support. Thanks to my sweet nephews and nieces for making auntie smile. Thanks tía Bruny and tío Nelson for providing me a home away from home. Thanks to all of you, I couldn't have done this without you.

DYNAMIC ASSESSMENT OF NK CELL INTERACTIONS WITH PEDIATRIC TUMOR CELLS TO PREDICT RESPONSE TO IMMUNOTHERAPY

Arianexys Aquino-López, BS

Advisory Professor: Eugenie S. Kleinerman, MD

Due to Natural Killer (NK) cells' capacity to target tumor cells without prior sensitization, adoptive NK cell therapy represents a promising immunotherapy approach for pediatric cancer patients. Our laboratory has developed an NK cell expansion protocol that generates large quantities of NK cells for therapeutic infusion. Given that NK cells are heterogeneous, with variable receptor expression and potential to target tumor cells, the purpose of my study was to determine whether subpopulations of NK cells with enhanced anti-tumor potential could be identified for increased potency of the NK cell infusion product. In addition, we previously showed that our expanded NK cells secret 20 times more IFNγ than resting NK cells. Opposing effects have been reported for IFNγ on tumor sensitivity to NK-mediated lysis. Therefore, another aim of my study was to evaluate the effect of IFNγ on tumor sensitivity to NK cell mediated lysis, tumor expression of NK cell ligands, and NK:tumor interactions using a standardized panel of cell lines corresponding to 6 types of pediatric malignancies.

My results demonstrate the presence of unique NK cell subpopulations in the expanded product that are absent in primary NK cells. These subpopulations co-express higher levels of multiple activating receptors than primary NK cells. Moreover, compared to the NK cell subpopulations that are common to both primary and expanded NK cells, the unique subpopulations showed increased degranulation (CD107a) and IFNγ secretion in response to tumor cell encounter.

I also demonstrate that IFNγ has a variable impact on NK-mediated lysis of pediatric tumor cell lines, with some cell lines becoming more resistant to NK cells and others becoming more sensitive. Broad screening of NK cell ligands on these cell lines using mass cytometry, and flow cytometry, show that both exogenous and NK cell secreted IFNγ cause significant upregulation of PD-L1, ICAM-1, and MHC-class I, but this upregulation varies widely between the cell lines. Modeling of the data suggests that the effect of IFNγ on NK cell-mediated tumor lysis is mostly dependent on relative changes in MHC-class I and ICAM-1 expression. In cell lines with increased sensitivity after IFNγ treatment, ICAM-1 upregulation exceeded that of MHC-class I upregulation. This ICAM-1 upregulation resulted in increased conjugate formation between the NK cells and tumor cells. Timelapse imaging of neurobastoma cells with increased sensitivity revealed that IFNγ treatment also decreased the time for NK cell encounter of tumor cells (t_{seek}). Blocking of ICAM-1 weakened the increased sensitivity observed after IFNγ treatment for selected cell lines and NK donors. Although ICAM-1 and MHC-class I were identified as key role players, the effects of MHC-class I and ICAM-1 are not always predictable.

This identification of hyperactive NK cell subpopulations with enhanced IFNγ secretion and a better understanding of the impact of IFNγ on NK:tumor interactions provides important information that can be used to further improve NK cell immunotherapy of cancer.

Table of Content

List of Illustrations

List of Tables

Abbreviations

ADCC	Antibody Dependent Cell Cytotoxicity
ALL	Acute Lymphoblastic Leukemia
AML	Acute Myelogenous Leukemia
ATRT	Atypical Teratoid Rhabdoid Tumor
B-ALL	B cell Acute Lymphpblastic Leukemia
CAR	Chimeric Antigen Receptor
CCSS	Childhood Cancer Survivor Study
CMV	Cytomegalovirus
COG	Children's Oncology Group
CTLs	Cytotoxic T Lymphocytes
CyTOF	Cytometry by Time of Flight
DR4	Death Receptor 4
DR5	Death Receptor 5
EBV-LCL	Epstein-Barr virus transformed lymphoblastoid cell line

E:T	Effector to Target Ratio
EWS	Ewing's Family Tumors
GMP	Good Manufacturing Practices
GVL	Graft vs Leukemia
HLA	Human Leukocyte Antigen
ICAM-1	Intercellular Adhesion Molecule
IFNγ	Interferon gamma
Ig	Immunoglobulin
IL	Interleukin
IS	Immune Synapse
KIR	Killer Immunoglobulin like Receptor
LAK	Lymphokine Activated Killer Cells
LFA-1	Lymphocyte Function Associated antigen 1
mb-IL21	membrane bound interleukin 21
MFI	Mean Fluoresence Intensity

MHC	Major Histocompatibility Complex
MMI	Mean Mass Intensity
NB	Neuroblastoma
NCR	Natural Cytotoxicity Receptor
NK	Natural Killer
PBMC	Peripheral Blood Mononuclear Cells
PD-1	Programmed cell death protein-1
PD-L1	Programmed death-ligand 1
PPTP	Pediatric Preclinical Testing Program
RMS	Rhabdomyosarcoma
scFv	single chain variable fragment
SCT	Stem cell Transplant
SPADE	spanning-tree progression analysis for density-normalized events
TCR	T cell receptor
TILs	Tumor Infiltrating Lymphocytes

TIMING Timelapse Imaging in Nanowell Grids

TRAIL TNF related apoptosis inducing ligand

CHAPTER I: INTRODUCTION: BACKGROUND, RATIONALE AND RESEARCH PLAN

Pediatric Cancer: Epidemiology and Current Therapies

Although pediatric malignancies are considered rare diseases, approximately 1 of 285 children in the United States (U.S.) will be diagnosed with cancer before reaching age 20 (1). Second only to accidents, cancer is a leading cause of death for children between the ages of 5-14 years (1). The most common cancer types among children and teenagers (0-19 years) are leukemia, brain & CNS tumors, and lymphoma. In a prospective study including children diagnosed with cancer between 1991 and 2000, the 5-year survival rates were 74% for leukemia, 72% for brain & CNS tumors, and 87% for lymphoma (1). Although there has been some improvements in survival for Acute Lymphoblastic Leukemia (ALL) and Non-Hodgkin's Lymphoma, there has been little or no progress for solid tumors including rhabdomyosarcoma (RMS), osteosarcoma, Ewing sarcoma (EWS) or gliomas for the past 20 years (2). For those children that survive, it is at the expense of increased morbidity and complications later in life. According to the Childhood Cancer Survivor Study (CCSS), when compared to their healthy siblings, pediatric cancer survivors have an increased incidence of long term complications (3, 4). Survivors that received chemotherapy or radiation had ~5 times higher risk of developing disabling, life threatening or fatal conditions, when compared to their siblings (4). Also, by age 50, half of the childhood cancer survivors experience some type of cardiovascular, renal, hepatic, pulmonary, and/or gonadal dysfunction (4).

One of the most serious late effects of chemotherapy and radiation in cancer survivors is the increased risk of developing secondary malignancies (4). For 5-year survivors of childhood cancer, secondary malignancies related to treatment are the leading cause of premature mortality (5) . Radiation has been associated to increased risk of developing secondary solid tumors, while chemotherapy has been linked to increased risk of developing secondary hematologic malignancies (5, 6). Therefore, there is a need to improve therapeutic options for pediatric cancer patients not only to increase survival rates, but also to decrease morbidity associated with current therapeutic regimens.

Cancer Immunotherapies: Natural Killer Cells for Pediatric Cancers

The immune system protects the body from pathogens including bacteria, viruses and parasitic worms. In addition, the immune system provides cancer surveillance and serves to eliminate tumor transformed cells (7). Natural Killer (NK) cells and macrophages from the innate immune system, as well as T cells and B cells from the adaptive immune system, serve to provide anti-tumor responses. Cancer immunotherapy uses the immune system components, or agents that modulate the immune system, to provide an anti-tumor effect and is a promising tool for the treatment of pediatric malignancies (8). In the recent years multiple immunotherapies have been developed for cancer treatment, some of these approaches include checkpoint inhibitor antibodies (anti-CTLA4, anti-PD-1/PD-L1), tumor infiltrating lymphocytes (TILs), T cells with Chimeric Antigen Receptors (CAR-T cells), adoptive cell therapies, among others (8).

Immune checkpoints function in our body to regulate T cell activity and avoid autoimmune responses. However, some tumor cells use these same inhibitory checkpoints (i.e. CTLA-4, and PD-1/PD-L1 axis) to acquire tolerance and evade the immune system (8). Checkpoint inhibitor antibodies block T cell inhibition and allow for enhanced T cell activity. However, Cytotoxic T lymphocytes (CTLs) rely on the T cell receptor (TCR) recognition of tumor antigens presented in the context of major histocompatibility complex (MHC) molecules, therefore the therapeutic efficacy of checkpoint inhibitors, in part, relies on an efficient interaction between the TCR and the antigen presented in the context of MHC (9). Similarly other therapies, such as TILs rely on the TCR interaction with antigens presented on MHC. In 40-90% of human tumors the MHC class I molecules, also known as Human Leukocyte Antigen class I (HLA-class I) is downregulated (10, 11). In the pediatric cancer field neuroblastoma and Ewing sarcomas, have been reported to have low HLA-A,B,C expression (11). This downregulation can affect the efficacy of CTL responses. To overcome this limitation CAR T cell therapies have been developed. CAR stands for chimeric antigen receptor, and its structure is composed of an antibody in the form of single chain Fv (scFv) as the extracellular domain and an intracellular T cell signaling domain. CAR T cells are capable of direct antigen recognition and do not require the antigen to be presented in the context of MHC. In order for CAR T cells to be safe, and to avoid unwanted effects in healthy tissues, the antigen should be expressed preferentially on malignant cells (12, 13). Although CAR T cell therapies are capable of overcoming MHC downregulation, their efficiency relies on the expression of a known antigen expressed on cancer cells. CAR T cells have shown promise for cancer types with known cancer antigens such as CD19

for B-cell acute lymphoblastic leukemia (B-ALL), CD30 for lymphomas, or CD33 for Acute Myelogenous Leukemia (AML) (14-18).

Despite the promising results of the immunotherapeutic approaches described above, alternative therapies should be investigated for scenarios where MHC is altered or downregulated, and also for tumors were no specific antigens have been identified. While MHC downregulation serves to escape from T cell recognition, it makes target cells more susceptible to NK cells. Because NK cells are an important component of the innate immune system with the capacity of recognizing and eliminating cancer cells without prior sensitization, our laboratory focuses on adoptive NK cell therapy for the treatment of pediatric malignancies (19, 20). For adoptive cell therapy NK cells are isolated, manipulated *ex-vivo* to enhance anti-tumor response, and reinfused to patients (8). The potential of NK cells for selectively targeting tumor cells, without affecting healthy cells, can decrease the risk of complications later in life, making them a promising therapy for pediatric cancer patients.

To evaluate the efficiency of new therapeutic options against pediatric cancers the Children's Oncology Group (COG) has developed the Pediatric Pre-clinical Testing Program (PPTP) *in-vitro* panel. This is a panel of over 20 cell lines which includes 6 different types of pediatric malignancies comprising leukemia, lymphoma, brain tumors, Ewing's family tumors (EWS), neuroblastoma (NB) and rhabdomyosarcoma (RMS). This panel has been now used for the *in-vitro* testing of more than 50 pediatric cancer therapies (21) and will serve as our *in-vitro* model to test adoptive NK cell immunotherapy.

Natural Killer Cell Biology and Functions

NK cells are part of the innate immune system and they comprise 5-15% of our peripheral blood lymphocytes (20). They are typically defined as CD56+/CD3- cells with the capacity of recognizing tumor cells without prior sensitization (22, 23) . NK cells are heterogeneous and their activity is regulated by a series of inhibitory and activating receptors which recognize ligands expressed by target cells. The 3 main receptor families present on NK cells include: natural cytotoxicity receptors (NCR's), C-type lectin (CD94/NKG2) and killer cell immunoglobulin like receptors (KIRs). NCR's (NKp30, NKp44, NKp46) are all activating receptors. Other important NK cell activating receptors such as DNAM1 and NKG2D have been described. C-type lectin and KIR families contain both activating and inhibitory variants (22). The major NK cell activating and inhibitory receptors and their respective ligands can be found in Table 1 (Adapted from Kannan GS, Aquino-Lopez A, Lee DA, *Blood Rev* 2016) (24). As observed in table 1, different KIRs recognize specific MHC class I molecules, therefore for a KIR to send inhibitory signals its corresponding MHC-class I molecule should be expressed in the target cell.

Activation of NK cells has been described by the "missing self" hypothesis, which states that the presence of major histocompatibility complex (MHC), which is ubiquitously expressed among healthy cells, provides NK cells with a "self" signal which is recognized by NK cell inhibitory receptors (KIRs and NKG2A) leading to inhibition of NK cell activity(25) (Fig 1, top panel).

Table 1. Major NK cell activating and inhibitory receptors and their ligands

Activating Family	Receptor	Ligand	Inhibitory Family	Receptor	Ligand
Natural Cytotoxicity Receptors (NCRs)	NKp30	BAT-3, HSPG, B7-H6	Killer Immunoglobulin like Receptors (KIRs)	KIR2DL1	HLA-C2 (Asn77/Lys80)
	NKp44	Viral Haemagglutinin		KIR2DL2 KIR2DL3	HLA-C1 (Ser77/Asn80)
	NKp46	HSPG, Viral Haemagglutinin		KIR3DL1	HLA-Bw4 (Asn77/Ile80)
C-type Lectin	CD94/NKG2C	HLA-E		KIR3DL2	HLA-A3, –A11
	CD94/NKG2E	HLA-E	C-type Lectin	CD94/NKG2A	HLA-E
	NKG2D	MICA,MICB, ULBP1–6			
Killer Immunoglobulin like Receptors (KIRs)	KIR2DS1	HLA-C2			
	KIR3DS1	HLA-Bw4 (peptide specific)			
	DNAM-1	PVR, Nectin			

Some tumor cells are known to downregulate MHC in order to avoid T cell attack and can also express activating ligands, making them susceptible targets for NK cell attack (Fig. 1, middle panel). In tumor cells where both inhibitory and activating ligands are present, the balance between activating and inhibitory signals will determine whether the NK cell gets activated (Figure 1, bottom panel. The response of an NK cell to a particular target will be determined not only by the expression of ligands in the target, but also by the combination of receptors expressed on the NK cell.

Once an NK cell is committed to kill a target cell it can do it through a variety of mechanisms including, granule release (degranulation) (26-28), death receptor pathway activation (28, 29), and IFNγ release (28). Upon degranulation NK cells release perforin and granzyme, which result in pore formation and target cell apoptosis respectively (27,

28). For death receptor pathway activation, TNF-related apoptosis inducing ligand (TRAIL) on NK cells binds death receptors (DR4 and DR5) on target cells inducing their apoptosis (28, 29).

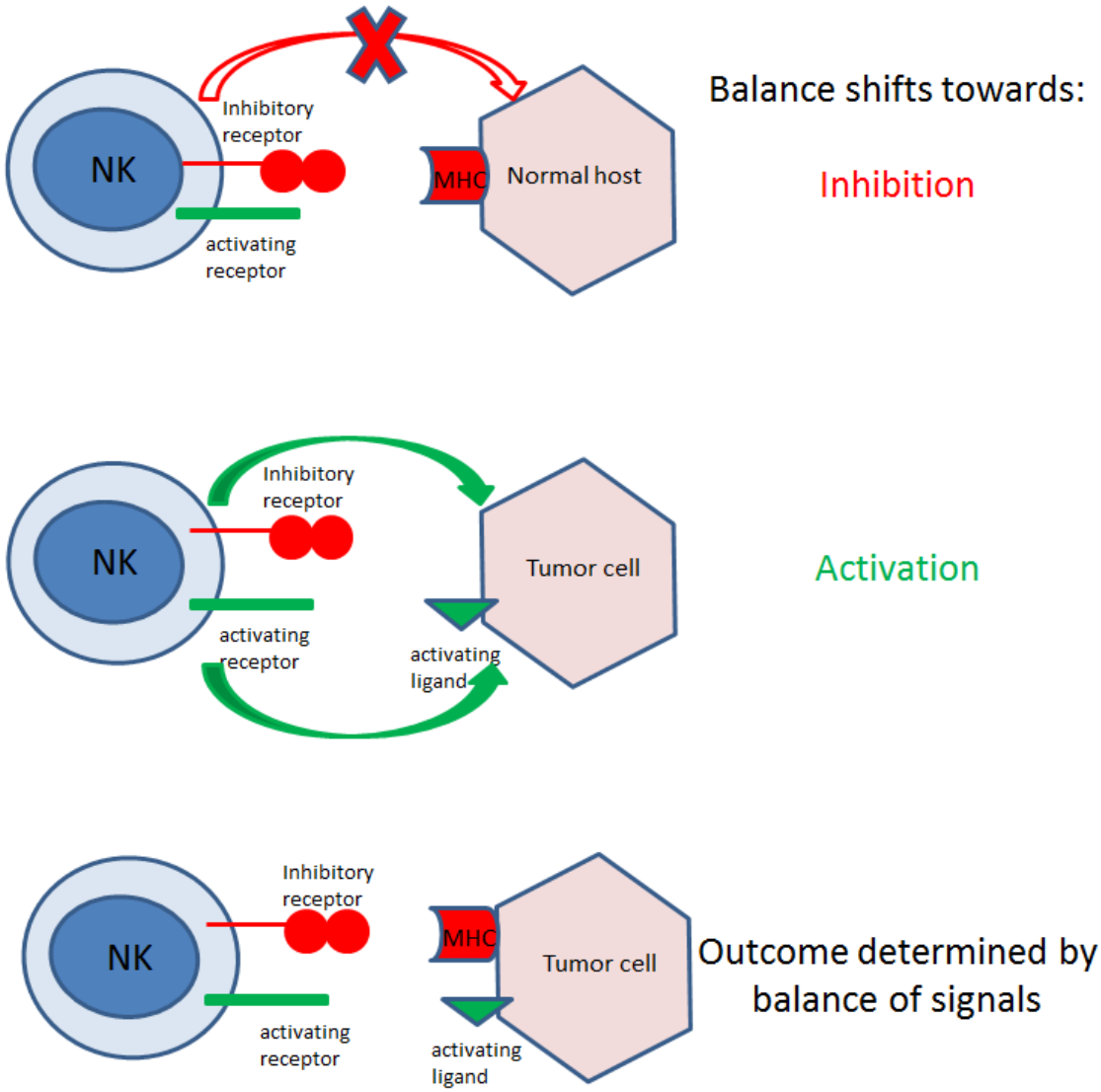

Figure 1. NK cell function is determined by the balance of inhibitory and activating signals.

Activated NK cells release IFNγ, a cytokine known to induce MHC upregulation which allows for enhanced antigen presentation for T cells (28). NK cells can also mediate tumor cell death through antibody dependent cell cytotoxicity (ADCC) (30). In ADCC the FcγR/ CD16 receptor of NK cells interacts with the Fc portion of antibodies coating tumor cells, this interaction leads to granule release and target cell destruction. ADCC mediated by NK cells is in part responsible for the beneficial effects of many antibodies used for cancer treatment (30, 31).

Adoptive NK cell Therapy: From Apheresis Product to Ex-vivo Expansion

Studies in patients with myeloid leukemia receiving stem cell transplant (SCT) showed that NK cells are among the first groups of cells to recover after transplant. Increased numbers of NK cells at day 30 post-transplant correlated with enhanced graft vs leukemia (GVL) effect, and improved survival (32). Since increased number of NK cells showed beneficial effects, investigators explored the idea of adoptive NK cell therapy as a way to increase NK cell numbers in the transplant setting for improved outcomes. Also NK cells have shown promise in non-transplant settings with therapeutic potential for multiple human cancers including leukemia (33), carcinomas (34, 35), lymphomas (36), and sarcomas (37, 38).

Apheresis was the initial platform used to obtain NK cells for adoptive therapy. However, given that NK cells compose only 5-15% of our peripheral blood lymphocytes (20), purification through apheresis resulted in infusion products ranging from $1x10^7$ – $5x10^7$ cells/kg which could be used as a single dose infusion (33, 35, 39, 40). Limitations

on the number of NK cells that could be obtained through apheresis, the expensive cost of the process, as well as its invasive nature, resulted in the development of *ex-vivo* expansion platforms that would allow for production of large quantities of NK cells for patient infusion. Multiple ex-vivo expansion platforms have been developed using cytokines such as IL-15, IL-2 and IL-21 to stimulate NK cell proliferation. Other ex-vivo expansion platforms rely on the use of feeder cells such as cells derived from EBV lymphoblastoid cells or modified K562 (leukemia) cells. Ex vivo expansion platforms published by multiple research groups are summarized on table 2. Overall, these expansion platforms reach a range of 5-550 fold expansion for NK cells in a maximum of 24 days.

However, our group has developed an NK cell expansion platform that results in the highest expansion fold reported in the literature for NK cells, with a 47,967 fold expansion after 21 days in culture (41). It relies on the use of K562 feeder cells modified to express membrane bound IL-21 (mb-IL21) in addition to 4-1BBL, from now on I will refer to these feeder cells as K562 mb-IL21 (41). Briefly in this expansion platform NK cells are stimulated weekly with K562-mb-IL21 for up to 3 weeks. NK cells expanded K562 mb-IL21 feeder cells, also referred as IL-21 expanded NK cells, are currently used in several trials at MD Anderson for leukemia, and also brain tumors (Refer to Table 3).

Table 2. NK cell Ex-vivo Expansion Platforms for Adoptive NK cell Therapy

Days in culture	Stimulation	NK Expansion Fold	Reference
14 days	IL-2	5	(42)
14 days	IL-2 or IL-2 + IL-15	5-20	(43)
13 days	Irradiated T & B cells as feeder + IL-15 or IL-2	25-28.5	(44)
7 days	IL-2 + IL-21 or IL-15 + IL-21	$CD56^{bright}$ 40-50 $CD56^{dim}$ 10	(45)
12 days	irradiated RPMI 8866 cells (EBV+ lymphoblastoid B-cell line) as feeder	40	(46)
21 days	Irradiated K562 with membrane-bound interleukin (IL)-15 and 41BB ligand as feeder	277	(47)
24 days	Irradiated K562-MICA-4-1BBL IL-15 as feeder	550	(48)
21 days	IL-2 + Irradiated K562 with Membrane-bound IL-21 (mbIL21) tCD19, CD64, CD86 and 4-1BBL as feeder	47,967	(41)

Table 3. Trials at MD Anderson infusing NK cells expanded on K562 mb-IL21 feeder cells

ClinicalTrials.gov Identifier	Disease	Study Title	Phase/ Primary Outcome
NCT01787474	AML	IL-21-Expanded NK Cells for Induction of Acute Myeloid Leukemia (AML)	Phase I/II- Maximum Tolerated Dose
NCT01904136	Leukemia Myeloproliferative Diseases	NK Cells to Prevent Disease Relapse for Patients High Risk Myeloid Malignancies	Phase I/II- Maximum Tolerated Dose
NCT01823198	AML Myelodysplastic Syndromes (MDS)	Natural Killer (NK) Cells With HLA Compatible Hematopoietic Transplantation for High Risk Myeloid Malignancies	Phase I/II- Maximum Tolerated Dose
NCT02271711	Brain Cancer	Fourth Ventricle Infusions of Autologous Ex Vivo Expanded NK Cells in Children With Recurrent Posterior Fossa Tumors	Phase I- Maximum Tolerated Dose
NCT02280525	Leukemia Lymphoma	Cord Blood Natural Killer (NK) Cells in Leukemia/Lymphoma	Phase I- Maximum Tolerated Dose

Prior studies from our lab demonstrated that IL-21 expanded NK cells secrete 100-fold more IFNγ than primary NK cells (median secretion of 2493 vs. 24 pg/mL) in response to targets (41). Similarly memory like-NK cells used by other groups for adoptive transfer to AML patients show increased IFNγ secretion when compared to control cells (49). Therefore, to optimize the use of expanded NK cells as adoptive cell therapy it is crucial to better understand how IFNγ affects tumor cell ligand expression and NK cell mediated lysis.

IFNγ and its Opposing Effects in Target Cell Sensitivity to NK-mediated Lysis

The pro-inflamatory cytokine IFNγ is mainly produced by activated CD8+ (Cytotoxic T Lymphocytes), CD4+ helper T cells, and NK cells (50). The secretion of IFNγ by immune cells, including NK cells, is known to upregulate MHC-class I expression on target cells, which allows for enhanced antigen presentation for T cells (28). However, in the context of NK cells, MHC serves as an inhibitory ligand recognized by NK cell inhibitory KIRs and NKG2A (51). Studies have shown an inverse correlation between MHC-class I expression and NK cell susceptibility (52). IFNγ has been reported to increase resistance of B-cell lymphoma, sarcoma, melanoma, B-cell leukemia and T-cell leukemia cells to Lymphokine Activated Killer (LAK) cells and NK cells, which has been attributed in part to upregulation of MHC-class I (53, 54). A study with primary cutaneous melanoma specimens revealed increased HLA expression for melanoma cells in proximity to NK cells. This study also revealed that after co-culturing melanoma cells with NK cells, the melanoma cells that were not eliminated had increased HLA expression and acquired resistance to NK cell mediated lysis (55).

However, IFNγ has also been reported to increase sensitivity of tumor cells to NK cell mediated lysis, and this has been attributed to upregulation Intercellular adhesion molecule-1 (ICAM-1/CD54) expression on target cells. ICAM-1 is important for the first steps in the immune synapse (IS) formation. NK cell adhesion to target cells is mediated by Lymphocyte Function Associated Antigen-1 (LFA-1) binding to adhesion molecules such as Intercellular adhesion molecule-1 (ICAM-1/CD54) (56). This adhesion is essential for the formation of an effective immune synapse (IS), and an efficient target cell lysis. LFA-1 engagement by ICAM-1 has also been shown to promote lytic granule convergence to the IS which is important for the cytotoxic effect of NK cells (56, 57). A study by Naganuma, et al. reported that IFNγ treatment of neuroblastoma cell line CHP-134 increased its sensitivity to Lymphokine Activated Killer (LAK) cells, and attributed this in part to increased ICAM-1 expression and formation of conjugates (58). In addition, Wang et al. reported increased NK cell mediated cytolysis for THP-1 cells (AML) after IFNγ treatment overnight. They attributed this increase in sensitivity for THP-1 cells to increased ICAM-1 expression on tumor cells and enhanced adhesion of NK cells to target cells after IFNγ treatment (59).

Aim of the study

Traditional chemotherapy and radiation increase the risk of life threatening complications later in life for childhood cancer survivors. Therefore, there is a critical need to develop new therapies that will allow us to eradicate the tumor, while decreasing morbidity. Adoptive transfer of NK cells, is a promising therapeutic approach for the pediatric population. NK cells have the potential of selectively targeting tumor cells and this can result in decreased risk of complications later in life. In order to study NK cells we isolate and expand NK cells from human donors. Each donor has a very heterogeneous pool of NK cells with variability in their receptor expression and their potential to kill tumor cells. Therefore, **we hypothesize** that particular subpopulations of NK cells with increased cytotoxic activity against pediatric malignancies can be identified and expanded for enhanced cytotoxic activity of the NK cell infusion product. Also, our laboratory has shown that mb-IL21 expanded NK cells have high levels of IFNγ secretion when compared to primary NK cells. We **hypothesize** that IFNγ has a variable effect in the tumor cell sensitivity to NK-mediated lysis and alters the NK cell receptor-ligand interactions for pediatric cancer cells. In order to test these hypotheses we developed three specific aims as follows:

Specific Aim 1: To determine if subpopulations of NK cells with high cytotoxic potential can be identified and expanded for enhanced NK cell product efficiency.

Specific Aim 2: To determine the effect of exogenous IFNγ on NK cell mediated lysis of a panel of pediatric cancer cell lines and the mechanism involved.

Specific Aim 3: To determine the impact of NK cell secreted IFNγ on tumor NK cell ligand expression.

CHAPTER II: MATERIALS AND METHODS

Isolation and Expansion of Human NK cells

Buffy coats from four anonymized donors were obtained from Gulf Coast Regional Blood Center (Houston TX). Exemption and waiver of consent for the research use of buffy coat fractions obtained from anonymized donors at Gulf Coast Regional Blood Center (Houston, TX) was granted by the Institutional Review Board of the University of Texas MD Anderson Cancer Center under protocol PA13-0978. For NK cells obtained from patient infusion products, consent for the research use was granted by the Institutional Review Board of the University of Texas MD Anderson Cancer Center under protocol 2012-0708. NK cells were isolated using the RossetteSep Human NK cell enrichment cocktail (Stem Cell Technologies) and expanded as described previously using K562 Clone9.mbIL21 as feeder cells for 21 days (41). Expanded NK cells were cryopreserved, and subsequently thawed and recovered for 1-2 days prior to their use. During recovery NK cells were cultured in NK cell media consisting of RPMI 1640 (Corning) supplemented with 50 IU/ml recombinant human IL-2 (Proleukin, Novartis Vaccines and Diagnostics, Inc), 20% Fetal Bovine Serum (Thermofisher), L-glutamine (Gibco), and penicillin/streptomycin (Corning).

Tumor Cells

TC-71, NALM-6, and Ramos-RA1 were obtained as kind gifts from colleagues (Drs. ES Kleinerman, LJN Cooper, and J Chandra, respectively). Karpas-299 was obtained from the German Collection of Microorganisms and Cell Cultures (DSMZ). RS4;11, MOLT-4, and CCRF-CEM were obtained from the America Type Culture

Collection (ATCC). The remaining cell lines were obtained from the Children's Oncology Group (COG) Cell Line and Xenograft Repository. Brain tumor cell lines BT-12, SJ-GBM2, CHLA-266, Ewing sarcoma (EWS) cell lines CHLA-9, CHLA-10, CHLA-258, TC-71, neuroblastoma (NB) cell lines NB-1643, NB-EBc1, CHLA-90, CHLA-136, rhabdomyosarcoma (RMS) cell line RD, and leukemia cell line COG-LL-317 were cultured in IMDM (Lonza) supplemented with 20% FBS (Thermofisher), 4mM L-Glutamine (Gibco), 1X ITS (Lonza) and penicillin/streptomycin (Corning). Lymphoma cell lines Karpas-299, Ramos-RA1, leukemia cell lines NALM-6, RS4;11, MOLT-4, CCRF-CEM, Kasumi-1, and RMS cell lines Rh41, Rh30, were cultured in RPMI 1640 (Corning) supplemented with 10% Fetal Bovine Serum (Thermofisher), L-glutamine (Gibco), and penicillin/streptomycin (Corning). Cultures were periodically tested to confirm absence of Mycoplasma using MycoAlert Mycoplasma Detection Kit (Lonza). Identity was confirmed by STR DNA fingerprinting either using the AmpFℓSTR Identifiler kit (Applied Biosystems) or the *Power Plex 16HS Kit* (*Promega)* according to manufacturer instructions. The STR profiles were compared to known fingerprints as published by ATCC or the COGcell STR Genotype Database (http://strdb.cogcell.org). STR profiles were last performed on March 2016 (SJ-GBM2, NB-1643, MOLT-4), October 2015 (RD, Rh-41, Rh30, BT-12, CHLA-10, NB-EBc1, NALM-6, and Ramos-RA1), or September 2012 (CHLA-266, CHLA-9, CHLA-258, TC-71, CHLA-90, CHLA-136, RS4;11, COG-LL-317, CCRF-CEM, Kasumi-1 and Karpas-299). Banks of STR validated, mycoplasma-free cell lines were cryopreserved. Cell lines were kept in culture no longer than 8 passages or 4 weeks prior to use.

IFNγ treatment of tumor cells

Cell lines that grow in suspension were seeded at $0.5x10^6$ cells/mL and treated with 50ng/mL of IFNγ (Peprotech) for 48 hours. Adherent cells were cultured to a 60-70% confluence and treated with 50ng/mL of IFNγ (Peprotech) for 48 hours. Untreated tumor cells were seeded in parallel. After treatment cells were washed in IFNγ free media, and adherent cells were detached with non-enzymatic cell dissociation buffer (Gibco) to avoid degradation of cell surface proteins. Treated and untreated cells were evaluated for surface expression of NK cell ligands by mass cytometry, and sensitivity to NK cell mediated lysis by calcein release assay.

Cytotoxicity

The fluorescence based calcein release assay was used to assess cytotoxicity, as previously described (41, 60). Adherent cells were detached with non-enzymatic cell dissociation buffer (Gibco) and cells were filtered by using a 70μm cell strainer (Corning) to obtain a single cell suspension. Target cells were labeled with 5 μg/mL of calcein-AM (Sigma-Aldrich) for 1 hour at 37°C. NK cells were co-cultured with target cells at different effector to target (E:T) ratios (10:1, 5:1, 2.5:1, 1.25:1, 0.6:1 and 0.3:1) for 4 hours at 37°C. Supernatant fluorescence was determined at 485 nm^{Exc}/530 nm^{Emm} using the SpectraMax $Plus^{384}$ spectrophotometer. For cytotoxic assays with ICAM-1 blocking, NK cells were loaded with Fc receptor blocker (Biolegend, 422302) prior to co-culture with target cells. Anti-ICAM-1 antibody (Biolegend, 322703) or IgG1 isotype (Biolegend, 400124) were added to calcein loaded target cells at 10μg/mL for 20 minutes at room temperature prior to co-culture with NK cells.

Mass Cytometry

Antibodies for mass cytometry were labeled with heavy metals using Maxpar-X8 labeling reagent kits (DVS Sciences) according to manufacturer's instructions and titrated for determination of optimal concentration. The antibodies and their respective heavy metal labeling for tumor cells staining can be found in Table 4. Since NK cell receptors may have multiple ligands (e.g., NKG2D binds to MICA, MICB, and ULBP1-5), or unknown ligands, chimeric receptor:IgG-Fc fusion proteins were tagged with heavy metals and used for identification of ligands on tumor cells. Antibodies used for staining of tumor cells and NK cells can be found on tables 4-6. For all cells 1.5 x 10^6 cells were stained for viability with 2.5μM cell ID cisplatin (Fluidigm, 201064) in serum free RPMI for 1 minute and washed twice with complete media. Subsequently, surface staining was performed as previously described (61). Staining media was prepared by adding 5%FBS and 0.1% sodium-azide to PBS.

During the intracellular staining step of tumor cells, 2 different isotopes of cisplatin Pt-194 (Fluidigm, 201194) and Pt-198 (Fluidigm, 201198) were used to barcode untreated and IFNγ treated samples, respectively, allowing samples to be combined in a single tube, minimizing acquisition time and variability between runs.

For functional mass cytometry experiments, NK cells from patient infusion products were co-cultured with 721.221 target cells at a 2:1 E:T ratio for 3 hours in the presence of metal conjugated anti-CD107a and protein transport inhibitor Golgi stop. After 3 hours, cells were stained with surface and intracellular staining was performed as previously described (61).

Data was acquired on a CyTOF instrument (DVS Sciences). Files containing only live single cells were exported using FlowJo V10 Software and uploaded into Cytobank for further analysis (Figure 2) (62). Heatmaps corresponding to median expression of ligands on tumor cells were generated using Cytobank (62).

Table 4. CyTOF Panel for Staining of Cancer Cells

Isotope	Antibody or Chimeric protein (Fc)	Antibody Clone	Source	Catalog #
149Sm	CD244/2B4_Fc	-	R&D	1039-2B-050
150Nd	HLA-E	3D12	BioLegend	342602
152Sm	NKp80_Fc	-	R&D	1900-NK-050
154Sm	NKp30_Fc	-	SinoBiological	10480-H03H
156Gd	NKp44_Fc	-	R&D	2249-NK-050
161Dy	CD261/DR4	DJR1	BioLegend	307202
162Dy	CD54/ICAM-1	HCD54	BioLegend	322702
163Dy	CD262/DR5	DJR2-4(7-8)	BioLegend	307402
165Ho	DNAM-1_Fc	-	R&D	666-DN-050
166Er	MHC-class I	W6/32	BioLegend	311402
168Er	NKG2D/CD314 _Fc	-	R&D	1299-NK-050
169Tm	NKp46_Fc	-	R&D	1850-NK-025
170Er	CD270	122	BioLegend	318802
172Yb	CD274/PD-L1	29E.2A3	BioLegend	329702
174Yb	HLA-DR	L243	BioLegend	307602
175Lu	CD95/Fas	DX2	BioLegend	305602

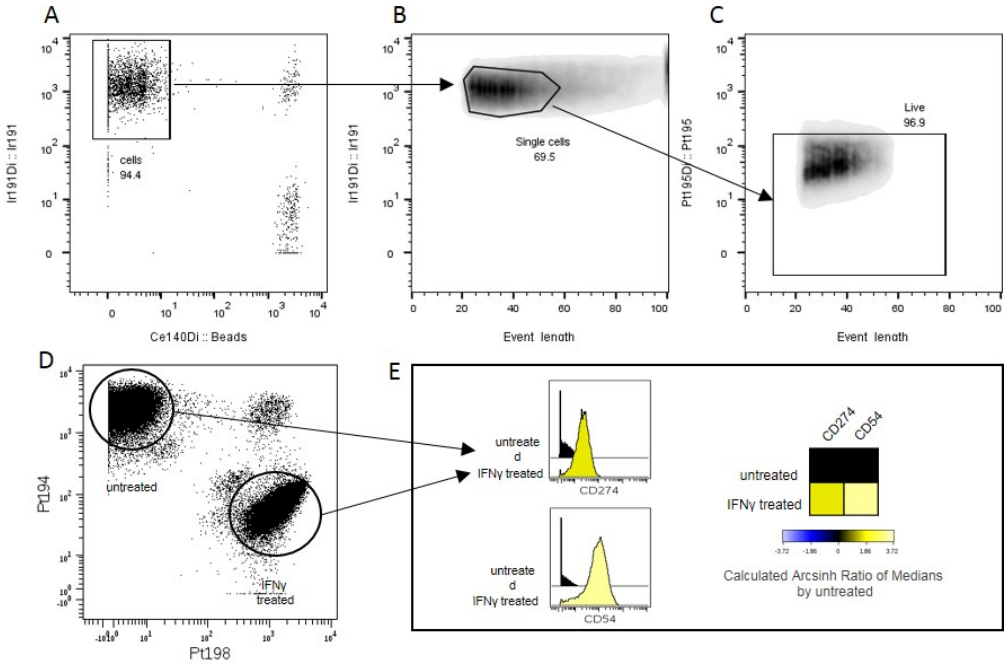

Figure 2. Gating Strategy and de-barcoding of untreated and IFN gamma treated cancer cells

(A) Cells were gated to remove beads from the anlaysis followed by (B) gating for single cells and removal of aggregates**. (C)** Dead cells exclusion. Live, single cells were exported as FCS files into Cytobank for de-barcoding **(D)** of treatment conditions. Untreated cells were positive for Pt-194 and IFNγ treated cells were positive for Pt-198. **(E)** Gated populations were analyzed and used for the generation of heat maps based on median expression of surface ligands

Table 5. CyTOF Panel for Phenotyping of Healthy Donor NK cells through Expansion

Isotope	Antibody	Antibody Clone	Source	Catalog #
139La	CD94	DX22	BioLegend	305502
	KIR3DL1-PE	DX9	Miltenyl Biotec	130-092-473
141Pr	Anti-PE	PE001	BioLegend	408102
143Nd	CD357	621	BioLegend	311602
	KIR2DL1-FITC	143211	R&D	FAB1844F
144Nd	Anti-FITC	FIT-22	DVS-Fluidigm	3144006B
147Sm	CD278/ICOS	C398.4A	BioLegend	313502
148Nd	CD134/OX-40	Ber-ACT35	BioLegend	350002
149Sm	CD223/LAG3	Poly	R&D	AF2319
150Nd	CD314/NKG2D	1D11	BioLegend	320802
151Eu	CD3	UCHT1	BioLegend	300443
152Sm	CD137/4-1BB	4-1BB	BD	555955
153Eu	CD272/BTLA	MIH26	BioLegend	344502
154Sm	NKp46	9E2	BioLegend	331902
156Gd	TIM-3	F38-2E2	BioLegend	345002
158Gd	CD244	C1.7	Biolegend	329502
160Gd	TIGIT	MBSA43	eBioscience	16-9500-82
161Dy	NKp80	5D12	BioLegend	346702
162Dy	CD56	NCAM16.2	BD	559043
163Dy	NKp44	P44-8	BioLegend	325102
164Dy	NKp30	P30-15	BioLegend	325202
165Ho	CD16	3G8	DVS-Fluidigm	3165001B
166Er	CD159a/NKG2A	131411	R&D	MAB1059
167Er	CD226/DNAM-1	TX25	Biolegend	337102
168Er	CD11a /LFA-1	HI111	BioLegend	301202
169Tm	NKG2C	134522	R&D	MAB1381
	KIR2DL2/3-APC	DX27	Miltenyl Biotec	130-092-617
170Er	Anti-APC	APC003	BioLegend	408002
171Yb	CD62L	DREG-56	BioLegend	304802
172Yb	CD57	HCD57	DVS-Fluidigm	3712009B
174Yb	CD253/TRAIL	RIK-2	BioLegend	308202
175Lu	CD279/PD-1	J105	MBL	D133-3

Table 6. CyTOF Panel for Functional Activity of Patient Infusion Products

Marker	Metal or Fluorophore	Clone	Source	Catalog #
CD94	139La	DX22	BioLegend	305502
PE*	141Pr	PE001	BioLegend	408102
CD357	143Nd	621	BioLegend	311602
FITC*	144Nd	FIT-22	DVS-Fluidigm	3144006B
CD4	145Nd	RPA-T4	BioLegend	300502
CD8a	146Nd	RPA-T8	BioLegend	301002
CD278/ICOS	147Sm	C398.4A	BioLegend	313502
CD134/OX-40	148Nd	Ber-ACT35	BioLegend	350002
CD223/LAG3	149Sm	Poly	R&D	AF2319
CD314/ NKG2D	150Nd	1D11	BioLegend	320802
CD107a	151 Eu	H4A3	DVS-Fluidigm	3151002B
CD272/BTLA	153Eu	MIH26	BioLegend	344502
NKp46	154Sm	9E2	BioLegend	331902
TIM3	156Gd	F38-2E2	BioLegend	345002
IFNg	158Gd	B27	DVS-Fluidigm	3158017B
TIGIT	160Gd	MBSA43	eBioscience	16-9500-82
NKp80	161Dy	5D12	BioLegend	346702
CD56	162Dy	NCAM16.2	BD	559043
NKp44	163Dy	P44-8	BioLegend	325102
NKp30	164Dy	P30-15	BioLegend	325202
CD16	165Ho	3G8	DVS-Fluidigm	3165001B
NKG2A	166Er	131411	R&D	MAB1059
CD226/DNAM-1	167Er	TX25	BioLegend	337102
CD11a	168Er	HI111	BioLegend	301202
NKG2C	169Tm	134522	R&D	MAB1381
APC*	170Er	A85-1	BD	560089
CD62L	171Yb	DREG-56	BioLegend	304802
CD57	172Yb	HCD57	DVS-Fluidigm	3712009B
CD253/TRAIL	174Yb	RIK-2	BioLegend	308202
CD3	175Lu	UCHT1	BioLegend	300443
KIR3DL/DS1	PE	Z27.3.7	Beckman Coulter	41116015
KIR2DL1	FITC	143211	R&D	FAB1844F
KIR2DL2/DL3	APC	DX27	Miltenyi	130-092-617

(Provided by Jolie Schafer, used with permission)

SPADE Clustering analysis

Clustering analysis of NK cell mass cytometry data was performed using spanning-tree progression analysis of density-normalized events (SPADE V3.0) software (Peng Qiu, et al., 2011) (63). For figures 6 and 8 live single NK cells were gated (CD56+/CD3-) and clustered using the following markers: NKp80, CD56, NKp44, NKp30, NKG2A, CD226, CD11a, CD272, TIM-3, CD244, CD357, CD134, CD314/NKG2D, CD278, CD226, CD137, CD57, and CD253. For figure 10 live single NK cells were gated (CD56+/CD3-) and clustered using the following markers: NKp80, CD56, NKp44, NKp30, NKG2A, CD226, CD11a, CD272, TIM3, CD16, CD94, CD357, CD134, CD314, CD278, CD223, NKp46, NKG2C, CD62L, CD57 and CD253.

Conjugation Assay

The determination of effector conjugation to target cells was performed as described by Burshtyn *et al*, with some minor modifications (64). Briefly, NK cells and tumor cells were stained with green dye PKH67-GL (Sigma, MINI67) and red dye PKH26-GL (Sigma, MINI26), respectively, in 5μM dye at $5x10^6$ cells/mL for 5 minutes at room temperature. Dye staining was stopped by adding two volumes of FBS and two volumes of complete media. Cells were washed twice with complete media and let rest for at least 1 hour at 37°C. 10^5 NK cells were combined with $2x10^5$ tumor cells in 200μL, centrifuged at 20g for 1 minute (to initiate contact), and incubated at 37°C for 30 min. Cells were resuspended by gentle vortexing, fixed with 200 μL of 4% formaldehyde, and analyzed by flow cytometry. For antibody blocking experiments NK cells were pre-incubated with 5μL of Fc blocker (Biolegend, 422302) for 10 minutes to avoid antibody dependent cell

cytotoxicity (ADCC). ICAM-1 was blocked on tumor cells by adding 10μg/mL of anti-CD54/ICAM-1 clone HCD54 (Biolegend, 322703) for 20 minutes at room temperature.

Timelapse Imaging in Nanowell Grids

Timelapse experiments were performed in collaboration with Gabrielle Romain and Navin Varadarajan from the University of Houston. Experiment was performed as described by Romain et al, 2014 (65). Briefly, NK cells were labeled with PKH67 membrane dye and tumor cells (NB-1643) were labeled with PKH26 dye. Labeled cells-were co-cultured at 1:1 E:T ratio on the nanowell array. The chip was then incubated on media containing Annexin V-Alexa 647 for detection of cell death. Images were obtained every 6 minutes for a total of 6 hours.

NK Cytokine Secretion Assay

$5x10^5$ tumor cells were seeded in the bottom and top chambers of a 6 transwell plate (Fisher Scientific, 0.4μm pore size). $1x10^6$ NK cells (Day 21 expanded) were co-cultured with tumor cells at the top chamber of experimental wells (2:1 E:T ratio). Addition of 50ng/mL of IFNγ, in absence of NK cells or tumor cells at the top chamber, served as our positive control. Small pore size allows for transfer of cytokines (i.e. IFNγ) but not NK or tumor cells to the bottom chamber. Tumor cells were also seeded in absence of NK cells and/or exogenous IFNγ on the top chamber to evaluate baseline expression of ligands. After 48 hour incubation at 37^{o}C, tumor cells at the bottom chamber were detached with non-enzymatic buffer (Gibco) and stained with anti-MHC-class I-FITC (Biolegend, clone W6/32), anti-ICAM-1-PE (Biolegend, clone HA58) and anti-PD-L1-APC (Biolegend, clone 29E.2A3) for 20 minutes at room temperature. To evaluate the

effect of NK-secreted IFNγ we blocked IFNγ in the supernatant by adding 10μg/mL of anti-IFNγ (Biolegend, clone B27) to the bottom chamber. Addition of 10μg/mL non-specific anti-IgG1 antibody (Biolegend, clone MOC-21) served as our Isotype control.

Statistical Analysis

Statistics were performed in GraphPad Prism Software. For determination of Δ in % Lysis after IFNγ treatment (Figure 1) we used data from 6 different E:T ratios. For each donor we calculated the average difference in lysis after IFNγ treatment (%lysis IFNγ treated - %lysis untreated). Significance was determined by using the t-test with a hypothetical value of zero for comparison.

Paired and unpaired t-tests were used across experiments with a $p<0.05$ for significance. Description of specific tests used for each analysis are depicted in the figure legends.

CHAPTER III: IDENTIFICATION OF NK CELL SUBPOPULATIONS WITH UNIQUE PHENOTYPE AND ENHANCED FUNCTION

Rationale

To use NK cells for adoptive therapy we isolate and expand them from human donors. However, each donor has a very heterogeneous pool of NK cells with variability in their receptor expression and their potential to kill tumor cells. Therefore, **we hypothesize** that particular subpopulations of NK cells with increased cytotoxic activity against pediatric malignancies can be identified and selected for better NK cell product activity against pediatric cancer cells.

In order to test this hypothesis pediatric tumor cells corresponding to 6 tumor types were evaluated for their expression of NK cell ligands. Since NK cell activity is based on receptor-ligand interactions, knowledge of the NK cell ligands expressed by tumor cells would allow us to determine which tumor cells are potentially susceptible to NK cells, and which NK cell subpopulations would have enhanced activity, based on receptor expression. Knowledge of which subpopulations would be more active can allow us to select them to obtain a product enriched on NK cells with enhanced function.

Results

Pediatric Solid Tumor Cells Express High Levels of NK-Activating Ligands

Using mass cytometry we evaluated the expression of 16 NK cell ligands on 22 pediatric cancer cell lines. Cell lines were obtained from the PPTP *in vitro* panel and are listed on Table 7. Expression of NK cell ligands was quantified in terms of median level

of expression and percent positive cells (Figure 3). Our results show that MHC-class I and HLA-E, which are known NK cell inhibitory ligands, are expressed in more than 70% of tumor cells for most cell lines, with the exception of Rh41, a RMS cell line with 35% cells expressing MHC-class I. However, it is important to consider that the anti-MHC-class I antibody clone used in this study (W6/32) has been shown to recognize classical (HLA-A, HLA-B, HLA-C) and non-classical HLA (HLA-E) (66). When evaluating expression of activating ligands on tumor cells we noticed that compared to leukemia cell lines, many solid tumor cell lines, including RMS, brain tumor, EWS, and NB show higher levels of ligands for activating receptors such as NKG2D, DNAM-1 and the NCRs (NKp30, NKp44, NKp46) in terms of median expression, and also percent positive cells (Figure 3-4).

After quantifying the percent of cells with activating ligands for the 6 tumor types, statistically significant differences were observed between leukemia cells and solid tumor cells (Figure 4). While NKG2D ligands were present on 32% of leukemia cells, they were observed on an average of 80% of RMS and 68% of EWS cells ($p= 0.014$, $p= 0.009$ respectively). DNAM-1 ligands on the other hand were observed only on 15% of leukemia cells but were on 96% of RMS cells ($p<0.0001$), 65% of brain tumor cells ($p<0.0001$), 95% of EWS cells ($p<0.0001$) and 56% of NB cells ($p=0.026$). Ligands for the NCR NKp30 were on 35% of the leukemia cells but 76 % of the NB cells ($p=0.025$). Ligands for another NCR, NKp44 were on 16% of the leukemia cells but on 56 % of the NB cells ($p=0.042$). These results are important because although adoptive NK cell therapy is currently on trials mostly for leukemia, the expression of activating ligands on solid tumors suggests that NK cells may be a promising therapy for solid tumors as well.

Table 7. Pediatric Pre-clinical Testing Program In-Vitro Panel

Cell line	Diagnosis	
RD	Rhabdomyosarcoma (RMS)	Embryonal
Rh41		Alveolar
Rh30		Alveolar
BT-12	Brain Tumor	ATRT
SJ-GBM2		Glioblastoma multiforme
CHLA-266		ATRT
CHLA-9	Ewing's Family Tumors (EWS)	PNET
CHLA-10		PNET
TC-71		Ewings
NB-1643	Neuroblastoma (NB)	MYCN amplified
NB-EBc1		N/A
CHLA-90		N/A
CHLA-136		MYCN amplified
NALM-6	Leukemia	Pre-B cell ALL
RS4;11		Pre-B cell ALL
COG-LL-317		T-cell ALL
MOLT-4		T-cell ALL
CCRF-CEM		T-cell ALL
Kasumi-1		AML
Karpas-299	Lymphoma	Anaplastic Large Cell
Ramos-RA1		Burkitt's

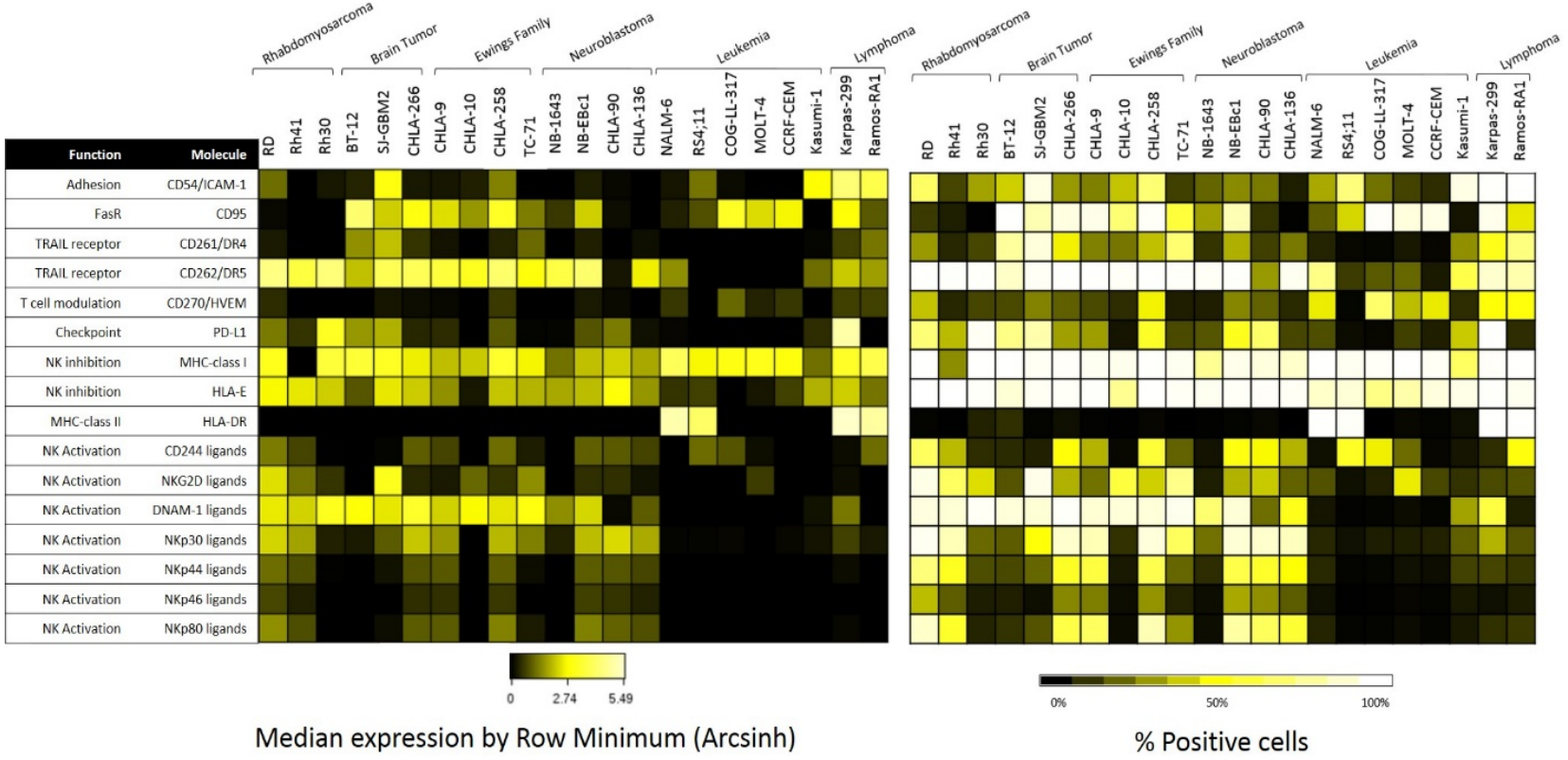

Figure 3. Expression of NK cell ligands in pediatric cancer cell lines.

Pediatric cancer cell lines were evaluated by mass cytometry for the baseline expression level of multiple NK cell ligands. The evaluated markers and their function can be found at the table above. **Left Panel.** Median expression level normalized by row minimum (obtained by evaluating the arcsinh ratio of the median expression compared to the row minimum). **Right Panel.** Percent positive cells for each given marker (Figure obtained from (67)).

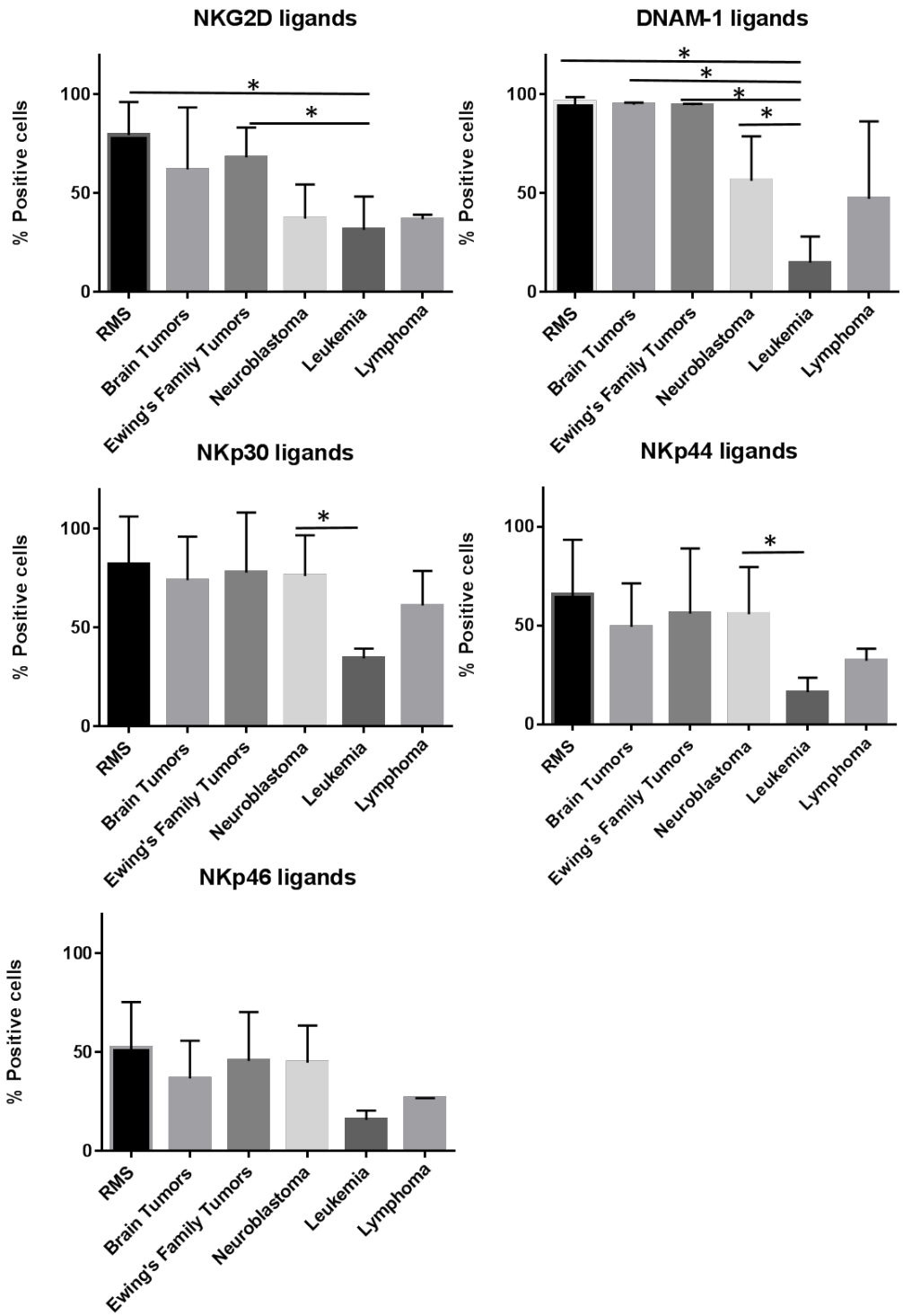

Figure 4. Quantification of percentage positive cells expressing activating ligands, classified by tumor type.

RMS (n=3), Brain Tumor (n=3), EWS (n=4), NB (n=4), Leukemia (n=6), Lymphoma (n=2). Unpaired T-test, *significant $p<0.05$

Increased Expression of Activating and Inhibitory Receptors on IL-21 Expanded NK cells

Given that pediatric solid tumors showed high levels of NK cell activating ligands for receptors such as NKG2D, DNAM-1, NKp30 and NKp44 our goal was to generate a product with high levels of these receptors. We first evaluated the expression of these receptors on IL-21 expanded cells and compared them to primary NK cells for 4 donors using mass cytometry. We observed that the number of cells expressing NKG2D, DNAM-1, NKp30 and NKp44 for day 21 expanded cells was significantly higher than for primary NK cells (Figure 5, Top Panel). Not only was the number of cells higher after expansion, but also the mean expression of activating receptors NKG2D, DNAM-1, NKp30 and NKp44 was statistically higher for IL-21 expanded cells, when compared to primary cells (Figure 5, Bottom Panel). We also evaluated other molecules associated with activation, including OX-40, 4-1BB, Lag-3, ICOS and GITR, and observed increased number of cells expressing them, as well as mean expression after expansion (Figure 5). Interestingly, we also observed increased number of cells expressing inhibitory receptors including KIR's, NKG2A, BTLA and TIM-3 after expansion (Figure 5, Top Panel). The mean expression for these was also significantly higher after expansion, when compared to primary NK cells. The expression of markers such as NKp80 and CD57, which have been associated to NK cell maturation, is decreased for expanded NK cells when compared to primary cells.

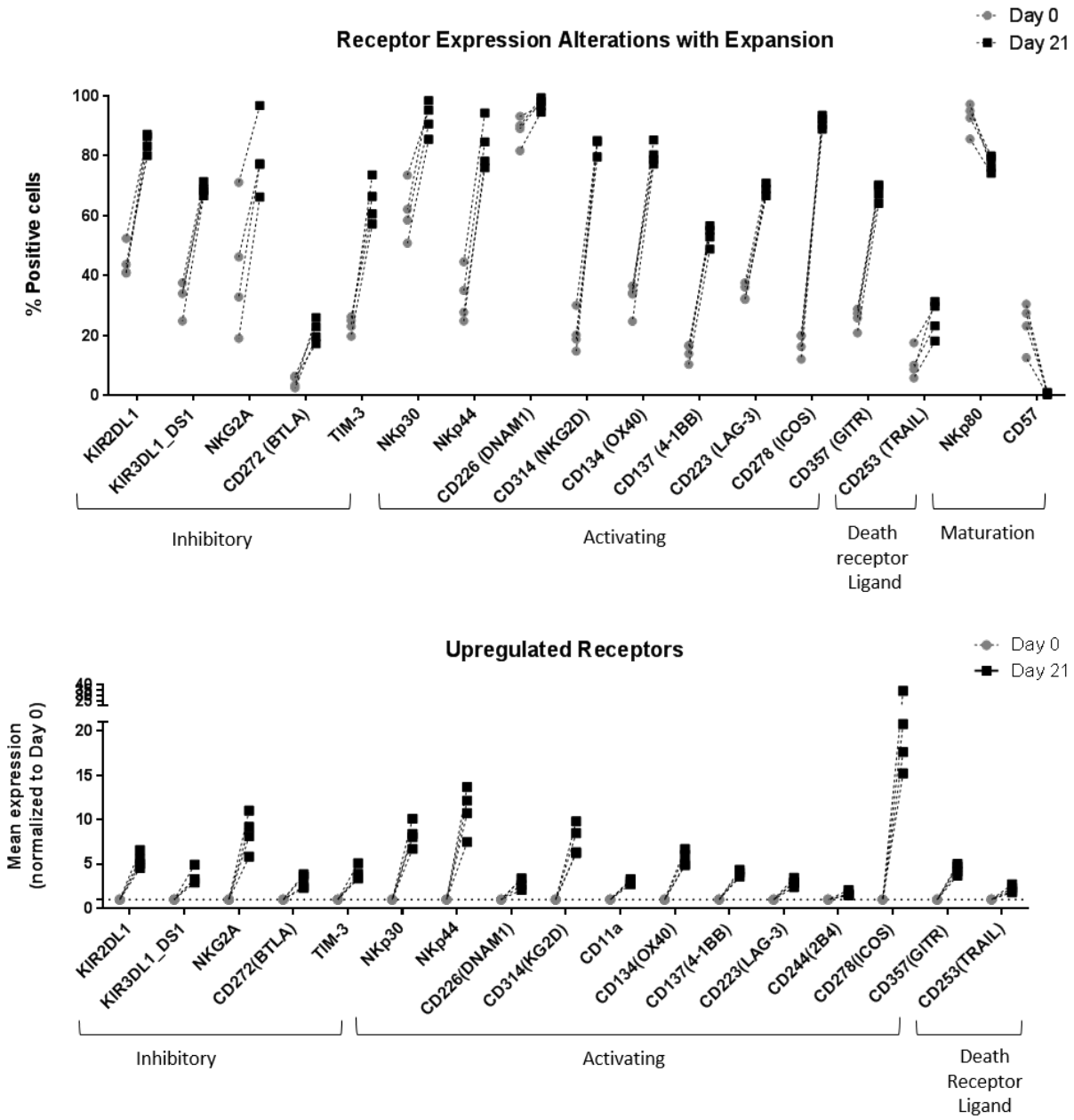

Figure 5. Alterations on NK cell receptor expression for IL-21 expanded NK cells

Presence of multiple NK cell activating and inhibitory receptors was evaluated by mass cytometry for primary NK cells and expanded NK cells of 4 anonymous donors. Only receptor alterations that were statistically significant are depicted on the figure (paired t-test, $p<0.05$). **Top Panel** represents percent positive cells. **Bottom Panel** represents Mean expression normalized to Day 0.

Identification of Unique Subpopulations on IL-21 Expanded NK cells from Healthy Donors

Given that we observed higher levels of NK-activating receptors on the IL-21 expanded NK cell product, we sought to determine whether particular clusters of NK cells were responsible for these overall changes in the product phenotype. We used the SPADE algorithm to cluster NK cell subpopulations based on their receptor expression. Interestingly, after comparing primary NK cells with day 21 expanded NK cells, we observed a number of clusters present after expansion that were absent for primary NK cells (Figure 6). These unique subpopulations have high expression of the activating receptors NKp30, NKp44, DNAM-1, and NKG2D. In addition, they also express high levels of other molecules associated with activation such as CD11a (LFA-1), ICOS, OX40 and 4-1BB. Inhibitory receptors such as KIRs, NKG2A and TIM-3 were also observed on high levels for these subpopulations. After gating for these subpopulations on all 4 donors we determined that these unique subpopulations, constituted an average of 41.7% of the IL-21 expanded NK cell product after 21 days in expansion (Figure 7). To determine whether we could find these populations earlier in the expansion we used the same SPADE clustering parameters and analyzed 3 healthy donors, at different time-points through the expansion, day 0, day 7, day 14, and day 21 (Figure 8). Our results indicate that these unique subpopulations can be identified as early as 1 week into the expansion process, with a similar phenotype co-expressing high levels of activating receptors NKp30, NKp44, DNAM-1, and NKG2D throughout the expansion. Interestingly, quantification of these unique subpopulations reveals that they are more abundant at day 7 (81%), but their abundance decreases throughout the expansion with decreased

frequencies at day 14 (64%) and day 21 (48%) (Figure 9). Next, we sought to determine the functionality of these unique subpopulations upon target cell encounter.

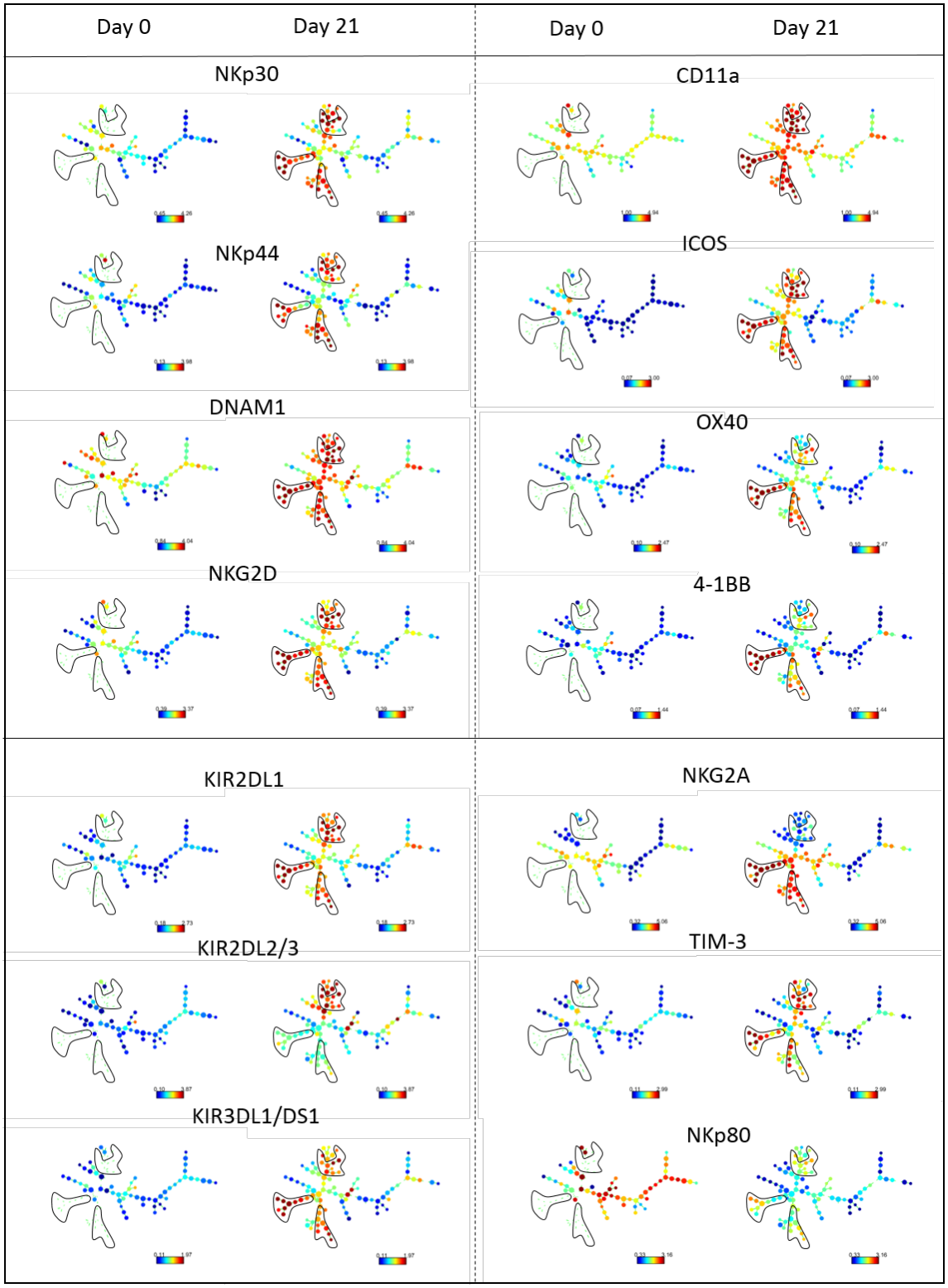

Figure 6. SPADE Clustering Identifies Unique Subpopulation on Expanded NK cells from Healthy Donors

Figure 6. SPADE clustering Identifies Unique Subpopulations on Expanded NK cells from Healthy Donors. NK cells from 4 donors were evaluated by mass cytometry for inhibitory and activating receptor expression. SPADE was used to cluster nodes based on NK cell receptor expression. Unique clusters, present on expanded NK cells but absent on primary NK cells, are highlighted by black contour. The figure shows representative results for 1 donor, but results were replicated across all donors. Blue indicates low expression, Red indicates high expression.

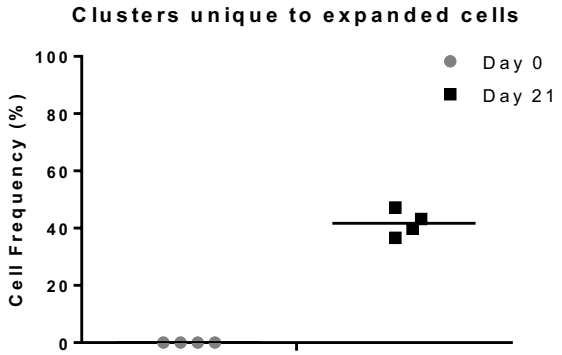

Figure 7. Quantification of Unique Subpopulations on Expanded NK cells from Healthy Donors

Unique subpopulations, unique to day 21 expanded NK cells, were gated and quantified. (n=4 donors)

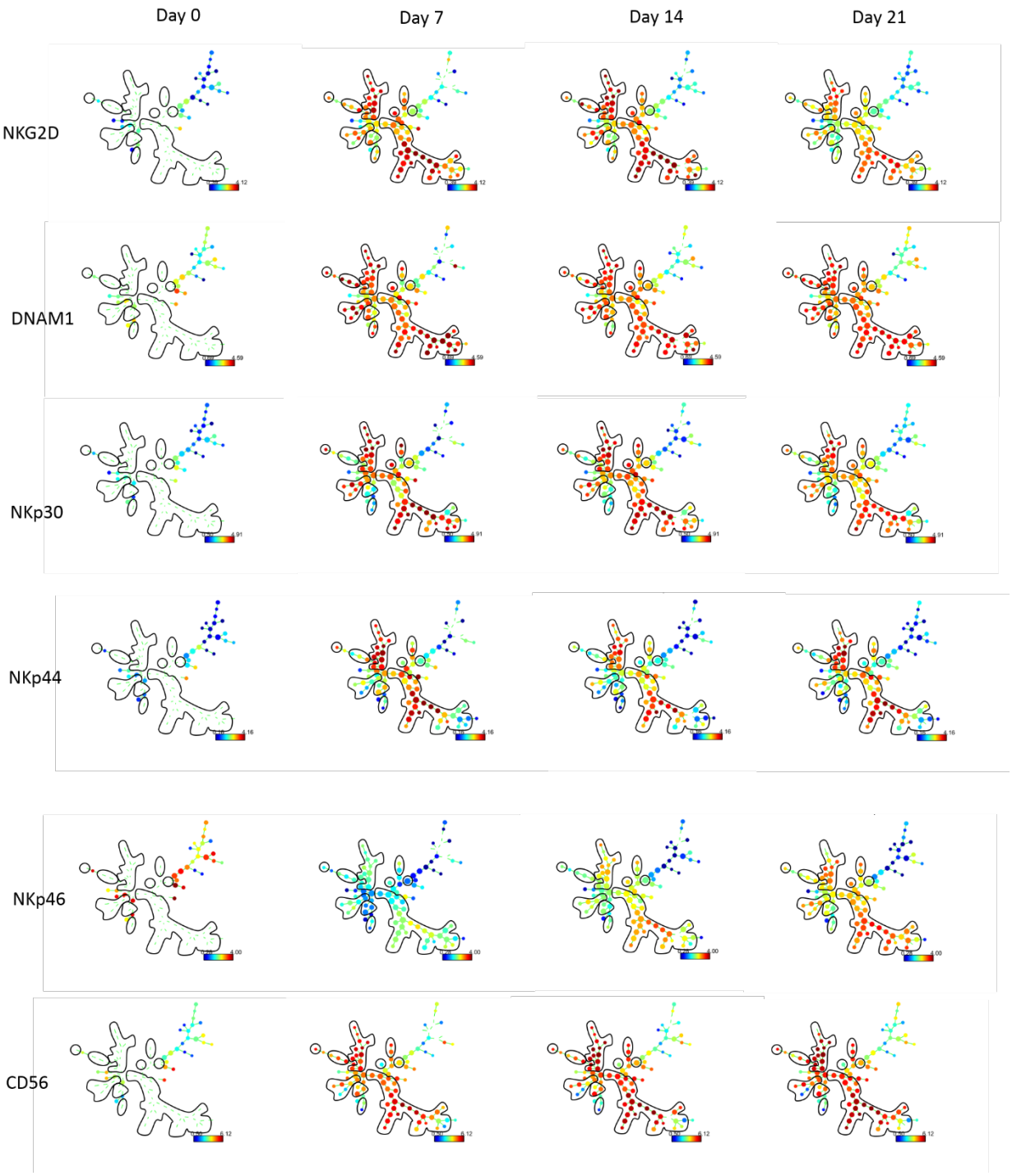

Figure 8. SPADE Clustering Identifies Unique Subpopulations Early in the Expansion Process

Figure 8. SPADE clustering Identifies Unique Subpopulations Early in the Expansion Process. NK cells from 3 donors were evaluated by mass cytometry for inhibitory and activating receptor expression. SPADE was used to cluster nodes based on NK cell receptor expression. Unique clusters, present on day 7, 14 and 21 expanded NK cells but absent on primary NK cells, are highlighted by black contour. The figure shows representative results for 1 donor, but results were replicated across all donors. Blue indicates low expression, Red indicates high expression.

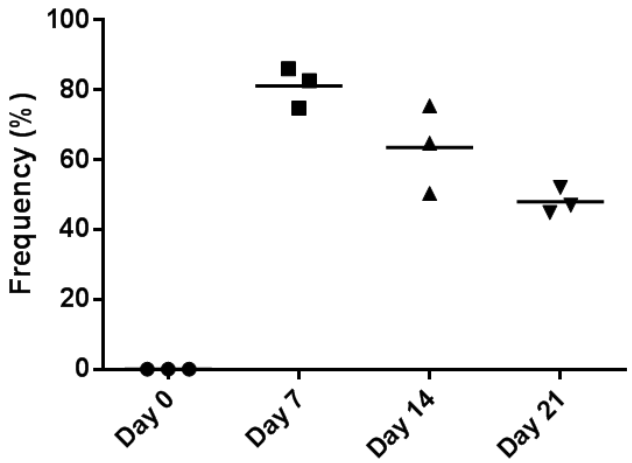

Figure 9. Quantification of Unique Subpopulations throughout Expansion

Unique subpopulations, unique to day 7, day 14 and day 21 expanded NK cells, were gated and quantified. (n=3 donors)

Unique Subpopulations Identified in Patient Infusion Products have Increased Function upon Target Cell Encounter

After identifying unique subpopulations co-expressing high levels multiple activating receptors on healthy donors we sought to determine whether they could be found on patient NK cell infusion products, and evaluated their functionality. We obtained NK cell infusion products from 6 leukemia patients enrolled in NCT01904136 trial, these consist of day 14 expanded donor NK cells prepared at the Good Manufacturing Practices (GMP) facility at MD Anderson Cancer Center for adoptive NK cell therapy (Refer to table 3). Data derived from patient infusion samples was obtained as a collaboration with Jolie Schafer from MD Anderson Cancer Center. To test the functionality of NK cells in the infusion product, we co-cultured them with 721.221 targets, a classical NK cell target devoid of MHC. Samples were then stained for the presence activating and inhibitory receptors, CD107a to evaluate for degranulation, and intracellular IFNγ levels.

First, we were able to identify on the patient infusion products the unique subpopulations previously described (Figure 10). These are highlighted by the black contours and were identified by the co-expression of high levels of multiple activating receptors including NKp44, NKp30, DNAM-1 and NKG2D. Upon quantification these unique subpopulations constituted an average of 29.3% of the patient NK cell infusion product (Figure 11). In order to evaluate their functionality we gated for these unique subpopulations on all 6 patient infusion products and evaluated their degranulation (CD107a) and also their cytokine production (IFNγ) compared to ungated cells and the

whole product. As observed in Figure 12A, the highest levels of CD107a and IFNγ expression within the infusion product are observed within these unique subpopulations (n=6 pooled samples). We quantified CD107a and IFNγ levels on the whole product, the gated unique subpopulations and ungated cells (Figure 12B, gating strategy). We observed that the %CD107a+ cells was significantly higher in the unique subpopulations when compared to the whole product or the ungated cells (p=0.0032, p=0.0010 respectively) (Figure 12C). Similarly, after quantifying the percent of IFNγ+ cells in the unique subpopulations versus the whole product or ungated cells we observed that the %IFNγ+ cells was significantly higher in the highlighted unique subpopulations (p=0.0015, p=0.0017 respectively) (Figure 10C). Similar results were observed in terms of mean expression with significantly higher levels of CD107a and IFNγ in the unique supopulations when compared to the whole product and ungated cells (Figure 12C). When we looked for the cell populations that were CD107a+/IFNγ+ we observed that double positive cells were significantly more frequent in the unique subpopulations, when compared to the whole product and the ungated cells (p=0.0020, p=0.0015 respectively)(Figure 12C).

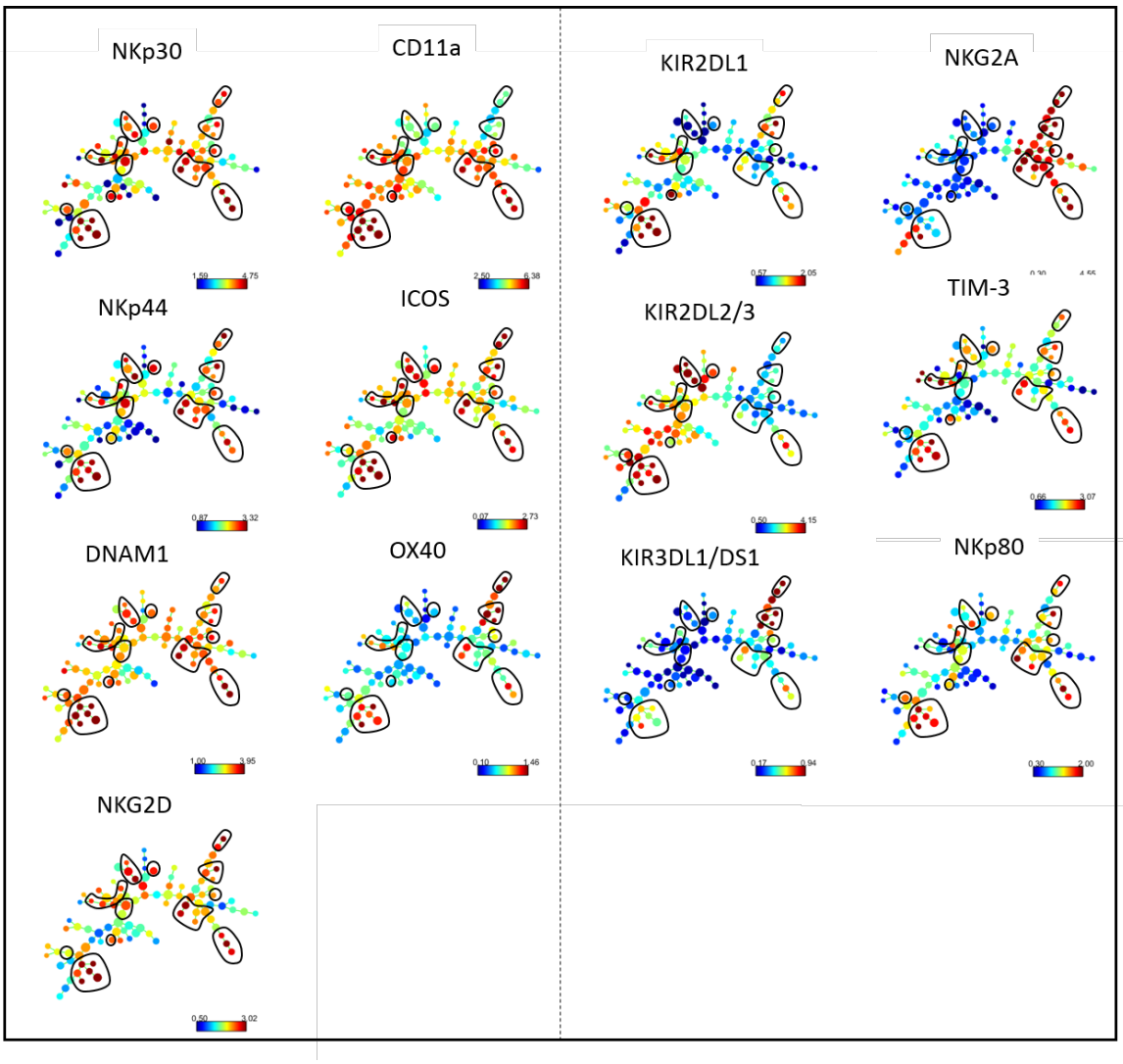

Figure 10. SPADE Clustering Identifies Unique Subpopulations Co-Expressing High Levels of Activating Receptors on Patient NK cell Infusion Products

Day 14 expanded NK cells were obtained from 6 patient infusion products and stained for NK cell receptor expression by mass cytometry. Clusters were generated using SPADE software, figure represents all 6 donors pooled together in a single SPADE three. Blue indicates low expression, Red indicates high expression. (Data derived from patient samples obtained as a collaboration with Jolie Schafer from MD Anderson Cancer Center, used with permission)

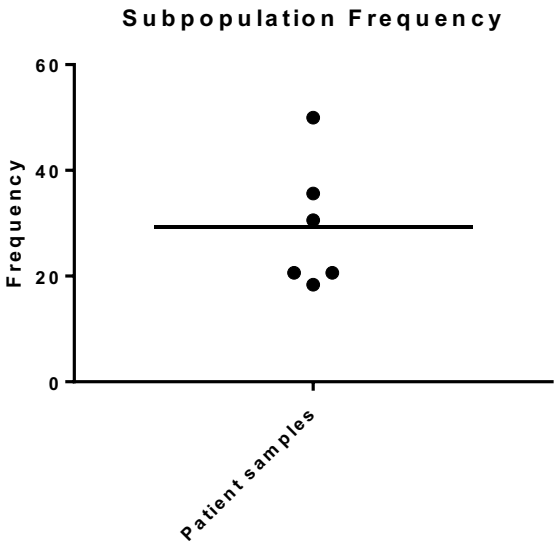

Figure 11. Quantification of Unique Subpopulations on Patient NK cell Infusion Products

Subpopulations co-expressing high levels of activating receptors DNAM-1, NKG2D, NKp30 and NKp44, were gated and quantified for patient NK cell infusion products. (n=6)

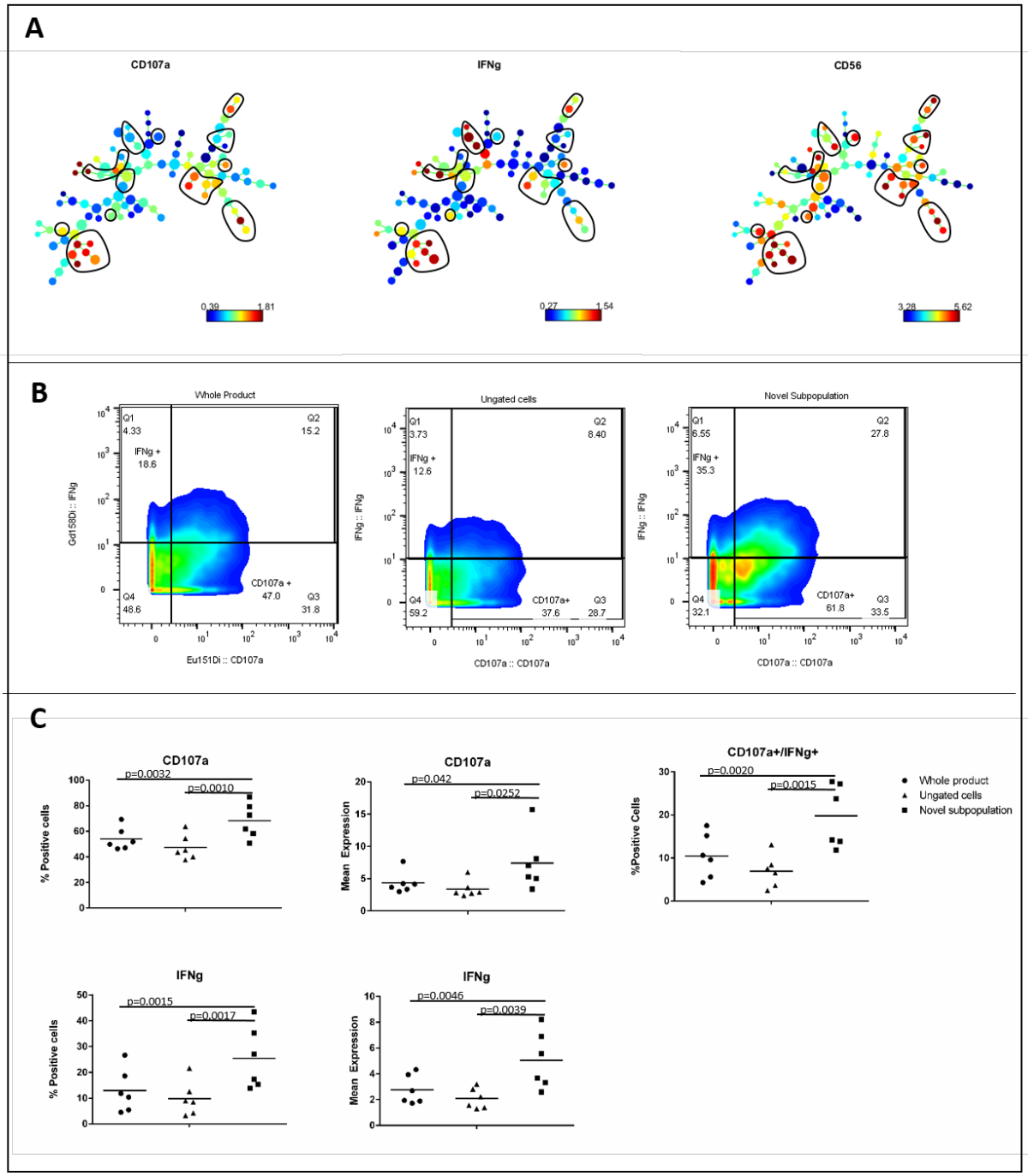

Figure 12. Subpopulations Co-expressing High Levels of Activating Receptors have Increased Functional Marker Expression upon Target Cell Encounter

Figure 12. Subpopulations Co-Expressing High Levels of Activating Receptors have Increased Functional Marker Expression upon Target Cell Encounter. Patient NK cell infusion products (Day 14 expanded) were co-cultured with 721.221 target cells. Subpopulations highlighted by black contour correspond to unique subpopulations co-expressing high levels of activating receptors NKp44, NKp30, NKG2D and DNAM1. (A) Levels of degranulation (CD107a) and cytokine secretion (IFNγ) after co-culture with target cells were evaluated for the gated unique subpopulations, ungated cells and the whole product. SPADE clusters represent all 6 donors pooled together. Blue indicates low expression, Red indicates high expression. (B) Gating strategy used to quantify functional markers. One representative donor. (C) Quantification of CD107a and IFNγ on unique subpopulations in comparison to whole product and ungated cells (n=6). Mean expression represents Mean Mass Intensity. Paired t-test, $p<0.05$ significant. (Data derived from patient samples obtained as a collaboration with Jolie Schafer from MD Anderson Cancer Center, used with permission)

Subsets with Enhanced Function are comprised within CD56^{bright} Populations

Our previous data revealed that unique subpopulations co-expressing high levels of activating receptors could be identified on patient NK cell infusion products. Moreover, we could demonstrate that these population of cells have increased function; however, selection based on co-expression of multiple activating receptors would be a complex process for clinical translation. Interestingly, our SPADE threes reveal that CD56^{bright} cells clustered together with the unique subpopulations with enhanced function (Figures 8,12), therefore we sought to determine whether gating based on CD56 expression could distinguish subpopulations with enhanced function upon target cell encounter, independent of their expression of other activating receptors. Our results show that CD56^{bright} cells constitute 70% of the IL-21 expanded cells (day 14) (n=6) (Figure 13A). We proceeded to evaluate the function of this subpopulation (Figure 13B). In terms of the degranulation marker (CD107a), we observed that CD107a+ positive cells were significantly more abundant within the CD56^{bright} subset, when compared to the CD56^{dim} cells (59% vs 42%, p=0.0014). Mean mass intensity (MMI) indicates that CD107a expression levels are significantly higher for CD56^{bright} cells (1.8 fold) when compared to CD56^{dim} cells (4.97 vs 2.71, p=0.0103). When IFNγ secretion was evaluated, IFNγ+ cells were also more abundant within the CD56^{bright} cells than on CD56^{dim} cells (16% vs 6%, p=0.0042). MMI reveals significantly higher IFNγ expression for CD56^{bright} cells (2.2 fold) when compared to CD56^{dim} cells (3.4 vs 1.5, p=0.0009). Since CD56^{bright} cells were more functional than their CD56^{dim} counterparts, we evaluated them for the surface expression of activating receptors (Figure 13C). Expression of NKp30 was significantly higher for CD56^{bright} cells (3 fold) when compared to CD56^{dim} cells (106.7 vs 35.4, p=0.0002).

Similarly, NKp44 was significantly higher for $CD56^{bright}$ cells (5.3 fold) when compared to $CD56^{dim}$ cells (27.3 vs 5.11, p=0.0002). Expression of the activating receptor DNAM-1 was significantly higher for $CD56^{bright}$ cells (2.2 fold) when compared to $CD56^{dim}$ cells (59 vs 26.9, p=0.0001). Finally, the activating receptor NKG2D was significantly higher for $CD56^{bright}$ cells (1.9 fold) when compared to $CD56^{dim}$ cells (22.13 vs 11.74, p=0.0009). In addition, given that NK cells mediate anti-tumor responses through ADCC, we evaluated for the presence of the CD16 (FcγR) receptor which is essential for this function. Our results reveal that the $CD56^{bright}$ cells have significantly higher levels of CD16 (4 fold) when compared to $CD56^{dim}$ cells (32.6 vs 7.9, p=0.012) (Figure 13C).

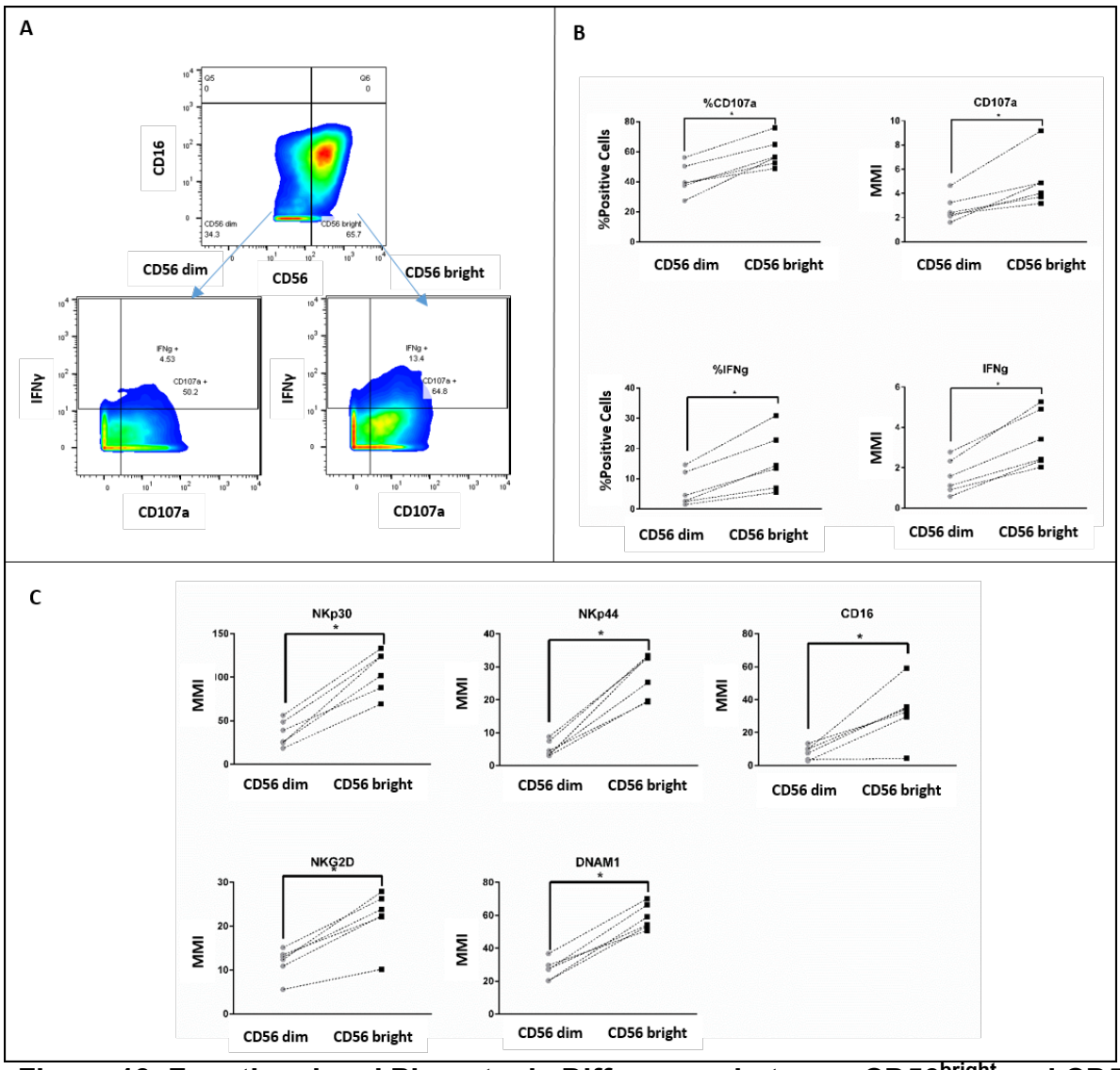

Figure 13. Functional and Phenotypic Differences between CD56^{bright} and CD56 ^{dim} Populations on Patient NK Infusion Products

Patient NK cell infusion products were co-cultured with 721.221 target cells. (A) Gating strategy for CD56^{bright} and CD56 ^{dim} populations. (B) CD56^{bright} and CD56 ^{dim} populations were evaluated for levels of degranulation (CD107a) and cytokine secretion (IFNγ). (C) Quantification of activating receptor expression (n=6). MMI, Mean Mass Intensity. Paired t-test, $p<0.05$ significant. (Patient samples obtained as a collaboration with Jolie Schafer from MD Anderson Cancer Center, used with permission)

Discussion

Tumor cells corresponding to 6 pediatric cancer types were evaluated for their expression of NK cell ligands. Although currently most adoptive NK cell therapy trials are focused on leukemia, after evaluating NK-ligand expression in multiple tumor types we observed that, compared to leukemia cells, many of the solid tumor cell lines had significantly higher number of cells expressing ligands for the activating receptors DNAM-1, NKG2D, NKp30 and NKp44 activating ligands (Figures 3-4). Given that NK cell activity is based on receptor-ligand interactions, the high expression of activating ligands on these solid tumor cells including RMS, brain tumor, EWS and NB suggests that NK cells could be a promising approach to target them.

To better target these solid tumor cells we would need an infusion product enriched on NK cells expressing the receptors DNAM-1, NKG2D, NKp30 and NKp44. After comparing primary NK cells with expanded NK cells from healthy donors we observed that the activating receptors DNAM-1, NKG2D, NKp30 and NKp44 were present in more than 80% of our day 21 expanded NK cell product (Figure 5). Also our expanded NK cells have significantly higher expression of the activating receptors DNAM-1, NKG2D, NKp30 and NKp44 compared to primary NK cells (Figure 5). Interestingly, we also observed that our expanded NK cells have significantly higher levels of inhibitory receptors including KIRs and NKG2A when compared to primary cells (Figure 5).

When we looked closely to our healthy donor expansion product and compared it to primary cells, by using SPADE clustering algorithm, we observed that there were

subpopulations of NK cells present at IL-21 expanded NK cells that were absent on primary NK cells (Figure 6). These unique subpopulations constituted about 81%, 64%, and 42-48% of day 7, day 14, and 21 expanded cells, respectively (Figure 7, 9). Unique subpopulations co-expressed high levels of the activating receptors DNAM-1, NKG2D, NKp44 and NKp30, and also high levels of other molecules associated to NK cell activation including CD11a (LFA-1), OX40, ICOS and 4-1BB. Interestingly, some of these unique subpopulations also express higher levels of inhibitory receptors such as KIRs and NKG2A compared to primary NK cells (Figure 6).

We sought to determine the functionality of these unique subpopulations by exposing expanded NK cells from patient infusion products to target cells. In order to do this we evaluated day 14 expanded NK-infusion products for leukemia patients (n=6) participating at one of the MD Anderson Trials (NCT01904136). First, we could identify the unique subpopulations co-expressing high levels of DNAM-1, NKG2D, NKp44 and NKp30 on patient infusion products, and it constituted an average 29% of the infusion product (n=6) (Figures 10, 11). After identifying the subpopulations we evaluated their functionality upon encounter of target cells (721.221). Our data demonstrates that the %CD107a+ and %IFNγ+ cells was significantly higher on the unique subpopulations when compared to the rest of the infusion product (Figure 12). Similarly, the mean expression level of CD107a and IFNγ was significantly higher on the subpopulations when compared to the whole infusion product and the ungated cells (Figure 12). This indicates that IL-21 expanded cells contain unique NK cell subpopulations co-expressing multiple activating receptors, these populations are absent in primary NK cells, and more importantly they have increased function.

Isolation of these unique populations, perhaps after 1 week of expansion when they are more abundant, would presumably allow us to obtain the populations driving most of the cytotoxic effects. However, selection of NK cells based on co-expression of multiple activating receptors would be a complex process for clinical translation. Interestingly, our findings indicate that the unique hyperactive populations are comprised within the $CD56^{bright}$ component of our product (Figures 12-13). Gating for $CD56^{bright}$ cells reveals that these cells have higher expression of multiple activating receptors than their $CD56^{dim}$ counterparts. In addition, functional experiments reveal higher levels of CD107a and IFNγ for the $CD56^{bright}$ cells, when compared to the $CD56^{dim}$ counterparts, indicating they are more functional upon target encounter.

Overall these results suggest that solid tumors are a potential target for NK cell therapy. Also, we observed that the expansion process itself can optimize the NK cell product by increasing the expression of activating receptors. Finally, clustering analysis revealed unique subpopulations on IL-21 expanded NK cells that were absent in primary NK cells. More importantly these newly formed populations co-express high levels of activating receptors and have increased function when compared to the rest of NK cell product. Selection of this unique populations, which are comprised within the $CD56^{bright}$ component of our product, is a potential approach to enhance the efficiency of the infused product.

CHAPTER IV: IFNγ TREATMENT ALTERS NK CELL LIGAND EXPRESSION AND NK CELL MEDIATED LYSIS OF PEDIATRIC CANCER CELLS

This chapter is in part based upon Aquino-López A, Senyukov VV, Vlasic Z, Kleinerman ES, Lee DA: **Interferon Gamma Induces Changes in Natural Killer (NK) Cell Ligand Expression and Alters NK Cell-Mediated Lysis of Pediatric Cancer Cell Lines**. *Frontiers in immunology* 2017, 8:391.

Rationale

Previous data from our laboratory has shown that, compared to primary NK cells, IL-21 expanded NK cells secrete 20X more IFNγ (111 vs. 2,493 pg/mL, respectively). The literature reports opposing effects of IFNγ on tumor sensitivity to NK cell mediated lysis. It has been described that IFNγ causes MHC upregulation, which can result in target cell resistance to NK cell mediated lysis (53, 54). However, IFNγ has also been reported to increase tumor cell sensitivity to NK cell mediated lysis, which has been associated to upregulation of the adhesion molecule ICAM-1 (58, 59). These opposing effects reported might be due to the focused nature of the studies, where only particular tumor types are evaluated. Therefore, our aim was to determine the effect of exogenous IFNγ on NK cell mediated lysis of a panel of pediatric cancer cell lines and the mechanism involved. We determined the effect of IFNγ on the sensitivity of pediatric cancer cells to NK-mediated lysis by evaluating 6 different tumor types. We also evaluated how IFNγ affected NK-ligand expression and whether this correlated with changes in NK-mediated lysis. The effect of IFNγ treatment of tumor cells on NK:target kinetic interactions was also evaluated.

Results

IFNγ Has a Variable Impact on Tumor Cell Sensitivity to NK-mediated Lysis

Tumor cells from the PPTP *in-vitro* panel were treated with IFNγ to evaluate its effect on their sensitivity to NK cell mediated lysis. Several pediatric cancer types were assessed, including NB, RMS, EWS, brain tumor, leukemia and lymphoma. All cell lines were evaluated with 4 NK cell donors consistent across all cell lines. Our results show that 6 cell lines develop resistance to NK cell mediated lysis after IFNγ treatment, these include the EWS cell lines CHLA-9 (p=0.0037) and CHLA-10 (p=0.0292), leukemia cell lines Molt-4 (p=0.0030) and Kasumi-1 (p=0.0231), NB cell line CHLA-136 (p=0.0065) and the lymphoma cell line Ramos-RA1 (p=0.0007) (Figure 14). Although the NB cell line NB-EBc1 seems to develop resistance to NK cells after IFNγ treatment, this effect was not statistically significant (p=0.0669). For the cell lines where significance was achieved we observed a consistent effect across all 4 donors at multiple E:T ratios (Figure 15). We also observed that 2 cell lines had a significant increase in sensitivity to NK-mediated lysis after being treated with IFNγ. These are the glioblastoma cell line SJ-GBM2 (p=0.0155), and the NB cell line NB-1643 (p=0.0371) (Figure 11). In addition, we observed that the brain tumor cell line BT-12 had an increase in sensitivity to NK-mediated lysis after IFNγ treatment for 3 of 4 NK cell donors. If only these 3 donors are evaluated the increase in sensitivity is significant (p=0.0061). For cell lines were increased sensitivity was observed, the effect was also consistent across donors and at multiple E:T ratios (Figure 15). We observed no changes in sensitivity after IFNγ treatment for the remaining cell lines. If we stratify our data by tumor type, our results

show that IFNγ had no effect on sensitivity to NK-mediated lysis for any of the RMS cell lines. However, for EWS, leukemia and lymphoma cell lines the effect was variable and cell line dependent, with some cell lines showing increased resistance after IFNγ treatment, while for other cell lines IFNγ had no effect on sensitivity. For brain tumor cell lines, IFNγ treatment resulted in enhanced sensitivity to NK cells or had no effect on NK-mediated lysis. Interestingly, for NB cells the effect of IFNγ was completely variable with some cell lines showing increased resistance to NK-mediated lysis after IFNγ treatment, others showing increased sensitivity, and some showing no effect of IFNγ on their sensitivity (Figure 11). We also evaluated whether cell lines with different responses to IFNγ had significant differences in their baseline sensitivity to NK cells (Figure 16). Baseline NK-sensitivity of tumor cells was not significantly different for tumor cell lines with different responses to IFNγ ($p=0.3292$).

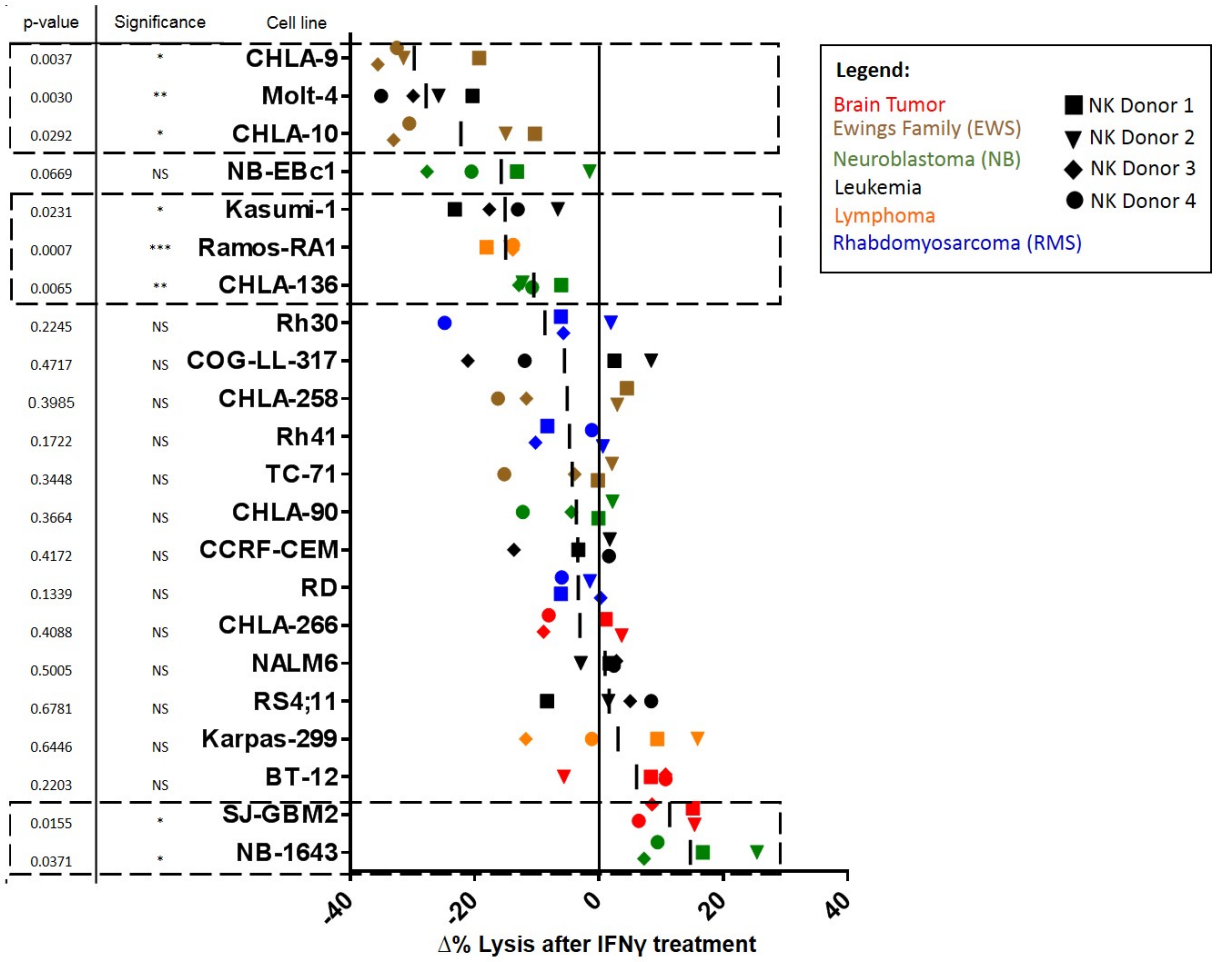

Figure 14. Waterfall plot of change in lysis by NK cells after treatment of pediatric cancer cell lines with IFNγ

NK cell cytotoxic activity towards IFNγ-treated and -untreated cancer cells was evaluated using calcein release assays. Changes in lysis (Δ% Lysis) of treated compared to untreated cancer cells were quantified for each NK cell donor. Each shape represents a different NK cell donor (the same four donors were used for all cell lines). Color coding corresponds to cell line cancer type. P-values are for probability that Δ% ≠ 0 (t-test). Squares with dashed lines indicate cancer cell lines with significant ($p \leq 0.05$) changes in NK cell mediated lysis after IFNγ treatment.

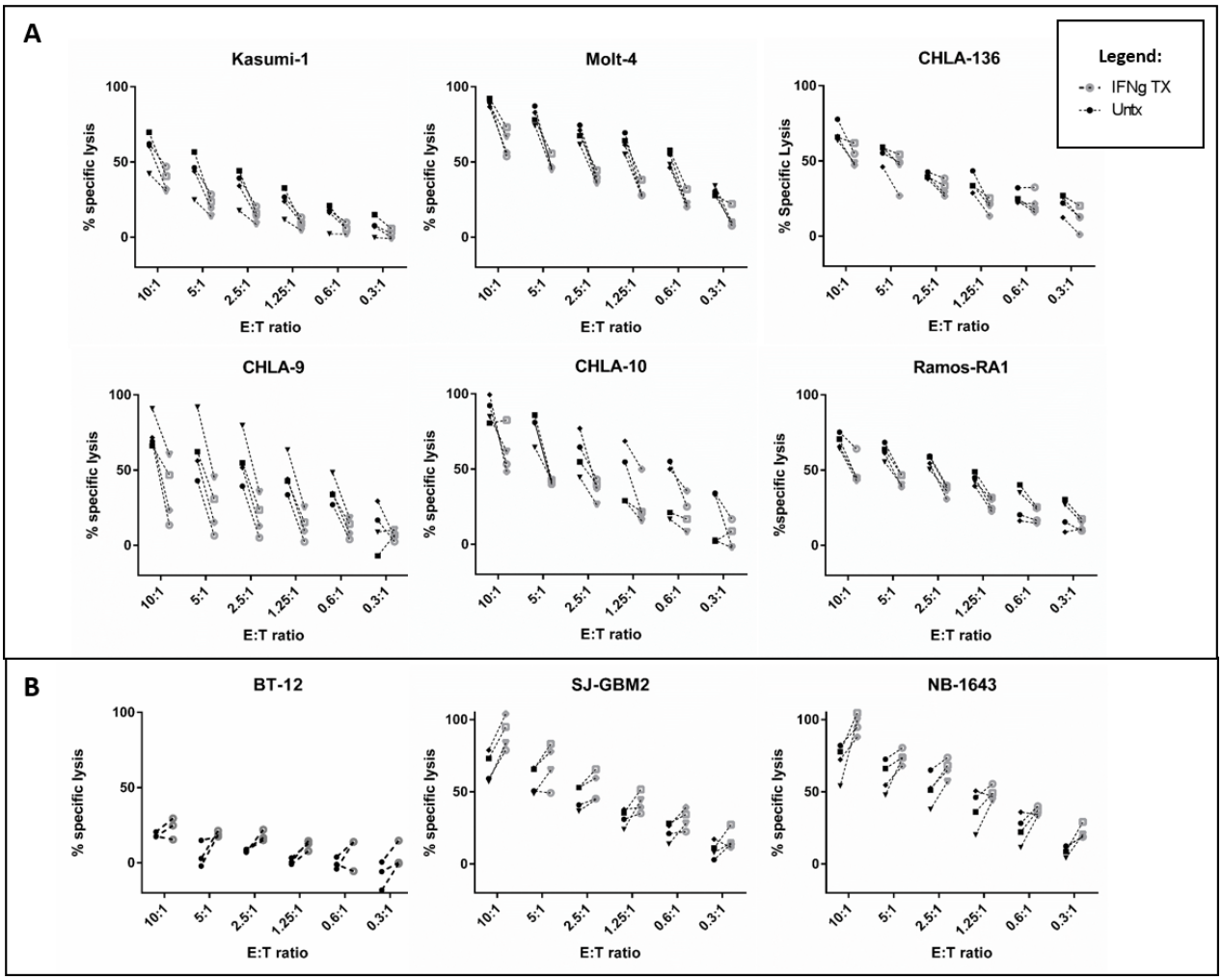

Figure 15. IFNγ has a variable impact on NK cell-mediated cancer lysis.

NK cell cytotoxic activity towards IFNγ treated (gray) and untreated (black) cancer cells was evaluated at 6 different effector to target (E:T) ratios using calcein release assays. (A) Cell lines showing decreased lysis (Leukemia (Molt-4, Kasumi-1), EWS (CHLA-9, CHLA-10), Lymphoma (Ramos-RA1), and NB (CHLA-136)) (B) Cell lines showing increased lysis (brain tumors (BT-12, SJ-GBM2) and NB (NB-1643)) after IFN γ treatment. The four NK cell donors are represented for all cell lines, except for BT-12 with 3 donors represented.

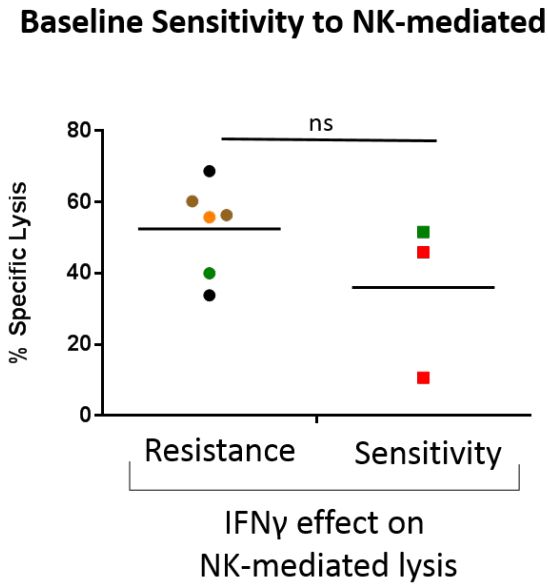

Figure 16. Baseline sensitivity of tumor cell lines classified by IFNγ effect.

Cell lines for which IFNγ had an impact on sensitivity to NK-mediated lysis were evaluated for their average baseline sensitivity at 2.5:1 E:T ratio (n=4 donors). Color coding: black-leukemia, orange- lymphoma, green-NB, red-Brain tumor. Unpaired t-test with Welch's correction, p=0.3292.

IFNγ alters surface expression of NK cell ligand expression for pediatric cancer cells

The 22 cell lines from the PPTP *in*-vitro panel were evaluated for NK-ligand expression using mass cytometry. Baseline expression levels of NK-ligands for all 22 cell lines were compared to expression levels after IFNγ treatment (Figure 17). After evaluating all cell lines for the effect of IFNγ in mean expression we observed that the ligands that were most upregulated by IFNγ were CD274/PD-L1, CD54/ICAM-1, HLA-DR, MHC-class I, CD95/FasR and CD270/HVEM (Figure 17A). We also evaluated the data in terms of median expression changes for each individual cell line after IFNγ treatment, and observed that the markers most upregulated were CD274/PD-L1, CD54/ICAM-1, HLA-DR, MHC-class I, CD95/FasR and CD270/HVEM (Figure 17B). When grouping cell lines by response to IFNγ we did not observe particular ligands being uniquely upregulated in cell lines that responded with significant changes in sensitivity after treatment (Figure 17B). However, when we stratified data by tumor type we observed that ligands such as PD-L1 were upregulated by IFNγ for cell lines corresponding to solid tumors (RMS, brain, EWS, NB), however they seemed to remain unaffected for lymphoma and leukemia cell lines (Figure 18). We also observed that IFNγ mediated ICAM-1 upregulation on brain tumor, EWS, NB and leukemia cells, however it was not observed for most RMS and lymphoma cell lines. HLA-DR upregulation by IFNγ was observed for EWS and NB cell lines. In terms of MHC-class I, IFNγ mediated upregulation was variable across different tumor types, however we observed a consistent upregulation for all NB cell lines. Fas receptor expression (CD95) was upregulated by IFNγ for leukemia, lymphoma and NB cells, but was not affected for

EWS, RMS and brain tumors. Finally, we observed that some brain tumor, EWS and NB cell lines upregulated CD270/HVEM after IFNγ treatment (Figure 18). Among all the cell lines evaluated lymphoma cells were the least responsive to IFNγ treatment in terms of ligand expression changes, however only two lymphoma cell lines were evaluated in this study.

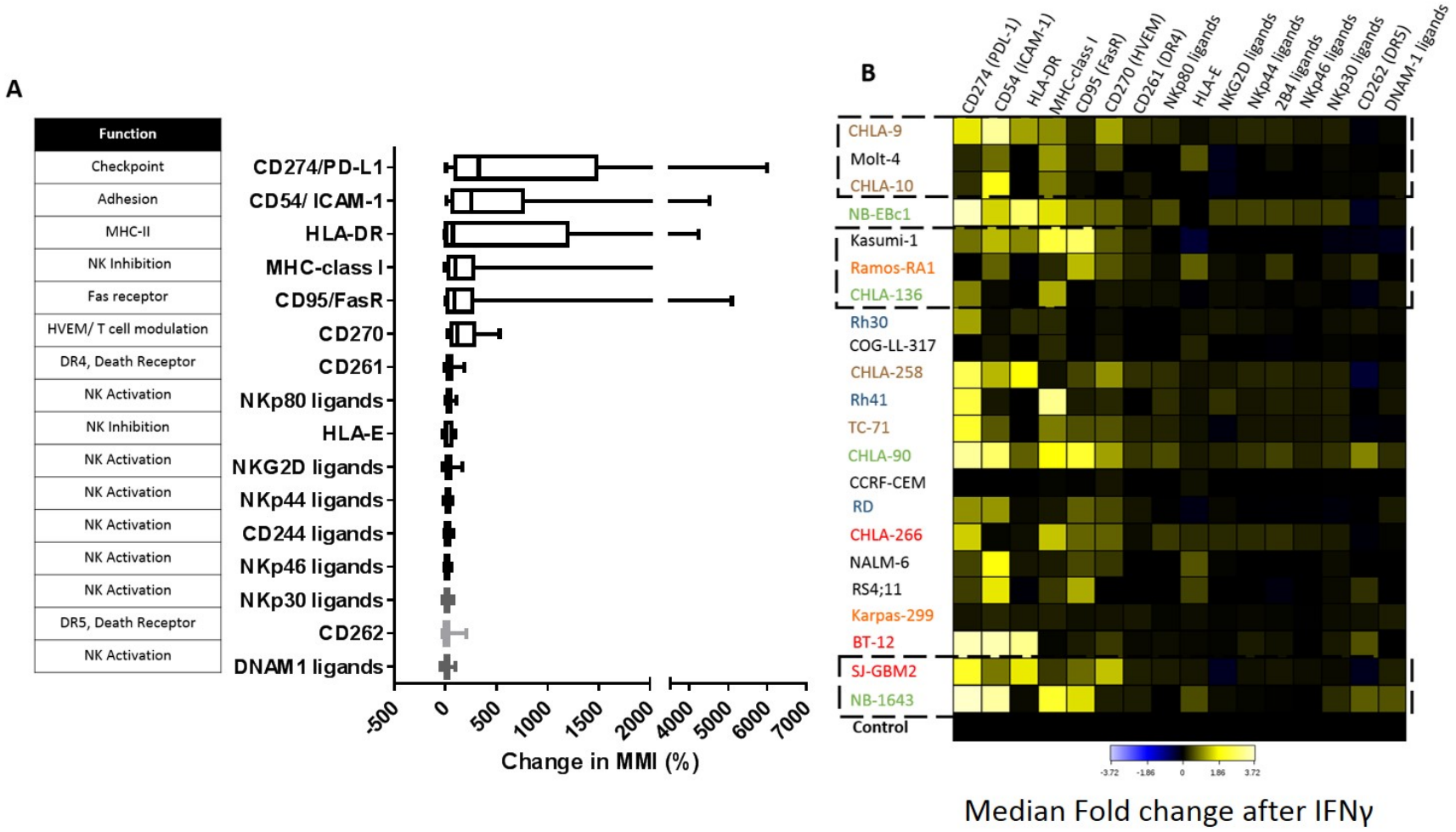

Figure 17. Impact of IFNγ treatment on the surface expression of NK cell ligands for pediatric cancer cell lines.

Figure 17. Impact of IFNγ treatment on the surface expression of NK cell ligands for pediatric cancer cell lines. (A) Change in expression level (Mean Mass Intensity (MMI)) was determined by quantifying the mean of each parameter at baseline and after IFNγ treatment for each cell line. Percent change in MMI after IFNγ treatment was calculated for each cell line and box plots were generated for each parameter using data obtained from all 22 cell lines. (B) Fold change in median expression for each parameter in all cell lines. Heat corresponds to the fold change in median expression after IFNγ treatment (obtained as the arcsinh ratio of median expression for the given markers compared to untreated cell line-Control). Cancer type color coding is the same as in Figure 1. Cell lines are arranged according to tumor response to IFNγ, squares with dashed lines indicate cell lines with significant changes in NK cell mediated lysis after IFNγ treatment

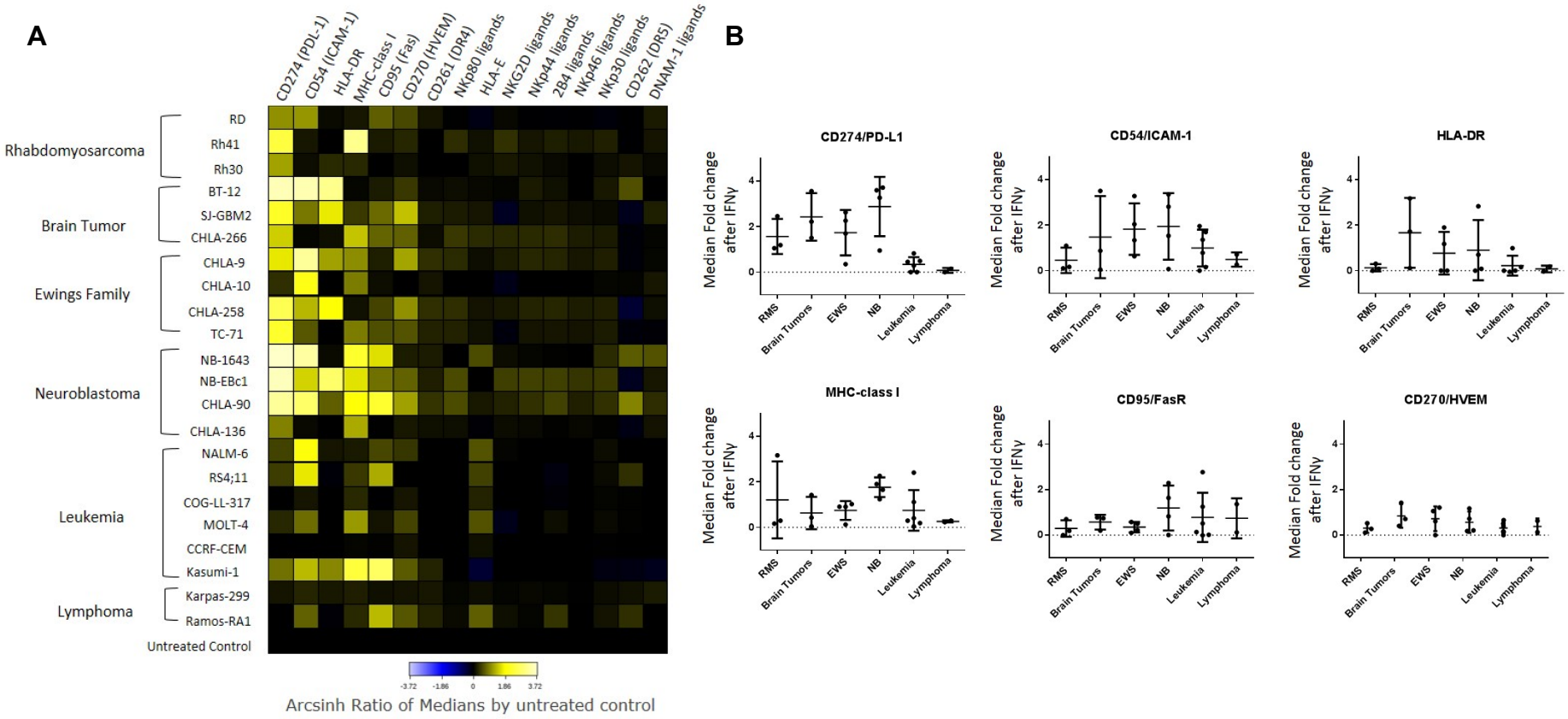

Figure 18. Major ligands affected by IFNγ classified by tumor type.

Figure 18. Major ligands affected by IFNγ classified by tumor type.

IFNγ induced changes in NK cell ligand expression were evaluated by cancer type. **A.** Heat corresponds to the fold change in median expression after IFNγ treatment (arcsinh ratio of median expression for given markers compared to untreated cell line-Control). **B.** Y-axis corresponds to the fold increase in marker median expression after IFNγ treatment, obtained by evaluating the arcsinh ratio of median expression for the given marker compared to untreated cell line.

IFNγ induced changes in ICAM-1 and MHC-class I correlate with changes in NK sensitivity

After evaluating the effect of IFNγ on tumor cell sensitivity to NK-mediated lysis and NK-ligand expression, we wanted to determine whether there were any correlations between changes in ligand expression and changes in NK-mediated tumor lysis. To do that, we first evaluated the expanded NK cells from our donors for the expression of receptors corresponding to PD-L1, ICAM-1 and MHC-class I, the ligands most upregulated by IFNγ (Figure 19). Our results showed that PD-1, the receptor for PD-L1 was expressed on 7% of the expanded NK cell product (n=4) (Figure 19). This suggests that changes in PD-L1 expression by IFNγ are unlikely to play a role in our model. In contrast the ICAM-1 binding integrin, LFA-1, was expressed in >99% of our expanded NK cells. In terms of KIR receptor expression in the expanded NK cell product we observed that 83.9% of the cells were KIR2DL2/3^{+}, 97.18% KIR2DL1/2DS5^{+}, and 89.15% KIR3DL1^{+}. In addition, the inhibitory receptor NKG2A was present in 97% of the expanded NK cells.

Since most of the expanded NK cells expressed receptors for MHC-class I (KIRs and NKG2A) and ICAM-1 (LFA-1) we decided to focus on the effect of IFNγ on these ligands and whether they correlated with changes in sensitivity to NK-mediated lysis (Figure 20). As stated above, MHC-class I upregulation is associated to NK-inhibition, while ICAM-1 upregulation is associated to adhesion, which is important for NK cell function. We quantified MHC-class I and ICAM-1 upregulation after IFNγ treatment for

the cell lines with altered sensitivity (Figure 20 A,B). The ratio of MHC-class I change over the change in ICAM-1 was also evaluated (Figure 20C).

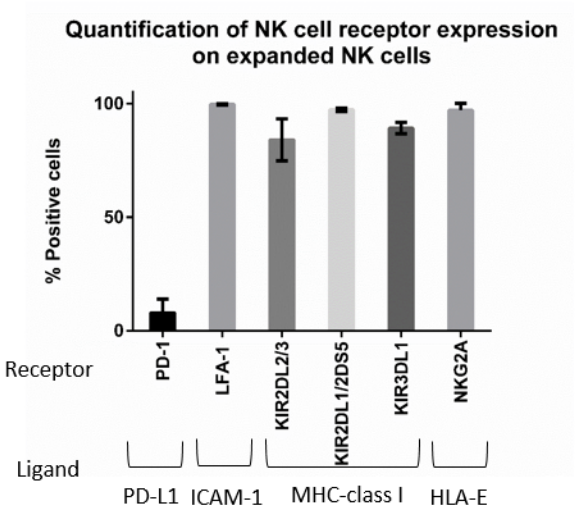

Figure 19. Phenotyping of expanded NK cells

Expression of PD-1, LFA-1, KIRs and NKG2A on the expanded NK cells was obtained by mass cytometry (n=4 donors).

For all the cell lines that became more resistant after IFNγ treatment we observed an increase in MHC-class I expression, which correlates with the increased resistance (Figure, 20A). However, for some of the cell lines with increased sensitivity after IFNγ treatment we also observed MHC-class I upregulation (Figure 20B). Interestingly, for the cell lines with increased sensitivity after IFNγ treatment MHC class-I/ICAM-1 change ratio was <1, indicating that upregulation of ICAM-1 exceeded MHC-class I upregulation (Figure 20B, 20C). Conversely, for 3 of the 6 cell lines where IFNγ induced resistance (Kasumi-1, MOLT-4 and CHLA-136) the MHC class-I/ICAM-1 change ratio was >1, which indicates that MHC-class I upregulation exceeded ICAM-1 upregulation (Figure 20A,

20C). Interestingly, ICAM-1 upregulation exceeded MHC-class I upregulation (ratio <1) for 3 of the cell lines in which IFNγ treatment resulted in decreased NK cell mediated lysis (EWS CHLA-9 and CHLA-10 and lymphoma cell line Ramos-RA1).

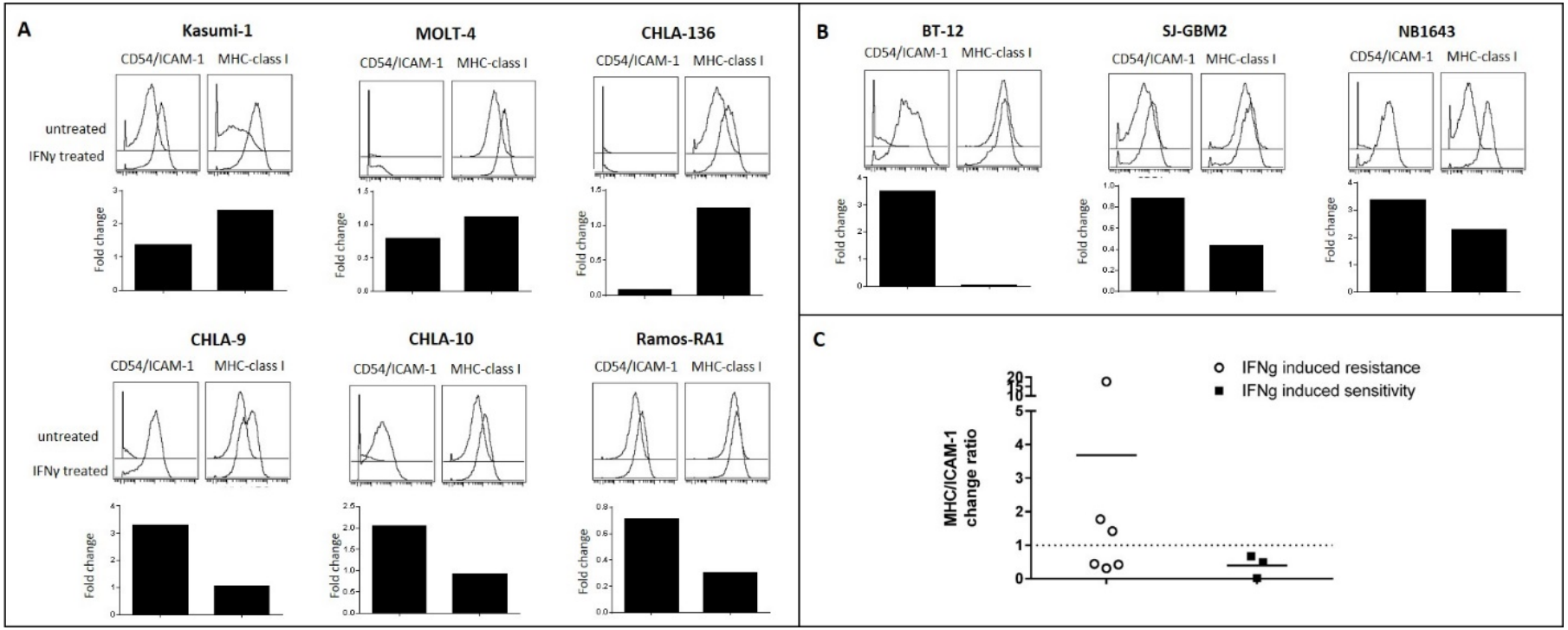

Figure 20. Effect of IFNγ treatment on ICAM-1 and MHC-class I expression for cancer cell lines with altered sensitivity.

Figure 20. Effect of IFNγ treatment on ICAM-1 and MHC-class I expression for cancer cell lines with altered sensitivity. The effect of IFNγ on ICAM-1 and MHC-class I expression for cell lines in which IFNγ treatment conferred (A) resistance or (B) sensitivity to NK cell mediated lysis. Histograms compare ICAM-1 (left) and MHC class I (right) expression for untreated cancer cells (top) and IFN γ treated cells (bottom). Bar graphs represent ICAM-1and MHC class I fold change in median expression after IFNγ treatment. (C) Ratio of MHC-class I/ ICAM-1 change after IFNγ treatment for cell lines with altered sensitivity**.** Fold change in median expression after IFNγ treatment for each parameter was quantified and the ratio was calculated. Ratio <1 indicates higher ICAM-1 upregulation, ratio >1 indicates higher MHC-class I upregulation after IFNγ treatment.

IFNγ induced ICAM-1 upregulation increases conjugate formation for cell lines with increased sensitivity

The effect of IFNγ on MHC-class I expression has been already associated to target cell resistance to NK-mediated lysis (53, 54), therefore we wanted to investigate possible mechanisms for the enhanced sensitivity observed after IFNγ treatment for the cell lines SJ-GBM2, NB1643 and BT-12. These cell lines presented with increased sensitivity to NK-mediated lysis after IFNγ treatment, despite presence of high levels of MHC-class I (Figure 15B, 20B). For these tumors upregulation of the adhesion molecule ICAM-1 exceeded MHC-class I upregulation, therefore we decided to determine whether IFNγ-mediated ICAM-1 upregulation correlated to increased NK function through increased NK:target conjugate formation (Figure 21). We also evaluated NK conjugates with Ramos-RA1, a cell line with ICAM-1 upregulation exceeding MHC-class I upregulation (ratio <1) for which IFNγ resulted in resistance. We observed IFNγ treatment resulted in a significant increase in conjugate formation for BT-12 ($p= 0.026$) and SJ-GBM2 ($p=0.011$) (Fig 21B). For the cell line NB-1643 although we were not able to show statistical significance we saw a trend towards increased conjugate formation ($p=0.069$). In contrast, IFNγ treatment did not increase conjugate formation for Ramos-RA1. Next, to determine whether the increased conjugate formation after IFNγ treatment was ICAM-1 mediated we blocked ICAM-1 on IFNγ treated cells (BT-12, SJ-GBM2 and NB1643). ICAM-1 blockade on IFNγ treated tumor cells, with anti-ICAM-1 antibody, resulted in a significant decrease in NK:target conjugate formation compared to isotype control antibody [BT-12 ($p=0.042$), SJ-GBM2 ($p=0.008$) and NB1643 ($p=0.041$)] (Figure 21C).

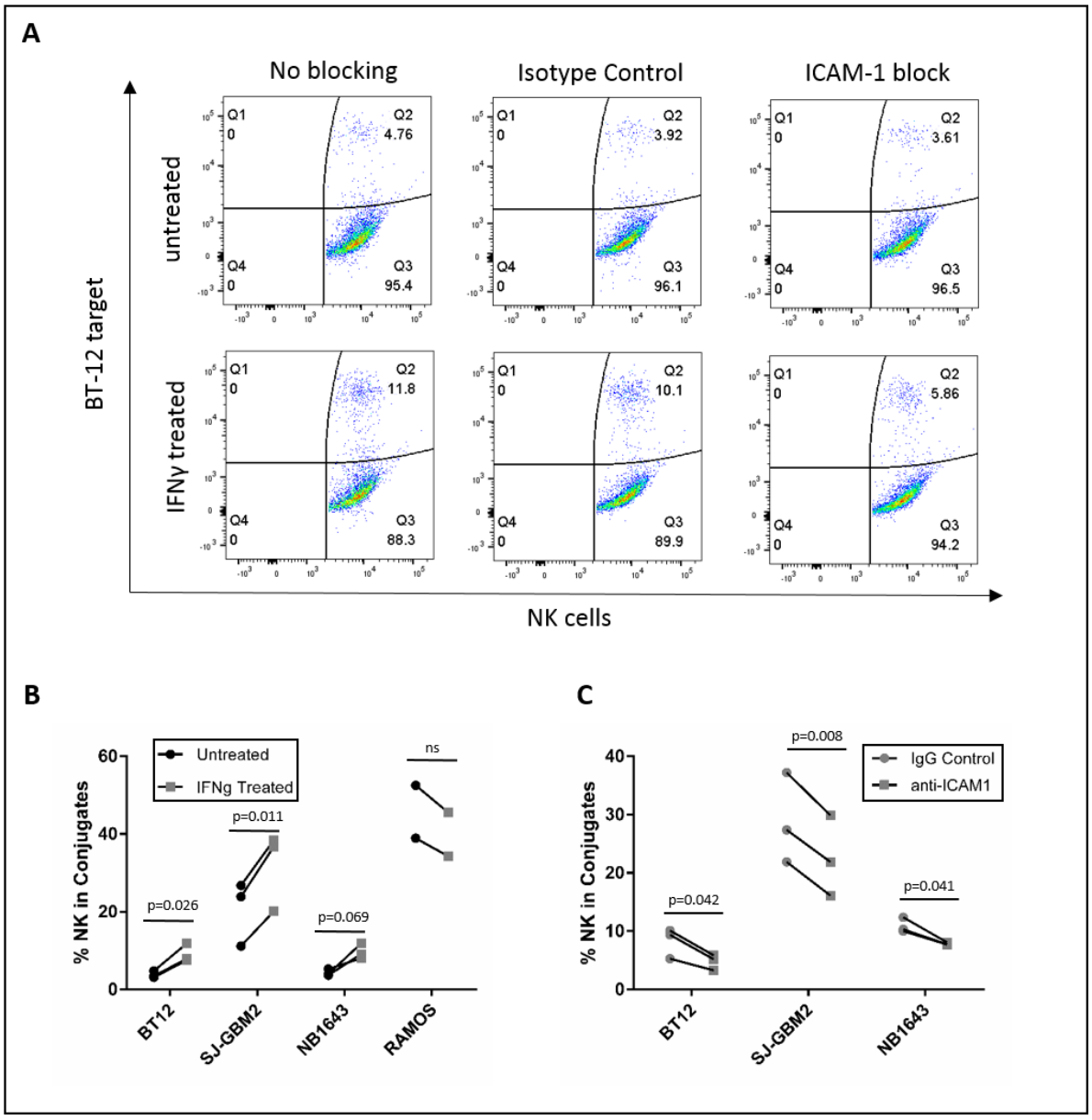

Figure 21. Conjugation Assay for Cell Lines with Increased Sensitivity after IFNγ treatment

(A) *y*-axis represents fluorescence of labeled target cells, *x*-axis represents fluorescence of labeled NK cells, and Q2 indicates dual fluorescence of NK cells conjugated with target cells. (B) Quantification of % NK cells in conjugate with BT-12, SJ-GBM2, NB1643 and Ramos-RA1. (C) Quantification of %NK cells in conjugate after ICAM-1 block for IFNγ treated BT-12, SJ-GBM2 and NB1643. (n=3 donors, Student's *t*-test).

Blocking of ICAM-1 weakens IFNγ induced increase in sensitivity for particular cell lines and donors

Using NK cells from 4 anonymous donors we showed that the cell lines BT-12, SJ-GBM2 and NB-1643 had increased sensitivity after IFNγ treatment. This also correlated with higher conjugate formation mediated by ICAM-1. Therefore, we sought to determine the effect of ICAM-1 blocking on the NK-mediated lysis of IFNγ treated cells. Blocking of ICAM-1 on the IFNγ treated tumor cells resulted in a significant decrease of the NK-mediated lysis for brain tumor cells (BT-12) ($p=0.0146$) (Figure 22). Similarly, blocking of ICAM-1 on the IFNγ treated NB-1643 tumor cells resulted in a significant decrease of the NK-mediated lysis ($p=0.0120$) (Figure 22). However, these results represent experimental replicates using a single anonymous NK cell donor, for whom HLA and KIR typing information is unavailable.

Pediatric tumor cell lines were previously evaluated in our laboratory to determine their HLA expression (Table 8, unpublished). Knowing tumor HLA expression, we typed donors and selected them based on the expression of licensed KIRs (KIR2DL3, KIR3DL1) corresponding to the tumor MHC molecules. This ensures KIR-MHC interactions occur and play a role on the balance. These three selected donors were used for subsequent functional experiments.

Table 8. HLA Typing for Selected Tumor Cells

Cell line	HLA-C1 Binds KIR2DL2/3	HLA-C2 Binds KIR2DL1	HLA-BW4 Binds KIR3DL1
BT-12	X		X
SJ-GBM2	X		X
NB-1643	X	X	X

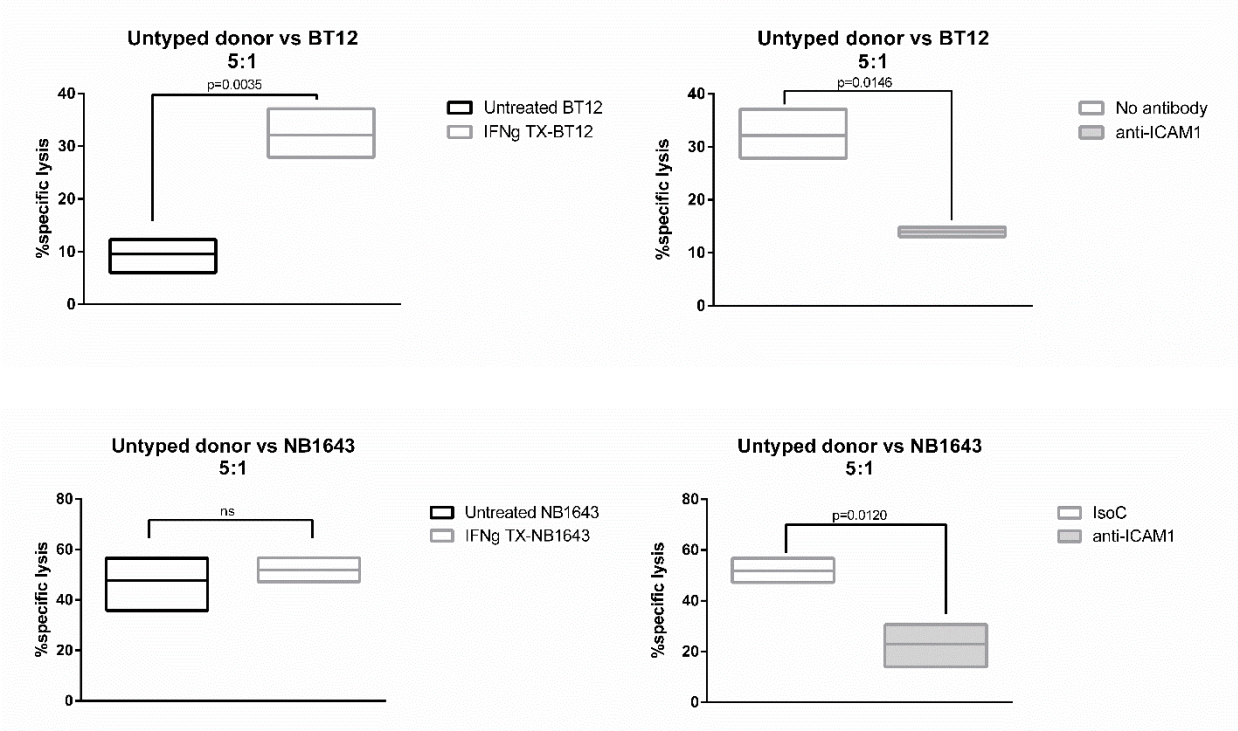

Figure 22. The Effect of ICAM-1 blockade on NK cell mediated lysis for IFNγ treated cell lines BT-12 and NB-1643.

(Left panel) Evaluation of NK-mediated lysis for untreated and IFNγ treated cell lines with one representative anonymous NK donor. (Right panel) Evaluation of the effect of ICAM-1 blockade in NK-mediated lysis for IFNγ treated tumor cells.

Results for functional experiments using the three selected donors show an increased NK-mediated lysis after IFNγ treatment for the brain tumor cell line BT-12. Although these results are not statistically significant, the trend goes accordingly with our previous results for at least 2 of the donors (Figures 23-24). Similarly, blocking ICAM-1 on IFNγ treated BT-12 cells resulted in decreased NK-mediated lysis, for 2 of the three donors (Figures 23, 24). We also evaluated the glioblastoma cell line, SJ-GBM2 with the three selected donors, interestingly we were unable to see increased sensitivity after IFNγ treatment, but a slight decrease in sensitivity (not significant) (Figure 23). Blocking of ICAM-1 did not affect NK-mediated lysis for IFNγ treated glioblastoma cells (Figure 23). Finally, when the NB cell line (NB-1643) was evaluated with these three selected NK cell donors, IFNγ treatment caused a slight, but significant increase in NK-mediated lysis ($p=0.03$) (Figure 23). However, blocking of ICAM-1 caused a decrease in NK-mediated lysis for only one of the three donors (Figures 23, 25).

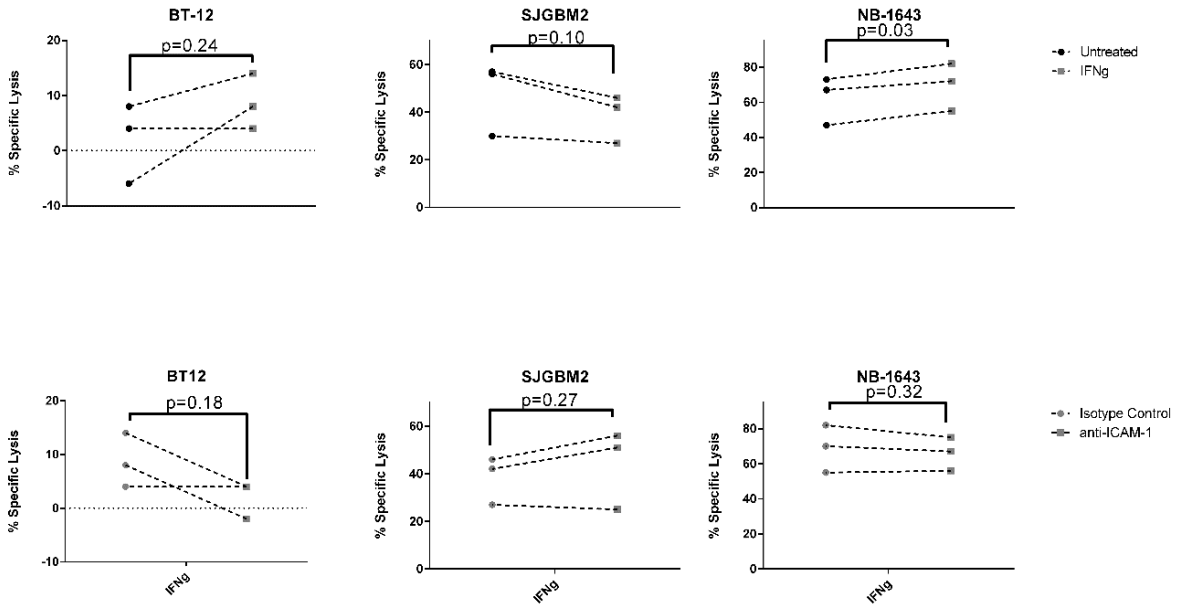

Figure 23. The Effect of ICAM-1 blockade on NK cell mediated lysis for IFNγ treated cell lines BT-12, NB-1643 and SJ-GBM2.

NK cell donors known to express licensed KIRs for the MHC molecules expressed by the tumor cells were used for these experiments (n=3). Top Panel. Calcein release assays at 5:1 E:T ratio were used to evaluate the effect of IFNγ on NK-mediated tumor lysis. Bottom Panel. For IFNγ treated tumor cells, anti-ICAM-1 antibodies were used to block ICAM-1, non-specific IgG1 antibodies were used as isotype control. Each graph depicts the results for 3 NK cell donors. Paired t-test ($p<0.05$, significant).

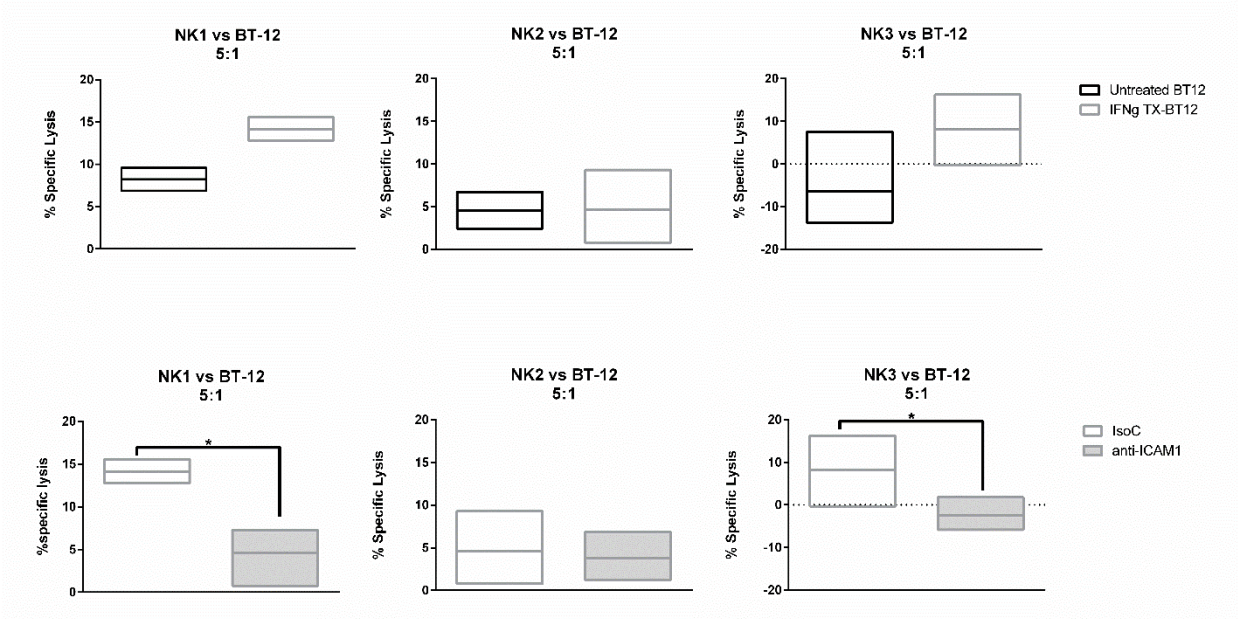

Figure 24. The Effect of ICAM-1 blockade on NK cell mediated lysis for IFNγ treated cell line BT-12

NK cell donors known to express licensed KIRs for the MHC molecules expressed by the tumor cells were used for these experiments. Top Panel. Calcein release assays at 5:1 E:T ratio were used to evaluate the effect of IFNγ on NK-mediated tumor lysis. Bottom Panel. For IFNγ treated tumor cells, anti-ICAM-1 antibodies were used to block ICAM-1, non-specific IgG1 antibodies were used as isotype control. Each graph depicts experimental replicates of a single NK cell donor. Unpaired t-test with Welch's correction ($p<0.05$, significant).

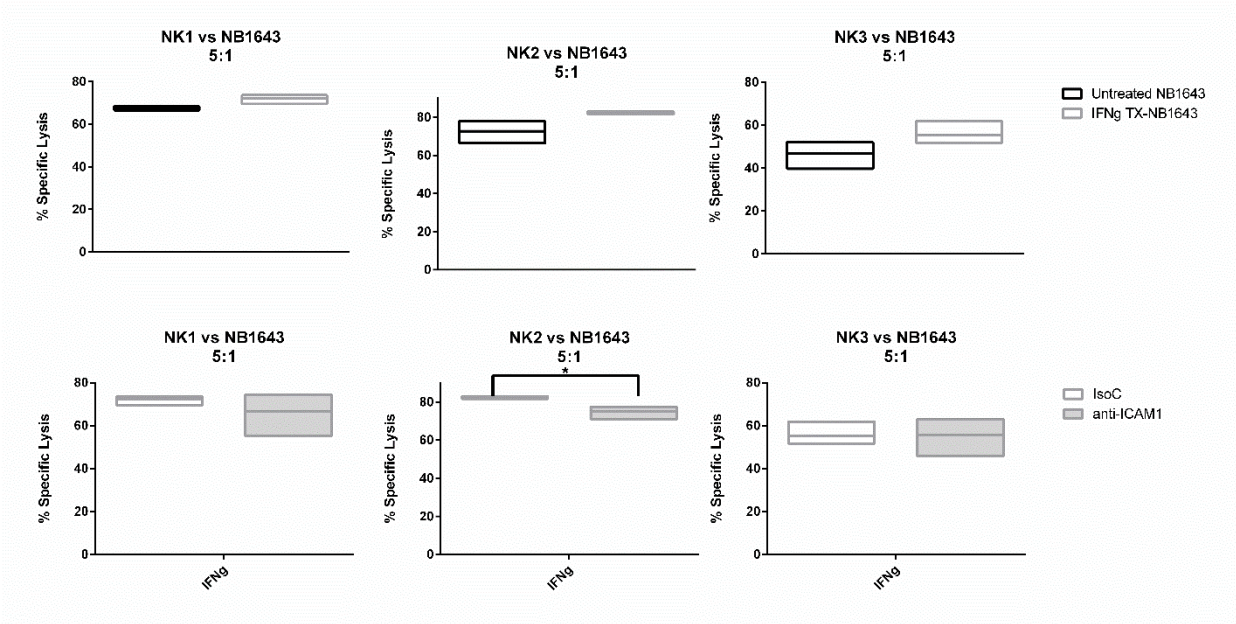

Figure 25. The Effect of ICAM-1 blockade on NK cell mediated lysis for IFNγ treated cell line NB-1643.

NK cell donors known to express licensed KIRs for the MHC molecules expressed by the tumor cells were used for these experiments. **Top Panel.** Calcein release assays at 5:1 E:T ratio were used to evaluate the effect of IFNγ on NK-mediated tumor lysis. **Bottom Panel.** For IFNγ treated tumor cells, anti-ICAM-1 antibodies were used to block ICAM-1, non-specific IgG1 antibodies were used as isotype control. Each graph depicts experimental replicates of a single NK cell donor. Unpaired t-test with Welch's correction ($p<0.05$, significant).

IFNγ treatment of Neuroblastoma cells Reduces the Time Required for NK cell Contact

To better understand how IFNγ treatment alters the kinetic interactions between NK cells and tumor cells we performed Timelapse imaging in nanowell grids (TIMING) experiments in collaboration with Gabrielle Romain and the Varadarajan Lab at University of Houston. NK cells were co-cultured in nanowells with NB-1643 tumor cells at 1:1 E:T ratio. Subsequently NK:tumor interactions in the nanowells were imaged every 6 minutes for 6 hours. Imaging allowed for quantification of the absolute time for the first NK:target contact (t_{seek}) and also the time from contact to death (t_{death}) (Figure 26). Annexin V staining was used to evaluate for tumor cell death. When we evaluated time from contact to death we observed that treatment of NB-1643 cells with IFNγ did not have an impact on t_{death} (Figure 27B). As we can observe in Figure 20B, by 2 hours after NK:target contact, 55-60% of the tumor cells were dead for both, IFNγ treated and untreated target cells (Figure 27B). However, after evaluating t_{seek} we observed that when NB-1643 tumor cells were treated with IFNγ, the time to elapsed until the first NK:target contact was reduced, compared to untreated tumor cells (Figure 27A). As depicted in figure 27A, it took at least 2 hours in co-culture for 71.6% of the NK cells to establish contact with the untreated NB-1643 tumor cells, but when tumor cells were treated with IFNγ, 73.7% of the NK cells had established contact with them by the first hour. We also evaluated the cumulative percentage of NK cells that had established contact with target cells over time (Figure 28A). As we can observe in Figure 28A for 50% of the NK cells to establish contact with the untreated NB-1643 cells it took 42 minutes, however, when the same tumor cells were treated with IFNγ 50% of the NK

cells had established contact with them by 12 minutes. Statistical analysis by Two Way ANOVA reveals that IFNγ treatment causes a statistically significant increase in the % of NK cells in conjugate ($p<0.0001$). We also quantified the average t_{seek} for both tumor treatment conditions and our results reveal that IFNγ treatment significantly decreases the t_{seek} of NB-1643 cells when compared to untreated tumor cells (75 min vs 47 min, respectively) ($p<0.0001$) (Figure 28B).

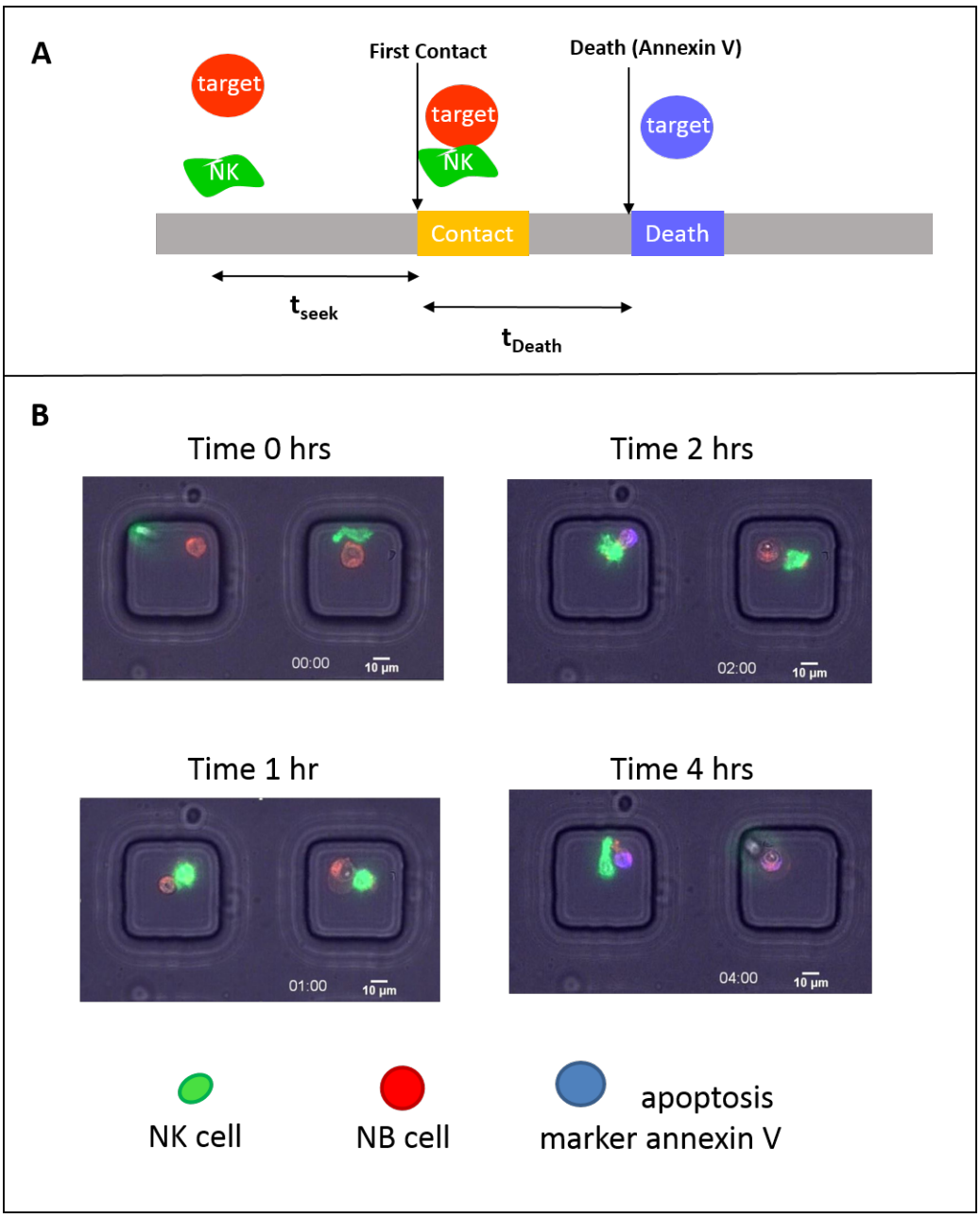

Figure 26. Timelapse Imaging: Assay Description and Representative Images.

NK cells were stained with green membrane dye and NB-1643 tumor cells were stained with red membrane dye. IFNγ treated and untreated tumor cells were evaluated for kinetic interactions with NK cells. Annexin V staining was used as an indicator of tumor cell apoptosis. (Performed in collaboration with Gabrielle Romain and Navin Varadarajan from the University of Houston)

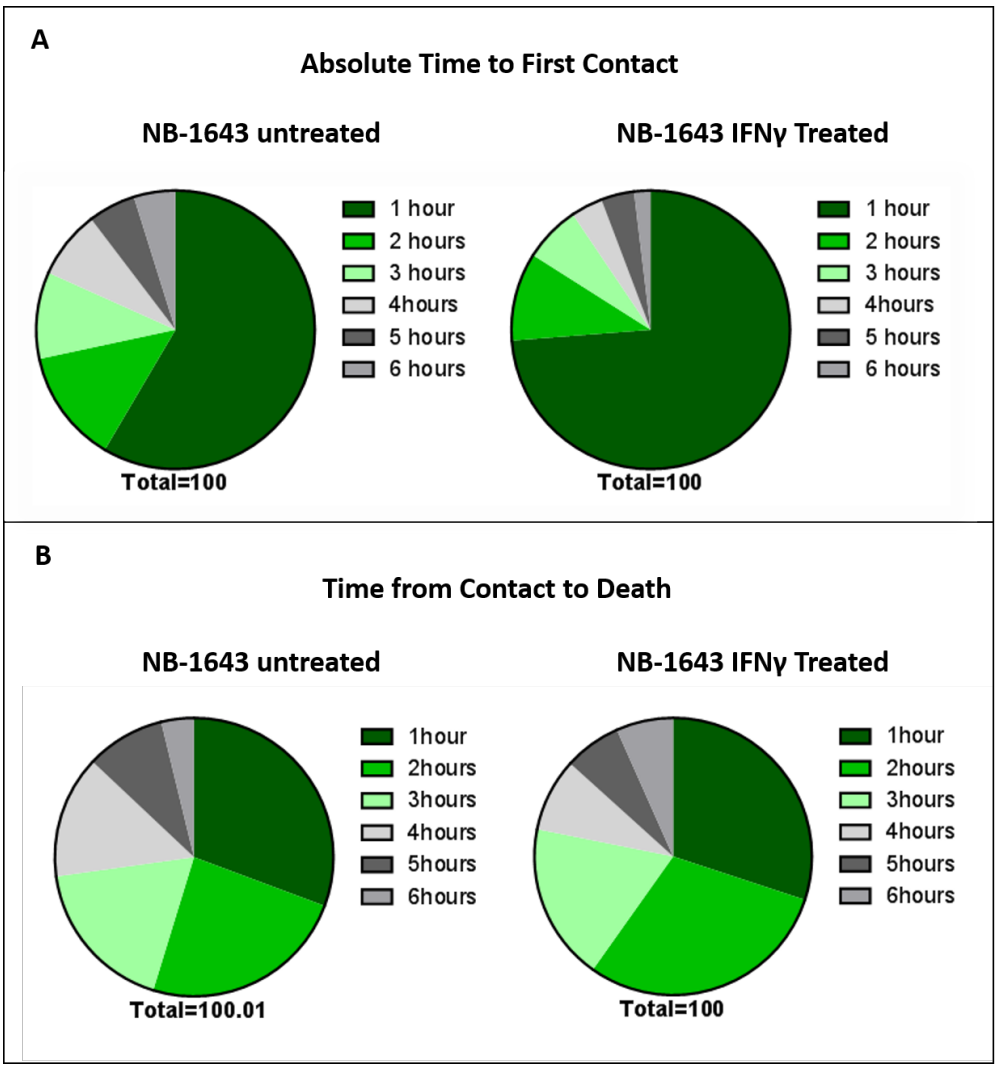

Figure 27. Timelapse quantification of t_{seek} and t_{death} for NK cells co-cultured with untreated and IFN treated NB-1643

NK cells were co-cultured with IFNγ treated or untreated NB-1643 tumor cells at 1:1 E:T ratio for 6 hours. **A.** Pie charts represent the t_{seek} (absolute time to contact) for NK cells that established contact with target cells (NK with untreated target: n=744) (NK with IFNγ treated target: n= 625). **B.** Pie charts represent the t_{death} (time from contact to death) for tumor cells after NK cell contact. (Performed in collaboration with Gabrielle Romain and Navin Varadarajan from the University of Houston)

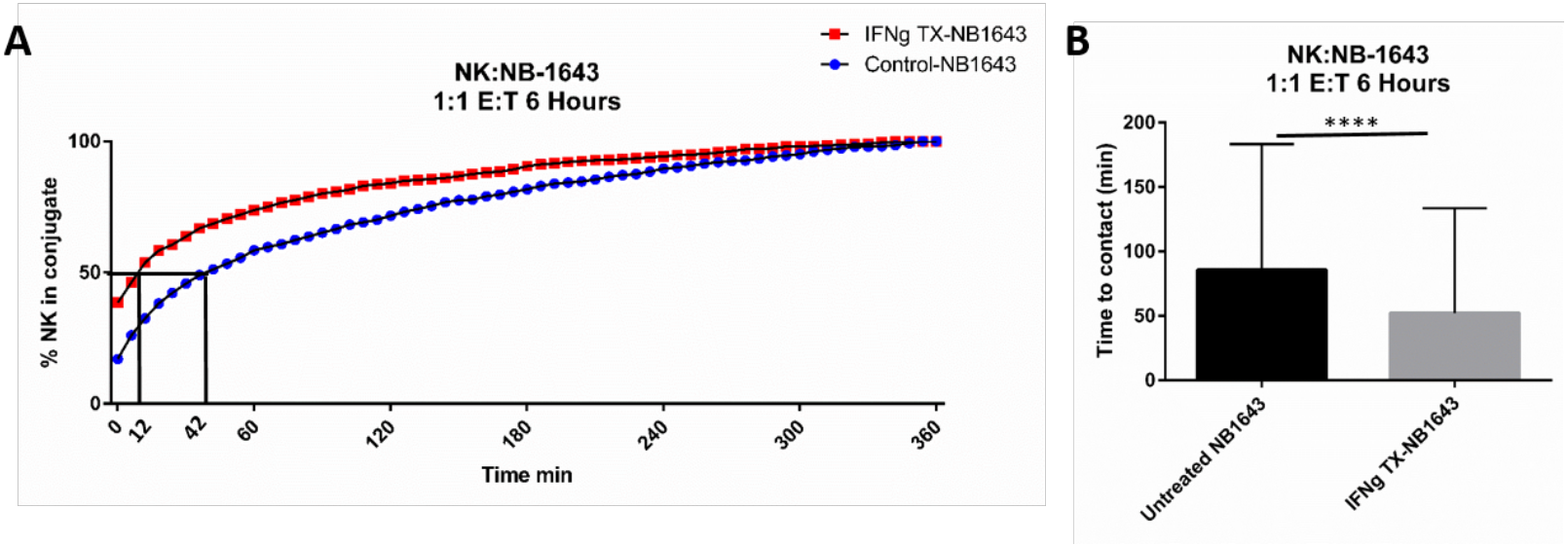

Figure 28. Timelapse imaging for dynamic quantification of NK in conjugates with NB-1643.

NK cells were co-cultured with IFNγ treated or untreated NB-1643 tumor cells at 1:1 E:T ratio for 6 hours. NK cells that established contact with target cells were gated for the analysis (NK with untreated target: n=744) (NK with IFNγ treated target: n= 625). **A.** *Y-axis* represents the cumulative percentage NK cells (at a 1:1 E:T) that had established contact with the tumor cell at particular time points. Two Way ANOVA revealed that tumor treatment condition (untreated vs IFNγ treated) alters the %NK in conjugate ($p<0.0001$). **B.** Quantification of the average t_{seek} for NK cells co-cultured with untreated and IFNγ treated NB-1643 cells. Unpaired t-test with Welch's correction reveals significance ($p<0.0001$). (Performed in collaboration with Gabrielle Romain and Navin Varadarajan from the University of Houston)

Discussion

IL-21 expanded NK cells are currently used in clinical trials to target myeloid malignancies and also brain tumors (NCT01787474, NCT01904136, NCT01823198, NCT02271711). Previous data from our laboratory has shown that these IL-21 expanded NK cells secrete 20X more IFNγ than primary NK cells (2,493 vs. 111 pg/mL, respectively) (41). In a similar manner, memory-like NK cells, which have been used as adoptive cell therapy for AML patients, have shown enhanced production of IFNγ when compared to control NK cells (49). IFNγ has been reported to have opposing effects on tumor sensitivity to NK cell mediated lysis. It can result in target cell resistance to NK cell mediated lysis through MHC upregulation (53, 54). However, other studies have shown increased tumor cell sensitivity after IFNγ treatment, which has been linked to ICAM-1 upregulation (58, 59). Opposing effects reported might be due the focused nature of the studies, were only particular tumor types are evaluated. Given that high levels of IFNγ are secreted by NK cell infusion products, and IFNγ has been reported to have opposing effects on tumor sensitivity to NK-therapy, we sought to determine the effect of IFNγ on NK cell interactions with tumor cells derived from multiple pediatric tumor types.

A broad selection of 22 pediatric tumor cell lines, including 6 different tumor types, were evaluated for the effect of IFNγ on their sensitivity to NK-mediated lysis. Sensitivity was evaluated using IL-21 expanded NK cells from 4 independent donors, consistent through all 22 cell lines. Our results demonstrate that IFNγ has a variable effect on tumor cell sensitivity to NK-mediated lysis. Six of the cell lines evaluated, including leukemia, EWS, lymphoma and NB cells, showed a significant decrease in NK-mediated lysis after

IFNγ treatment. In contrast, for 3 cell lines including NB and brain tumor cells, IFNγ treatment resulted in a significant increase in sensitivity to NK-mediated lysis. The remaining 13 cell lines did not show a statistically significant effect of IFNγ on NK-mediated lysis, although some show trends that could be significant with additional donor replicates. When evaluated by tumor type we observed that IFNγ had no impact on NK-mediated lysis of RMS cell lines. However, for EWS, leukemia and lymphoma cell lines IFNγ treatment resulted in increased resistance or no effect on sensitivity. For brain tumor cell lines, IFNγ treatment had no effect or resulted in enhanced sensitivity to NK-mediated lysis. While for NB, the IFNγ effect was completely variable, with some cell lines showing IFNγ induced increased resistance, increased sensitivity, or no effect on their sensitivity (Figure 14). These results suggest that IFNγ effect on tumor NK-mediated lysis is variable and cell line dependent.

To better understand this variability, CyTOF was used to evaluate the effect of IFNγ on tumor NK-ligand expression. First, we observed that, overall, none of the ligands evaluated were downregulated by IFNγ. In contrast, ligands such as CD274/PD-L1, CD54/ICAM-1, HLA-DR, MHC-class I, CD95/FasR and CD270/HVEM were upregulated in various cell lines corresponding to multiple tumor types. These findings are consistent with previously published studies, with the exception of CD270/HVEM (58, 59, 68-73) . Although HVEM is involved in T cell regulation (74), its role in NK cell biology has not been well described, and to our knowledge, no studies have yet reported its regulation by IFNγ.

Upregulation of MHC-class I, PD-L1 and ICAM-1 have been previously described in studies for individual tumor types, however no study had uncovered the variability of responses across different pediatric tumor types. Our results demonstrate that PD-L1 is upregulated by IFNγ on pediatric solid tumor cells (RMS, EWS, NB and brain tumors), however, no effect was observed for most of the pediatric leukemia and lymphoma cell lines. In terms of the adhesion molecule ICAM-1 we observed IFNγ mediated upregulation on leukemia, NB, EWS and brain tumors, but not for lymphoma and RMS cells. Previous studies have described IFNγ mediated upregulation of ICAM-1 on NB and leukemia cells, however, to our knowledge, no studies have demonstrated IFNγ mediated ICAM-1 upregulation on EWS cells (58, 59).

We observed upregulation of HLA-DR by IFNγ on some cell lines corresponding to EWS, NB, and brain tumor cells (Figure 15). HLA-DR, an MHC-class II molecule, is important for antigen recognition by helper CD4 T cells as well as their stimulation (75). Given that HLA-DR upregulation can stimulate other immune cells in the tumor microenvironment, it would be interesting to investigate its impact on tumor response to NK immunotherapy as well as other immune therapies.

Our findings also demonstrate IFNγ induced upregulation of CD95, known as FasR (Fas receptor), in a small number of cell lines corresponding to NB and leukemia (Figure 15). NK cells can express Fas ligand (FasL) and its interaction with FasR can result in tumor cell apoptosis (28). The levels of FasL expression on IL-21 expanded NK cells were not evaluated for our study, but it would an interesting factor to evaluate in further studies.

While some ligands were upregulated by IFNγ in just a few cell lines, the ligands CD274/PD-L1, CD54/ICAM-1, and MHC-class I were highly upregulated by IFNγ across multiple tumor types, therefore we wanted to determine whether changes in tumor lysis after IFNγ treatment could be correlated to changes in their expression. The PD-1/PD-L1 axis is associated to immune cell suppression, therefore we evaluated if PD-L1 upregulation by IFNγ played a role at our system. After evaluating for PD-1 expression on our expanded NK cells we observed that it was expressed only on 7% of the NK cells. In addition, changes in PD-L1 expression did not correlate with our changes in sensitivity, cell lines such as BT-12, SJ-GBM2 and NB-1643 which became more sensitive, had among the highest levels of PD-L1 upregulation by IFNγ (Figure 17B). Therefore, our data suggests that PD-L1 upregulation was not playing a role in our model.

LFA-1, KIRs and NKG2A were expressed in >90% of our IL-21 expanded NK cells, therefore we decided to focus on IFNγ mediated changes on their ligands, ICAM-1 and MHC-class I. For all the cell lines with increased sensitivity after IFNγ treatment, we observed that ICAM-1 upregulation exceeded MHC-class I upregulation (MHC class-I/ICAM-1 change <1). This suggests that, even in the presence of high levels of MHC-class I, IFNγ treatment can result in an increase in NK-mediated lysis, possibly due to ICAM-1/LFA-1 interaction. For three of the six cell lines that had increased resistance after IFNγ treatment we observed upregulation of MHC-class I exceeding ICAM-1 upregulation (MHC class-I/ICAM-1 change >1). These results suggest a shift of the NK cell activity balance towards inhibition due to increased expression of MHC-class I, which binds inhibitory receptors. However, there are three cell lines were IFNγ induced resistance despite ICAM-1 upregulation exceeding MHC-class I upregulation (ratio<1).

For these cell lines our model would have predicted increased sensitivity after IFNγ treatment. These results suggest that although MHC-class I and ICAM-1 changes can explain some of the changes in tumor sensitivity to NK-mediated lysis after IFNγ treatment, there must be other factors playing a role.

Brain tumor cell lines (SJ-GBM2, BT-12) and a NB cell line (NB-1643) showed increased sensitivity to NK-mediated lysis after IFNγ treatment even in the presence of MHC-class I upregulation. For these cells we observed ICAM-1 upregulation exceeding MHC-class I upregulation (MHC class-I/ICAM-1 change <1) after IFNγ treatment, therefore we wanted to determine whether the increased sensitivity could be correlated to increased NK:target conjugate formation mediated by ICAM-1 upregulation. After evaluating conjugate formation for SJ-GBM2, BT-12 and NB1643 we observed an increase in the %NK cells in conjugate with IFNγ treated tumor cells when compared to untreated cells (Figure 21). Blocking of ICAM-1 on the IFNγ treated tumor cells resulted in a decrease on the % NK cells in conjugate. Based on these results we can correlate the increased sensitivity observed after IFNγ treatment for these cell lines, with an increased effector-target conjugation mediated by ICAM-1 upregulation.

Since we observed an increase in ICAM-1 mediated conjugate formation after IFNγ treatment for these three cell lines, we evaluated whether blocking ICAM-1 decreased tumor lysis after IFNγ treatment. Initial experiments were performed with single anonymous donors and revealed that blocking of ICAM-1 significantly decreased NK-mediated lysis of IFNγ treated tumor cells (BT-12, NB-1643) (Figure 22). However, these experiments were performed with anonymous NK donors, and to ensure KIR-HLA

interactions played a role in the balance, HLA and KIR typed donors were necessary. For the subsequent functional experiments NK cell donors were selected for their expression of inhibitory KIR receptors corresponding to the tumor HLA. For the brain tumor cell line BT-12, our results show an increase in NK-mediated lysis after IFNγ treatment for two of the three donors. This increase in lysis was weakened by the presence of ICAM-1 blocking antibodies for two donors, indicating that at least for these 2 donors, ICAM-1 mediated increase in conjugate formation is in part responsible for the increase in sensitivity observed. For the NB cell line NB-1643, we observed a significant increase in NK-mediated lysis after IFNγ treatment, however, blocking of ICAM-1 resulted in a significant decrease in NK-mediated lysis for only one of the three donors, indicating that for this donor, ICAM-1 mediated increase in conjugate formation is in part responsible for the increase in sensitivity observed. Our results for the glioblastoma cell line SJ-GBM2 were surprising, we observed decrease in NK-mediated lysis after IFNγ treatment with our three selected NK donors, and blocking of ICAM-1 did not affect NK-mediated tumor lysis. Although the results indicate ICAM-1 upregulation plays a role in the increased sensitivity after IFNγ, the results are variable between donors. Donor variabilities such as cytomegalovirus (CMV) seropositive status and KIR haplotype were not considered for donor selection, these can play a role in the donor NK cell receptor repertoire and therefore NK cell activation balance.

To better understand the kinetic interactions between NK cells and IFNγ treated tumor cells we performed timelapse imaging experiments in collaboration with the Varadarajan lab at the University of Houston. Our results indicate that the t_{death} was not affected by IFNγ treatment of the tumor cells (Figure 27B). However, the t_{seek} is

significantly decreased for IFNγ treated tumor cells when compared to untreated tumor cells (Figure 27A, 28). These results go accordingly with our conjugation data which showed that IFNγ treatment of NB-1643 cells resulted in increased %NK cells in conjugate after 30 minutes in co-culture. These results suggest that differences in NK interactions with untreated and IFNγ treated tumor cells occur early, within the first 2 hours in co-culture.

Overall our data demonstrates that IFNγ has a variable impact on tumor sensitivity to NK-mediated lysis. The effect of IFNγ can be correlated to changes in NK-ligand expression. We have identified MHC-class I and ICAM-1 as some of the key molecules altered by IFNγ, whose changes can be correlated to changes in tumor sensitivity, however they cannot explain all of the effects observed. Our data also suggest that tumor exposure to IFNγ can facilitate ICAM-1 upregulation and enhance NK cell conjugate formation with brain tumor cells and NB cells, which correlates with enhanced NK cell activity.

As mentioned above, published literature has already linked IFNγ treatment with tumor resistance to NK cell mediated lysis, mediated MHC-class I upregulation (53, 54). In addition, other studies link IFNγ treatment to increased sensitivity of target cells to NK-mediated lysis, mediated by ICAM-1 upregulation (58, 59). The contradictory results from these studies are possibly due to the analysis of a small number of targets, and the focus on particular tumor types. This is, to our knowledge the first study to evaluate the effect of IFNγ on NK-mediated lysis and NK-cell ligand expression for a variety of at least six pediatric tumor types. Given that IL-21 expanded NK cells, which are used in clinical

trials, secrete large amounts of IFNγ (41), the information obtained through this study will be valuable to optimize adoptive NK cell immunotherapy as an alternative treatment for pediatric cancers.

CHAPTER V: DYNAMIC NK-TUMOR INTERACTIONS ALTER NK-LIGAND EXPRESSION ON SURROUNDING TUMOR CELLS

Rationale

Given that IL-21 expanded NK cells, currently used in multiple clinical trials, secrete 20X more IFNγ than primary NK cells, we evaluated the effect of IFNγ on NK:tumor interactions, tumor expression of NK-ligands and tumor sensitivity to NK-mediated lysis (41). In terms of NK-ligand expression, our results demonstrated that MHC-class I, ICAM-1 and PD-L1 were among the ligands most upregulated by exogenous IFNγ treatment. Although exogenous IFNγ treatment alters tumor ligand expression, whether NK cell secreted IFNγ was sufficient to induce similar changes remained unknown. Therefore, we sought to determine whether IFNγ secreted by IL-21 expanded NK cells was capable of inducing changes in ligand expression. We **hypothesize** that similar to our findings in presence of exogenous IFNγ treatment, IFNγ secreted by IL-21 expanded NK cells is capable of inducing upregulation of MHC-class I, ICAM-1 and PD-L1.

Results

NK secreted IFNγ upregulates MHC-class I, PD-L1 and ICAM-1 *in-vitro*

Using transwell plates as a tool, we co-cultured on the top chamber NK cells and tumor cells at a 2:1 E:T ratio for 48 hours, tumor cells alone were cultured on the bottom chamber. NK interactions with tumor cells on the top chamber allowed their activation and cytokine release. The small pore size allowed for passage of cytokines (i.e. IFNγ) to

the bottom chamber, allowing us to evaluate the effect of NK cell secreted cytokines on NK-ligand expression for tumor cells in the bottom chamber. By using anti-IFNγ blocking antibodies we verified whether changes in ligand expression observed were mediated by NK-secreted IFNγ (Figure 29). The three cell lines with increased sensitivity after IFNγ treatment (NB-1643, BT-12 and SJ-GBM2) were evaluated for the effect of NK cell secreted IFNγ on their ligands expression.

For the cell line BT-12, derived from an ATRT brain tumor, our results indicate that IFNγ secreted by activated NK cells mediates upregulation of MHC-class I, ICAM-1 and PD-L1 (Figure 30). The second transwell containing tumor cells only was used as our baseline expression for all ligands (Figure 29A). The presence of activated NK cell supernatant did not significantly impact the percentage of tumor cells expressing MHC-class I, but resulted in an increase in the mean expression of MHC-class I for tumor cells. For brain tumor cells (BT-12) in contact with the supernatant of activated NK cells there was a 2.2 fold increase in MHC-class I mean expression, and this effect was abrogated in the presence of α-IFNγ antibodies which decreased levels to virtually baseline levels (1.2 fold). In terms of ICAM-1 expression, the presence of NK secreted cytokines had an impact on the percentage of tumor cells expressing ICAM-1. For BT-12 tumor cells ICAM-1 expression was observed initially on 0.95% of the cells, however when tumor cells were in contact with the supernatant of activated NK cells this number increased to 15.9%. In terms of the mean expression, tumor contact with NK cell secreted cytokines caused a 2.4 fold increase in ICAM-1 expression, an effect that was abrogated in the presence of α-IFNγ antibodies (1.2 fold, 1.32%).

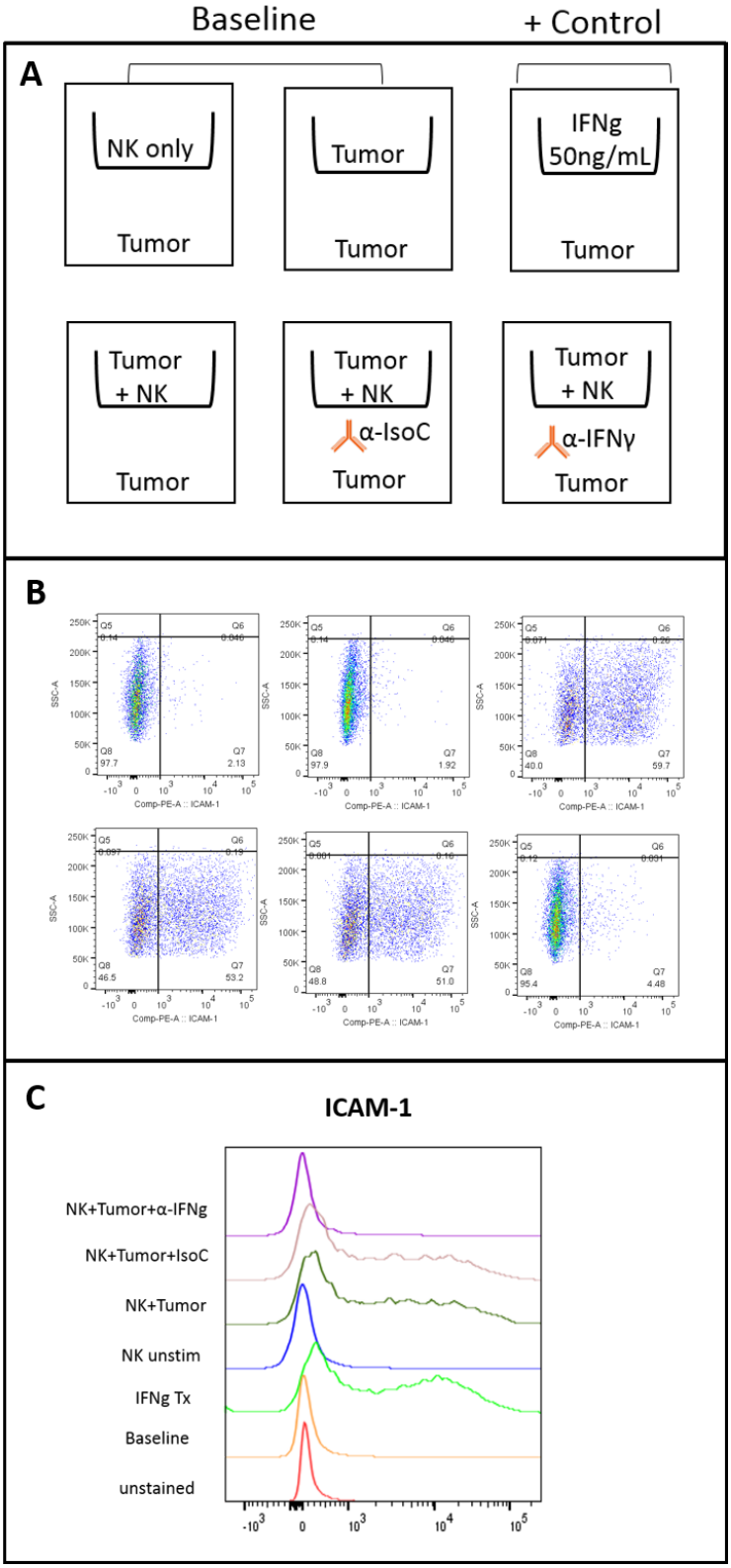

Figure 29. Cytokine Secretion Assay: Evaluation of the Effect of NK-secreted IFNγ

Figure 29. **Cytokine Secretion Assay: Evaluation of the Effect of NK-secreted IFNγ on Tumor NK-ligand Expression. A.** Transwell plate setup. NK + Tumor cells were co-cultured at the top chamber, 2:1 E:T ratio for 48 hours. Tumor cells on the bottom chamber were evaluated for the effect of IFNγ secreted by activated NK cells on their NK-ligand expression by flow cytometry. **B.** Representative Dot plots and gating strategy for ICAM-1 expression on NB-1643 tumor cells cultured under different conditions (setup as in A). **C.** Representative data for NB-1643 visualized as overlaid histograms.

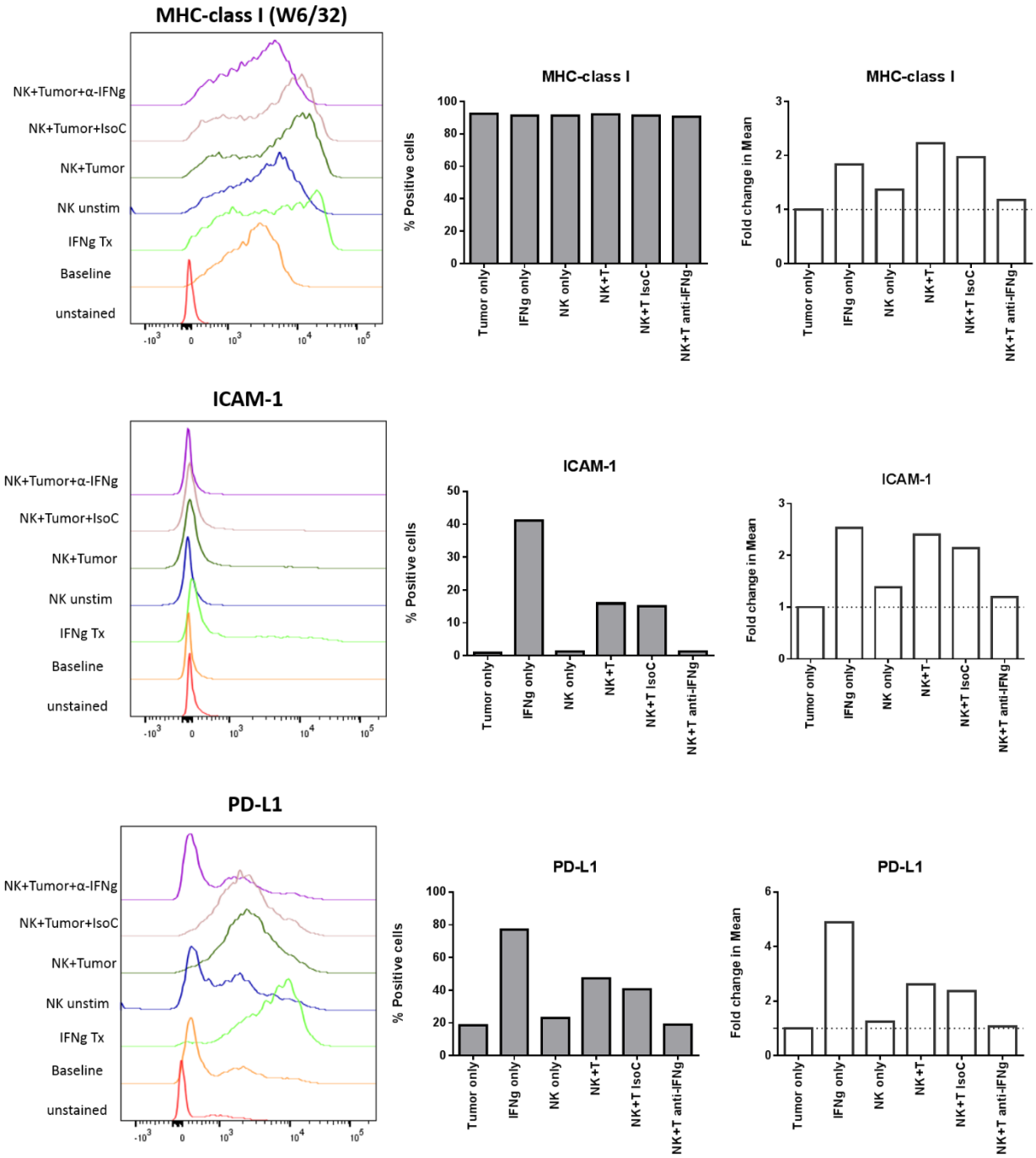

Figure 30. Effect of NK-secreted IFNγ on BT-12 NK-ligand Expression

NK cells and BT-12 tumor cells were co-cultured at 2:1 E:T ratio for 48 hours. Tumor cells in contact with activated NK cells supernatant were evaluated for ligand expression.

Finally, we evaluated the effect of NK cell secreted IFNγ on tumor PD-L1 expression, since this was another of the ligands highly upregulated by IFNγ. Our results indicate that for the BT-12 cell line, PD-L1 baseline expression was 18.7%, however in the presence of activated NK cells supernatant this number increased to 47.1%. A similar trend was observed in terms of mean expression, culturing tumor cells in the presence of activated NK cell supernatant increased PD-L1 expression by 2.6 fold. Again this effect was abrogated in the presence of α-IFNγ antibodies, which decreased PD-L1 levels to nearly baseline levels (1.1 fold, 19%) (Figure 30).

For the cell line NB-1643, a neuroblastoma, our results indicate that cytokines secreted by activated NK cells, particularly IFNγ, mediate upregulation of MHC-class I, ICAM-1 and PD-L1 (Figure 31). Similar to what we observed in the brain tumor cells, the presence of activated NK cell supernatant did not significantly impact the percentage of tumor cells expressing MHC-class I, but resulted in an increase in the mean expression of MHC-class I for NB tumor cells. For NB cells (NB-1643) in contact with the supernatant of activated NK cells there was a 2.6 fold increase in MHC-class I expression, an effect that was abrogated in the presence of α-IFNγ antibodies which decreased levels close to baseline levels (1.8 fold). In terms of ICAM-1 expression, initially ICAM-1 was expressed on 1.92% of the NB-1643 cells, however when tumor cells were in contact with the supernatant of activated NK cells this number increased to 53.2%. Tumor contact with the supernatant of activated NK cells caused a 3.5 fold increase in ICAM-1 expression, an effect that was abrogated in the presence of α-IFNγ antibodies which decreased ICAM-1 to levels close to baseline (1.8 fold, 4.48%). Finally, we evaluated the effect of NK cell secreted IFNγ on tumor PD-L1 expression, our results indicate that for

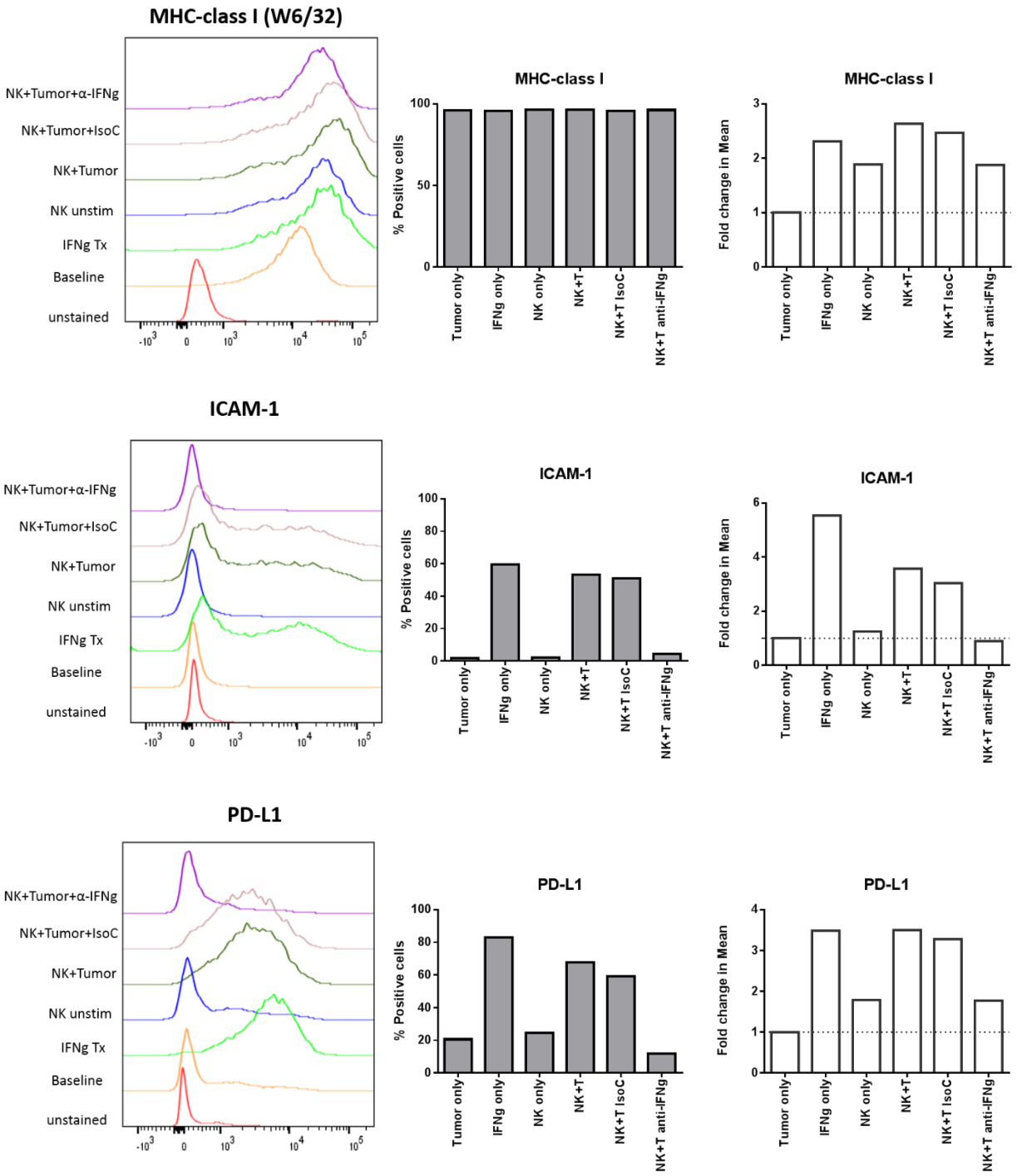

Figure 31. Effect of NK-secreted IFNγ on NB-1643 NK-ligand Expression

NK cells and NB-1643 tumor cells were co-cultured at 2:1 E:T ratio for 48 hours. Tumor cells in contact with activated NK cells supernatant were evaluated for ligand expression.

the NB-1643 cell line, PD-L1 baseline expression was 20.6%, however in the presence of activated NK cell supernatant this number increased to 67.7%. In terms of mean expression, culturing tumor cells in the presence of activated NK cell supernatant increased PD-L1 expression by 3.6 folds, an effect that was abrogated in the presence of α-IFNγ antibodies, which decreased PD-L1 levels to virtually baseline levels (0.9 fold, 12%) (Figure 31).

Finally, we evaluated the glioblastoma cell line SJ-GBM2, our results cnfirmed once again that the IFNγ secreted by activated NK cells can mediate upregulation of MHC-class I, ICAM-1 and PD-L1 (Figure 32). Similar to what we observed in the previous cell lines, BT-12 and NB-1643, the presence of NK secreted cytokines did not have a significant effect on the percentage of tumor cells expressing MHC-class I, however we observed an increase in the mean expression of MHC-class I. For glioblastoma cells (SJ-GBM2) in contact with the supernatant of activated NK cells there was a 1.5 fold increase in MHC-class I expression. This effect was abrogated in the presence of α-IFNγ antibodies which decreased levels to nearly baseline levels (1.1 fold). In terms of ICAM-1 expression, for SJ-GBM2 tumor cells, the baseline ICAM-1 expression was 15.7%. However, when tumor cells were cultured in the supernatant of activated NK cells this number increased to 42.3%. In terms of mean expression there was also a 1.9 fold increase in ICAM-1 expression for SJ-GBM2 cells in contact with the supernatant of activated NK cells. This effect was abrogated in the presence of α-IFNγ antibodies which decreased ICAM-1 levels to the baseline levels (1.1 fold, 18.4%). Finally, we evaluated the effect of NK cell secreted IFNγ on tumor PD-L1 expression. Our results indicate that for the SJ-GBM2 cell line, PD-L1 baseline expression was 6.6%.

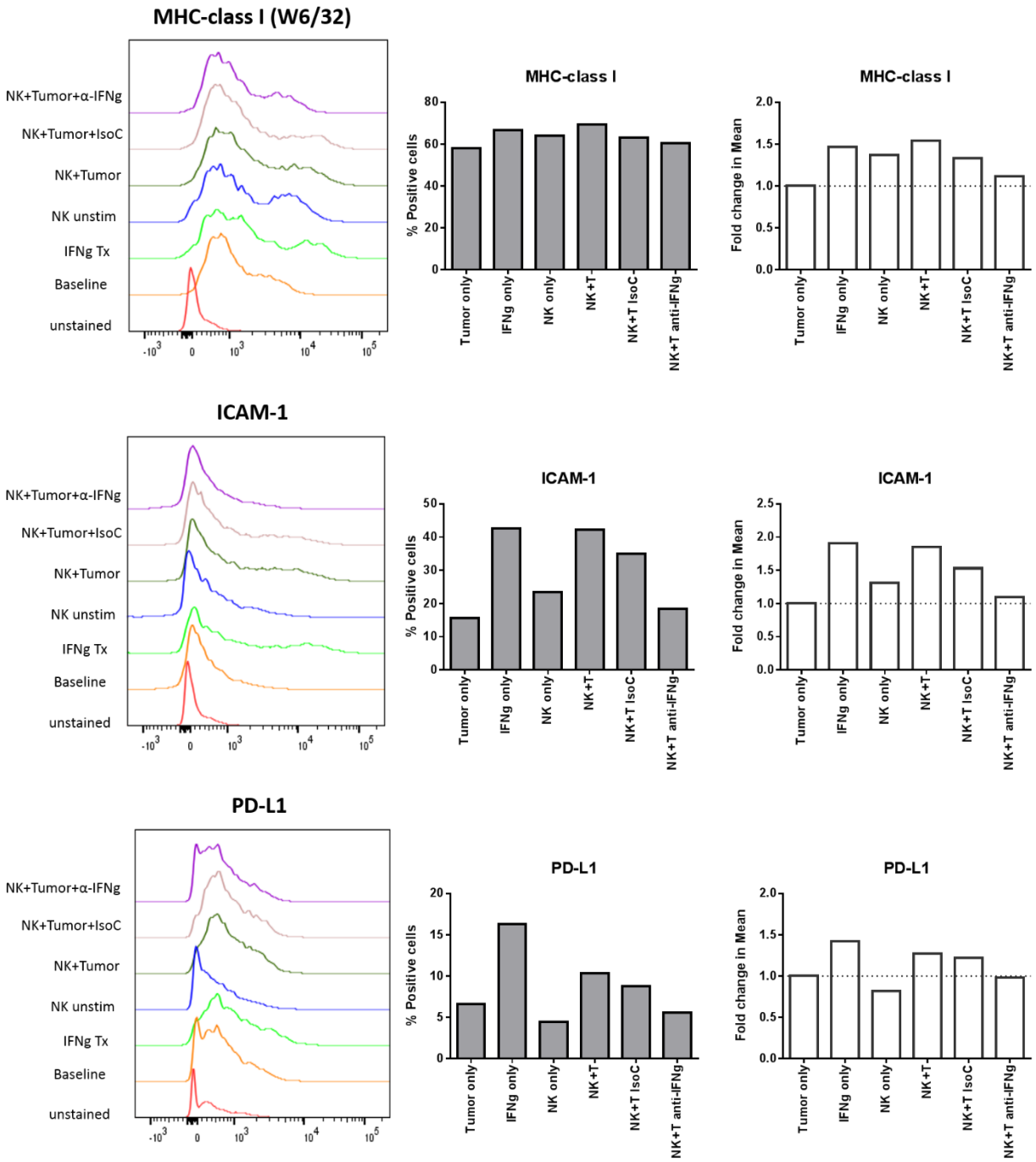

Figure 32. Effect of NK-secreted IFNγ on SJ-GBM2 NK-ligand Expression.

NK cells and SJ-GBM2 tumor cells were co-cultured at 2:1 E:T ratio for 48 hours. Tumor cells in contact with activated NK cells supernatant were evaluated for ligand expression.

By contrast, in the presence of activated NK cell supernatant this number increased to 10.3%. Culturing tumor cells in the presence of activated NK cell supernatant had a slight impact on mean PD-L1 expression causing a 1.3 fold increase compared to baseline. This effect that was abrogated in the presence of α-IFNγ antibodies, which decreased PD-L1 levels to levels similar to baseline (1 fold, 5.6%) (Figure 25).

The three cell lines evaluated had an increased sensitivity to NK-mediated lysis after exogenous IFNγ treatment and ICAM-1 upregulation exceeding MHC-class I upregulation (MHC/ICAM-1 change ratio <1). Therefore we sought to determine whether the MHC/ICAM-1 change ratio remained <1 in the presence of NK cell secreted IFNγ by calculating the fold change in median expression (Mean Fluorescence Intensity). For the brain tumor cell line BT-12, we saw upregulation of both MHC-class I (2.2 fold) and ICAM-1 (2.4 fold), with an MHC/ICAM-1 change ratio <1. Similarly for the NB cell line NB-1643, we saw upregulation of both MHC-class I (2.6 fold) and ICAM-1 (3.5 fold) with an MHC/ICAM-1 change ratio <1. Finally, when we evaluated the glioblastoma cell line SJ-GBM2 in presence of NK cell secreted IFNγ there was an upregulation of both MHC-class I (1.5 fold) and ICAM-1 (1.9 fold), leading to an MHC/ICAM-1 change ratio <1. Overall, the MHC/ICAM-1 change ratio remained <1 for all cell lines, indicating that NK cell secreted IFNγ caused ICAM-1 upregulation exceeding MHC-class I upregulation.

Discussion

IL-21 expanded NK cells, currently used in multiple clinical trials, secrete 20X more IFNγ than primary NK cells (41). In chapter IV we showed that exposing tumor cells to exogenous IFNγ can have an impact on their sensitivity to NK-mediated lysis, tumor kinetic interactions with NK cells, and tumor expression of NK-ligands. In terms of NK-ligand expression, our results showed that the ligands most upregulated by exogenous IFNγ treatment were MHC-class I, ICAM-1 and PD-L1 (Figure 17). These results demonstrate the capacity of exogenous IFNγ of altering tumor ligand expression, however, whether NK cell secreted IFNγ could induce similar changes remained uncertain. Given that IL-21 expanded NK cells secrete high levels of IFNγ, we sought to determine whether this secreted IFNγ was sufficient to induce changes on tumor NK-ligand expression.

In this chapter we demonstrate that, similar to what we observed with exogenous IFNγ treatment, culturing tumor cells (BT-12, SJ-GBM2 and NB-1643) in presence of activated NK cells supernatant can induce MHC-class I, ICAM-1 and PD-L1 upregulation (Figure 26). More importantly, we were able to demonstrate that the cytokine responsible for the upregulation was IFNγ. While addition of isotype control antibody (IgG1) did not have an effect in MHC-class I, ICAM-1 and PD-L1 upregulation, addition of IFNγ blocking antibodies weakened upregulation of all three ligands to nearly baseline levels for all three cell lines (Figure 33).

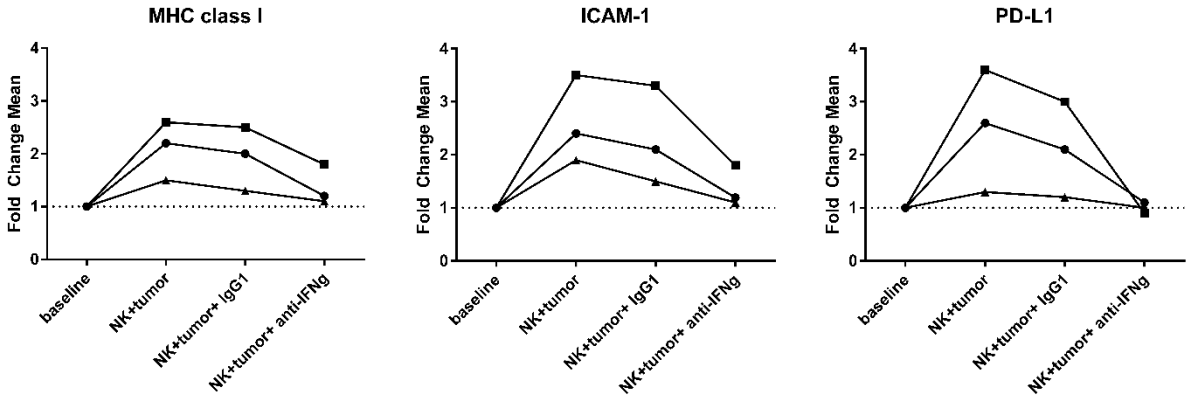

Figure 33. Summary of Results: Effect of NK-secreted IFNγ on Tumor NK-ligand Expression

Three tumor cell lines were evaluated for NK-ligand expression by flow cytometry, BT-12 (circle), NB-1643 (square) and SJ-GBM2 (triangle). NK cell donor was consistent for all cell lines.

After exogenous IFNγ treatment, the three cell lines evaluated showed an increased sensitivity to NK-mediated lysis and an MHC/ICAM-1 change ratio <1, indicating ICAM-1 upregulation exceeded MHC-class upregulation. Changes in MHC-class I expression and ICAM-1 expression induced by NK cell secreted IFNγ also resulted in an MHC/ICAM-1 change ratio <1 for all three cell lines, indicating that NK cell secreted IFNγ also induced ICAM-1 upregulation exceeding MHC-class I upregulation for these cell lines.

Overall these results highlight the importance of NK cell secreted pro-inflammatory cytokines, such as IFNγ, and the effect they have in tumor ligand expression. They also uncover the effect NK cells can have in surrounding cells, even in

the absence of direct NK:target contact. Given that IL-21 expanded NK cells secrete high levels of IFNγ, knowledge of the ligands upregulated by IFNγ is crucial to optimize adoptive NK cell therapy for cancer treatment and can be used as a tool to enhance NK cell anti-tumor effects.

CHAPTER VI: GENERAL DISCUSSION AND FUTURE DIRECTIONS

General Discussion

Current therapeutic approaches for pediatric cancer patients include chemotherapy and radiation. While these have improved survival rates for ALL and Hodgkin's Lymphoma, there has been little or no progress in terms of survival for patients with solid tumors, such as RMS, osteosarcoma, EWS or gliomas in 20 years (2). In addition, childhood cancer survivors who receive chemotherapy or radiation, have increased risk of complications later in life when compared to their siblings (4). Late effects of chemotherapy and radiation can include not only cardiovascular, renal, hepatic and gonadal dysfunction, but also the risk of developing secondary malignancies (4). Therefore, there is a critical need to develop alternative therapeutic approaches for pediatric cancer patients that could eradicate the disease, while decreasing the risks for complications later in life.

Given that NK cells have the capacity of eliminating cancer cells without prior sensitization, adoptive NK cell therapy is proposed as an alternative approach for the treatment of pediatric cancer patients (19, 20). The potential of NK cells for selectively targeting tumor cells can possibly decrease the risks for complications later in life for survivors, making them a promising therapy for pediatric cancer. To use NK cells as an adoptive cell therapy our approach includes their isolation and ex-vivo expansion. Our expansion protocol is based on mb-IL21 K562 feeder cells, and leads to a 47,967 expansion fold in 21 days (41). These IL-21 expanded NK cells are currently used at multiple clinical trials at MD Anderson Cancer Center (Table 3). However, the field of

adoptive NK cell therapy is in its early stages and a better understanding of the NK cell ligands expressed by tumor cells, as well as the interactions between IL-21 expanded NK cells and tumor cells, is required for optimization of NK cell immunotherapy.

NK cells have a heterogeneous distribution of inhibitory and activating receptors between individuals and within the same individual (76). Given that the activity of NK cells is dependent on NK cell receptor-ligand interactions, NK cell subpopulations within a single donor can have different potential to target malignancies, depending on the expression of NK cell ligands by the cancer cells. Through our work we characterized 22 pediatric cancer cell lines, corresponding to 6 types of pediatric cancer types (RMS, brain tumors, EWS, NB, leukemia and lymphoma) for their expression of NK-ligands. In addition, we identified NK cell subpopulations on IL-21 expanded NK cells co-expressing high levels of multiple activating receptors and with enhanced activity against target cells.

Furthermore, given that IL-21 expanded NK cells secrete high levels of IFNγ, we explored the effect of IFNγ on NK:tumor interactions, tumor sensitivity to NK-mediated lysis, and tumor expression of NK-ligands. Our results revealed that IFNγ has a variable impact on tumor sensitivity to NK-mediated lysis. For cell lines with enhanced sensitivity after IFNγ we observed ICAM-1 upregulation, leading to enhanced conjugate formation. Blocking of ICAM-1 weakened this enhanced sensitivity after IFNγ treatment for selected cell lines and NK donors. We were also able to show that IFNγ secreted by IL-21 expanded NK cells was enough to induce changes in tumor expression of NK cell ligands such as PD-L1, MHC-class I and ICAM-1. Information of the impact of IFNγ on NK-target

interactions and NK-ligand expression by tumors can be used to optimize the efficiency of the NK cell infusion product in the clinical practice.

Further optimization of adoptive NK cell therapy would require for us to consider other factors. Generation of a highly cytotoxic product is important, however infusion of this product might not be entirely beneficial if the NK cells are not able to migrate to the tumor tissue. Chemokines are small chemotactic proteins secreted by tumor cells. Their interaction with chemokine receptors on NK cells results in signaling that promotes NK cell trafficking and homing (77). Therefore, additional studies should explore NK cell chemokine receptor expression in our expanded NK cell product. In addition, chemokines secreted by multiple pediatric tumor types should be explored. Knowledge of the chemokines secreted by pediatric cancer cells would allow us to predict the chemokine receptor profile required on our NK cell product for an efficient NK cell migration to the tumor tissue.

Future Directions

Selection of CD56 bright NK-cell Subpopulations for the Treatment of Solid Tumors

In Chapter III we demonstrated that, compared to leukemia cells, solid tumor cells have higher expression of ligands for NK cell activating receptors, such as DNAM-1, NKG2D, NKp30 and NKp44 (Figures 3-4). Although current adoptive NK cell trails are mostly focused on leukemia, our results suggest that NK cell therapy can be a potential therapy for the treatment of pediatric solid tumors such as RMS, EWS, and brain tumors. Given that solid tumor cells express ligands for the activating receptors DNAM-1,

NKG2D, NKp30 and NKp44, a product enriched on cells co-expressing these receptors would be ideal to target them.

SPADE clustering revealed that IL-21 expanded NK cells from healthy donors contain unique subpopulations that are absent on primary NK cells. These unique populations co-express high levels of multiple activating receptors (NKp30, NKp44, DNAM-1 and NKG2D), and their frequency was the highest after 1 week of expansion (81%) (Figures 6-9). NK cells from patient infusion products also contained these unique subpopulations, and more importantly, we showed that these unique populations have enhanced degranulation, and IFNγ production, when compared to the rest of the product (Figure 12). These findings suggest that sorting for these hyperactive subpopulations after 1 week of expansion might be beneficial, since at this time-point their abundance is the highest (81%). However, sorting for populations co-expressing multiple activating receptors can be challenging to translate into the clinical practice. Interestingly, our data reveals that the unique hyperactive populations are contained within the $CD56^{bright}$ component of the expanded infusion product; therefore, enrichment of $CD56^{bright}$ cells is a possible approach to isolate cells with increased anti-tumor function at the 1 week time-point, for further expansion. Selective expansion of these $CD56^{bright}$ hyperactive subpopulations could possibly enhance the product's cytotoxic potential.

To test the efficiency of this approach we could sort $CD56^{bright}$ and $CD56^{dim}$ populations from the 1 week expanded product and perform *in-vitro* cytotoxicity assays to test their activity against solid tumor cells. We would expect to see increased tumor lysis for the $CD56^{bright}$ population when compared to the $CD56^{dim}$. Subsequently, we

could expand these populations for an additional week and evaluate them for phenotype and anti-tumor activity, by using CyTOF and calcein release assays respectively. This would allow us to determine whether they have phenotypic and/or functional differences. We would expect to see increased co-expression of multiple activating receptors in the $CD56^{bright}$ sorted cells, as well as increased anti-tumor activity, when compared to $CD56^{dim}$ cells.

This enrichment approach could be translated to the clinical practice by using commercially-available purification, stimulation and sorting platforms such as the Miltenyi Prodigy. These platforms allow for automated preparation of the product in a closed system, keeping samples from contamination. Multiple investigators have already used this platform for successful automated preparation of GMP-compliant NK and CAR-T cell infusion products (78, 79). Particularly, Granzin, et. al., proved the feasibility of automated NK cell expansions using an expansion protocol that also relies on feeder cells, in this case the Epstein-Barr virus transformed lymphoblastoid cell line (EBV-LCL) (79). Briefly, NK cell enrichment from peripheral blood mononuclear cells (PBMC's) was performed by CD3 depletion and CD56 enrichment, using Miltenyi's magnetic sorting platform. Subsequently, the product underwent automated expansion using the CliniMACS Prodigy, which was programmed for their expansion conditions (79).

Closed-system manufacturing could be envisioned combining the CliniMACS Prodigy technology for NK cell enrichment and expansion, with the MACS-Quant Tyto microchip, for fluorescence based cell sorting (80). After 1 week expansion, fluorescence based sorting could be used to enrich the $CD56^{bright}$ population from our infusion product.

Subsequent expansion of $CD56^{bright}$ populations for 1 additional week could possibly lead to a product with enhanced degranulation capacity and CD16 expression, which could ultimately improve our product's cytotoxic potential and capacity for ADCC. Although the MACS-Quant Tyto microchip is not yet clinically approved, its' capacity to sort at low pressures minimizes stress to cells, and given that it is a closed system it could be integrated into GMP-compliant protocols in the future (80).

Combination of adoptive NK cell therapy with anti-PD-L1 antibodies for brain tumors

NK cells play an important role in the antitumor effects of antibodies through ADCC (81), therefore it is not surprising that multiple current clinical trials explore the combination of NK cells and antibodies for the treatment cancer. For example, neuroblastoma cells express the tumor associated antigen (TAA) diaganglioside GD2 (82, 83), therefore several studies are evaluating NK cells and anti-GD2 antibodies for the treatment of neuroblastoma. A phase I trial at St. Jude Children's Hospital is evaluating the combination of humanized anti-GD2 (hu14.18 K322A), with NK cells and standard chemotherapy (NCT01576692). Similarly, two phase I trials at Memorial Sloan Kettering Cancer Center explore the combination of chemotherapy, NK cells and anti-GD2 antibodies (NCT02650648, NCT00877110). However, all these studies rely on the use of HLA-haploidentical NK cells obtained through apheresis from blood related donors, therefore NK cell quantities for infusion are limited.

Previous data from our laboratory has shown that IL-21 expanded NK cells have abundant CD16 expression and are capable of mediating ADCC (41). Moreover,

combination of our IL-21 expanded NK cells and anti-GD2 has already proven to be beneficial on a neuroblastoma pre-clinical model (84). However, given that TAA's have not been identified for all tumor types, it is worth exploring the combination of IL-21 expanded NK cells with other types of antibodies, including those that target checkpoint molecules such as PD-L1.

The PD-1/PD-L1 axis is involved in tumor immune escape. Binding of PD-1 on T cells to its ligands PD-L1 and PD-L2, which can be found on tumor cells, leads to inhibition of T-cell activation (8, 85). Our data demonstrates that IFNγ mediates upregulation of PD-L1 for solid tumors such as RMS, brain tumors, EWS and NB (Figure 18). Also, in chapter IV we described that upon tumor cell encounter, IL-21 expanded NK cells secrete enough IFNγ to induce upregulation of PD-L1 ligand on surrounding brain tumor cells and NB cells (Figures 30-31). Only a minority of the IL-21 expanded cells (7%) express the PD-1 receptor on their surface, and upregulation of PD-L1 on NB and brain tumor cells did not result in decreased NK-mediated tumor lysis (Figures 14,17), therefore these findings suggests that PD-L1 upregulation by IFNγ would not lead to inhibition of the IL-21 expanded NK cells.

The use of anti-PD-L1 antibodies to mediate additional signaling through ADCC in combination with IL-21 expanded NK cells would be a unique and promising approach to enhance NK cell cytotoxic effects for brain tumors. Initial contact of IL-21 expanded NK cells with tumor cells would lead to their activation and IFNγ release, promoting tumor PD-L1 upregulation. Subsequently, addition of the anti-PD-L1 antibody can induce NK

cell anti-tumor effects through ADCC, and by blocking of PD-L1 on tumor cells, the anti-tumor effects of T-cells could be enhanced.

Although there is currently a phase I/II clinical trial at Fuda Cancer Hospital, China, exploring the combination of anti-PD-1 (Nivolumab) and NK cell immunotherapy for solid tumors; Nivolumab targets PD-1 on T cells, rather than PD-L1 on the target cells. This combination therapy would not result in NK-mediated target death by ADCC (86). In addition, this study excludes patients under 30 years and also patients with brain metastases (NCT02843204).

We propose the use of anti-PD-L1 antibodies in combination with IL-21 expanded NK cells for brain tumors to enhance NK cell cytotoxic anti-tumor effects through ADCC. Given that many of the checkpoint antibodies available have been engineered to prevent ADCC, we should ensure that the anti-PD-L1 antibody used for this type of study has a native Fc region and is able to induce ADCC (86). Avelumab is an anti-PD-L1 antibody that functions to reactivate T-cells and may induce ADCC through its native Fc region (86). It was recently approved by the FDA for the treatment of Merkel cell carcinoma in patients 12 and older, making it an ideal alternative to test our hypothesis (87).

We could use orthotopic brain tumor models for ATRT and medulloblastoma, which have already been established at Dr. Gopalakrishnan laboratory (88). Gopalakrishnan's group demonstrated that after *in-vivo* locoregional delivery of IL-21 expanded NK cells to medulloblastoma bearing mice, there is tumor infiltration and NK cell persistence even after 3 weeks (88). This data was the pre-clinical evidence that

lead to the phase I trial mentioned in chapter I, in which, IL-21 expanded NK cells are being infused into the fourth ventricle of patients with brain tumors (NCT02271711).

Given that ATRT and medulloblastoma orthotopic brain tumor models have already been established at Dr. Gopalakrishnan, we could test the combination of IL-21 expanded NK cells with anti-PD-L1 antibodies in this model. For these models brain tumor cells transduced with firefly luciferase are injected into the brain of NSG mice. This allows for tracking of tumor progression by bioluminisence imaging. In addition, tumor infiltration by NK cells can be evaluated by CD45 staining of tissue samples through immunohistochemistry. For *in vivo* experiments we would expected to see decreased tumor progression when mice are treated with NK cells + anti-PD-L1, compared to the mice treated with NK cells only or anti-PD-L1 only.

Bibliography

1. Ward, E., C. DeSantis, A. Robbins, B. Kohler, and A. Jemal. 2014. Childhood and adolescent cancer statistics, 2014. *CA: a cancer journal for clinicians* 64: 83-103.

2. Pui, C. H., A. J. Gajjar, J. R. Kane, I. A. Qaddoumi, and A. S. Pappo. 2011. Challenging issues in pediatric oncology. *Nature reviews. Clinical oncology* 8: 540-549.

3. Armstrong, G. T., Q. Liu, Y. Yasui, J. P. Neglia, W. Leisenring, L. L. Robison, and A. C. Mertens. 2009. Late mortality among 5-year survivors of childhood cancer: a summary from the Childhood Cancer Survivor Study. *Journal of clinical oncology : official journal of the American Society of Clinical Oncology* 27: 2328-2338.

4. Armstrong, G. T., T. Kawashima, W. Leisenring, K. Stratton, M. Stovall, M. M. Hudson, C. A. Sklar, L. L. Robison, and K. C. Oeffinger. 2014. Aging and risk of severe, disabling, life-threatening, and fatal events in the childhood cancer survivor study. *Journal of clinical oncology : official journal of the American Society of Clinical Oncology* 32: 1218-1227.

5. Ng, A. K., L. B. Kenney, E. S. Gilbert, and L. B. Travis. 2010. Secondary malignancies across the age spectrum. *Seminars in radiation oncology* 20: 67-78.

6. Neglia, J. P., D. L. Friedman, Y. Yasui, A. C. Mertens, S. Hammond, M. Stovall, S. S. Donaldson, A. T. Meadows, and L. L. Robison. 2001. Second malignant neoplasms in five-year survivors of childhood cancer: childhood cancer survivor study. *Journal of the National Cancer Institute* 93: 618-629.

7. Corthay, A. 2014. Does the immune system naturally protect against cancer? *Frontiers in immunology* 5: 197.

8. Martin-Liberal, J., M. Ochoa de Olza, C. Hierro, A. Gros, J. Rodon, and J. Tabernero. 2017. The expanding role of immunotherapy. *Cancer treatment reviews* 54: 74-86.

9. Bukur, J., S. Jasinski, and B. Seliger. 2012. The role of classical and non-classical HLA class I antigens in human tumors. *Seminars in cancer biology* 22: 350-358.

10. Bubenik, J. 2004. MHC class I down-regulation: tumour escape from immune surveillance? (review). *International journal of oncology* 25: 487-491.

11. Haworth, K. B., J. L. Leddon, C. Y. Chen, E. M. Horwitz, C. L. Mackall, and T. P. Cripe. 2015. Going back to class I: MHC and immunotherapies for childhood cancer. *Pediatric blood & cancer* 62: 571-576.

12. Jaspers, J. E., and R. J. Brentjens. 2017. Development of CAR T cells designed to improve antitumor efficacy and safety. *Pharmacology & therapeutics*.

13. Haji-Fatahaliha, M., M. Hosseini, A. Akbarian, S. Sadreddini, F. Jadidi-Niaragh, and M. Yousefi. 2016. CAR-modified T-cell therapy for cancer: an updated review. *Artificial cells, nanomedicine, and biotechnology* 44: 1339-1349.

14. Brentjens, R. J., M. L. Davila, I. Riviere, J. Park, X. Wang, L. G. Cowell, S. Bartido, J. Stefanski, C. Taylor, M. Olszewska, O. Borquez-Ojeda, J. Qu, T. Wasielewska, Q. He, Y. Bernal, I. V. Rijo, C. Hedvat, R. Kobos, K. Curran, P. Steinherz, J. Jurcic,

T. Rosenblat, P. Maslak, M. Frattini, and M. Sadelain. 2013. CD19-targeted T cells rapidly induce molecular remissions in adults with chemotherapy-refractory acute lymphoblastic leukemia. *Science translational medicine* 5: 177ra138.

15. Sha, H. H., D. D. Wang, D. L. Yan, Y. Hu, S. J. Yang, S. W. Liu, and J. F. Feng. 2017. Chimaeric antigen receptor T-cell therapy for tumour immunotherapy. *Bioscience reports* 37.

16. Di Stasi, A., B. De Angelis, C. M. Rooney, L. Zhang, A. Mahendravada, A. E. Foster, H. E. Heslop, M. K. Brenner, G. Dotti, and B. Savoldo. 2009. T lymphocytes coexpressing CCR4 and a chimeric antigen receptor targeting CD30 have improved homing and antitumor activity in a Hodgkin tumor model. *Blood* 113: 6392-6402.

17. Walter, R. B. 2014. The role of CD33 as therapeutic target in acute myeloid leukemia. *Expert opinion on therapeutic targets* 18: 715-718.

18. O'Hear, C., J. F. Heiber, I. Schubert, G. Fey, and T. L. Geiger. 2015. Anti-CD33 chimeric antigen receptor targeting of acute myeloid leukemia. *Haematologica* 100: 336-344.

19. Robertson, M. J., and J. Ritz. 1990. Biology and clinical relevance of human natural killer cells. *Blood* 76: 2421-2438.

20. Almeida-Oliveira, A., M. Smith-Carvalho, L. C. Porto, J. Cardoso-Oliveira, S. Ribeiro Ados, R. R. Falcao, E. Abdelhay, L. F. Bouzas, L. C. Thuler, M. H.

Ornellas, and H. R. Diamond. 2011. Age-related changes in natural killer cell receptors from childhood through old age. *Human immunology* 72: 319-329.

21. Houghton, P. J., C. L. Morton, C. Tucker, D. Payne, E. Favours, C. Cole, R. Gorlick, E. A. Kolb, W. Zhang, R. Lock, H. Carol, M. Tajbakhsh, C. P. Reynolds, J. M. Maris, J. Courtright, S. T. Keir, H. S. Friedman, C. Stopford, J. Zeidner, J. Wu, T. Liu, C. A. Billups, J. Khan, S. Ansher, J. Zhang, and M. A. Smith. 2007. The pediatric preclinical testing program: description of models and early testing results. *Pediatric blood & cancer* 49: 928-940.

22. Cheent, K., and S. I. Khakoo. 2009. Natural killer cells: integrating diversity with function. *Immunology* 126: 449-457.

23. Kiessling, R., E. Klein, H. Pross, and H. Wigzell. 1975. "Natural" killer cells in the mouse. II. Cytotoxic cells with specificity for mouse Moloney leukemia cells. Characteristics of the killer cell. *European journal of immunology* 5: 117-121.

24. Kannan, G. S., A. Aquino-Lopez, and D. A. Lee. 2016. Natural killer cells in malignant hematology: A primer for the non-immunologist. *Blood Rev*.

25. Ljunggren, H. G., and K. Karre. 1990. In search of the 'missing self': MHC molecules and NK cell recognition. *Immunology today* 11: 237-244.

26. Frey, T., H. R. Petty, and H. M. McConnell. 1982. Electron microscopic study of natural killer cell-tumor cell conjugates. *Proceedings of the National Academy of Sciences of the United States of America* 79: 5317-5321.

27. Criado, M., J. M. Lindstrom, C. G. Anderson, and G. Dennert. 1985. Cytotoxic granules from killer cells: specificity of granules and insertion of channels of defined size into target membranes. *Journal of immunology* 135: 4245-4251.

28. Smyth, M. J., Y. Hayakawa, K. Takeda, and H. Yagita. 2002. New aspects of natural-killer-cell surveillance and therapy of cancer. *Nature reviews. Cancer* 2: 850-861.

29. Zamai, L., M. Ahmad, I. M. Bennett, L. Azzoni, E. S. Alnemri, and B. Perussia. 1998. Natural killer (NK) cell-mediated cytotoxicity: differential use of TRAIL and Fas ligand by immature and mature primary human NK cells. *The Journal of experimental medicine* 188: 2375-2380.

30. Weiner, L. M., R. Surana, and S. Wang. 2010. Monoclonal antibodies: versatile platforms for cancer immunotherapy. *Nature reviews. Immunology* 10: 317-327.

31. Long, E. O., H. S. Kim, D. Liu, M. E. Peterson, and S. Rajagopalan. 2013. Controlling natural killer cell responses: integration of signals for activation and inhibition. *Annual review of immunology* 31: 227-258.

32. Savani, B. N., S. Mielke, S. Adams, M. Uribe, K. Rezvani, A. S. Yong, J. Zeilah, R. Kurlander, R. Srinivasan, R. Childs, N. Hensel, and A. J. Barrett. 2007. Rapid natural killer cell recovery determines outcome after T-cell-depleted HLA-identical stem cell transplantation in patients with myeloid leukemias but not with acute lymphoblastic leukemia. *Leukemia* 21: 2145-2152.

33. Rubnitz, J. E., H. Inaba, R. C. Ribeiro, S. Pounds, B. Rooney, T. Bell, C. H. Pui, and W. Leung. 2010. NKAML: a pilot study to determine the safety and feasibility of haploidentical natural killer cell transplantation in childhood acute myeloid leukemia. *Journal of clinical oncology : official journal of the American Society of Clinical Oncology* 28: 955-959.

34. Iliopoulou, E. G., P. Kountourakis, M. V. Karamouzis, D. Doufexis, A. Ardavanis, C. N. Baxevanis, G. Rigatos, M. Papamichail, and S. A. Perez. 2010. A phase I trial of adoptive transfer of allogeneic natural killer cells in patients with advanced non-small cell lung cancer. *Cancer immunology, immunotherapy : CII* 59: 1781-1789.

35. Geller, M. A., S. Cooley, P. L. Judson, R. Ghebre, L. F. Carson, P. A. Argenta, A. L. Jonson, A. Panoskaltsis-Mortari, J. Curtsinger, D. McKenna, K. Dusenbery, R. Bliss, L. S. Downs, and J. S. Miller. 2011. A phase II study of allogeneic natural killer cell therapy to treat patients with recurrent ovarian and breast cancer. *Cytotherapy* 13: 98-107.

36. Bachanova, V., L. J. Burns, D. H. McKenna, J. Curtsinger, A. Panoskaltsis-Mortari, B. R. Lindgren, S. Cooley, D. Weisdorf, and J. S. Miller. 2010. Allogeneic natural killer cells for refractory lymphoma. *Cancer immunology, immunotherapy : CII* 59: 1739-1744.

37. Buddingh, E. P., M. W. Schilham, S. E. Ruslan, D. Berghuis, K. Szuhai, J. Suurmond, A. H. Taminiau, H. Gelderblom, R. M. Egeler, M. Serra, P. C. Hogendoorn, and A. C. Lankester. 2011. Chemotherapy-resistant osteosarcoma

is highly susceptible to IL-15-activated allogeneic and autologous NK cells. *Cancer immunology, immunotherapy : CII* 60: 575-586.

38. Cho, D., D. R. Shook, N. Shimasaki, Y. H. Chang, H. Fujisaki, and D. Campana. 2010. Cytotoxicity of activated natural killer cells against pediatric solid tumors. *Clinical cancer research : an official journal of the American Association for Cancer Research* 16: 3901-3909.

39. Meyer-Monard, S., J. Passweg, U. Siegler, C. Kalberer, U. Koehl, A. Rovo, J. Halter, M. Stern, D. Heim, J. R. Alois Gratwohl, and A. Tichelli. 2009. Clinical-grade purification of natural killer cells in haploidentical hematopoietic stem cell transplantation. *Transfusion* 49: 362-371.

40. Passweg, J. R., A. Tichelli, S. Meyer-Monard, D. Heim, M. Stern, T. Kuhne, G. Favre, and A. Gratwohl. 2004. Purified donor NK-lymphocyte infusion to consolidate engraftment after haploidentical stem cell transplantation. *Leukemia* 18: 1835-1838.

41. Denman, C. J., V. V. Senyukov, S. S. Somanchi, P. V. Phatarpekar, L. M. Kopp, J. L. Johnson, H. Singh, L. Hurton, S. N. Maiti, M. H. Huls, R. E. Champlin, L. J. Cooper, and D. A. Lee. 2012. Membrane-bound IL-21 promotes sustained ex vivo proliferation of human natural killer cells. *PloS one* 7: e30264.

42. Koehl, U., J. Sorensen, R. Esser, S. Zimmermann, H. P. Gruttner, T. Tonn, C. Seidl, E. Seifried, T. Klingebiel, and D. Schwabe. 2004. IL-2 activated NK cell

immunotherapy of three children after haploidentical stem cell transplantation. *Blood cells, molecules & diseases* 33: 261-266.

43. Klingemann, H. G., and J. Martinson. 2004. Ex vivo expansion of natural killer cells for clinical applications. *Cytotherapy* 6: 15-22.

44. Decot, V., L. Voillard, V. Latger-Cannard, L. Aissi-Rothe, P. Perrier, J. F. Stoltz, and D. Bensoussan. 2010. Natural-killer cell amplification for adoptive leukemia relapse immunotherapy: comparison of three cytokines, IL-2, IL-15, or IL-7 and impact on NKG2D, KIR2DL1, and KIR2DL2 expression. *Experimental hematology* 38: 351-362.

45. de Rham, C., S. Ferrari-Lacraz, S. Jendly, G. Schneiter, J. M. Dayer, and J. Villard. 2007. The proinflammatory cytokines IL-2, IL-15 and IL-21 modulate the repertoire of mature human natural killer cell receptors. *Arthritis research & therapy* 9: R125.

46. Torelli, G. F., A. Guarini, R. Maggio, C. Alfieri, A. Vitale, and R. Foa. 2005. Expansion of natural killer cells with lytic activity against autologous blasts from adult and pediatric acute lymphoid leukemia patients in complete hematologic remission. *Haematologica* 90: 785-792.

47. Fujisaki, H., H. Kakuda, N. Shimasaki, C. Imai, J. Ma, T. Lockey, P. Eldridge, W. H. Leung, and D. Campana. 2009. Expansion of highly cytotoxic human natural killer cells for cancer cell therapy. *Cancer research* 69: 4010-4017.

48. Gong, W., W. Xiao, M. Hu, X. Weng, L. Qian, X. Pan, and M. Ji. 2010. Ex vivo expansion of natural killer cells with high cytotoxicity by K562 cells modified to co-express major histocompatibility complex class I chain-related protein A, 4-1BB ligand, and interleukin-15. *Tissue antigens* 76: 467-475.

49. Romee, R., M. Rosario, M. M. Berrien-Elliott, J. A. Wagner, B. A. Jewell, T. Schappe, J. W. Leong, S. Abdel-Latif, S. E. Schneider, S. Willey, C. C. Neal, L. Yu, S. T. Oh, Y. S. Lee, A. Mulder, F. Claas, M. A. Cooper, and T. A. Fehniger. 2016. Cytokine-induced memory-like natural killer cells exhibit enhanced responses against myeloid leukemia. *Science translational medicine* 8: 357ra123.

50. Kalvakolanu, D. V., and E. C. Borden. 1996. An overview of the interferon system: signal transduction and mechanisms of action. *Cancer Invest* 14: 25-53.

51. Moretta, A., C. Bottino, M. Vitale, D. Pende, R. Biassoni, M. C. Mingari, and L. Moretta. 1996. Receptors for HLA class-I molecules in human natural killer cells. *Annual review of immunology* 14: 619-648.

52. Storkus, W. J., D. N. Howell, R. D. Salter, J. R. Dawson, and P. Cresswell. 1987. NK susceptibility varies inversely with target cell class I HLA antigen expression. *Journal of immunology* 138: 1657-1659.

53. de Fries, R. U., and S. H. Golub. 1988. Characteristics and mechanism of IFN-gamma-induced protection of human tumor cells from lysis by lymphokine-activated killer cells. *Journal of immunology* 140: 3686-3693.

54. Moore, M., W. J. White, and M. R. Potter. 1980. Modulation of target cell susceptibility to human natural killer cells by interferon. *International journal of cancer. Journal international du cancer* 25: 565-572.

55. Balsamo, M., W. Vermi, M. Parodi, G. Pietra, C. Manzini, P. Queirolo, S. Lonardi, R. Augugliaro, A. Moretta, F. Facchetti, L. Moretta, M. C. Mingari, and M. Vitale. 2012. Melanoma cells become resistant to NK-cell-mediated killing when exposed to NK-cell numbers compatible with NK-cell infiltration in the tumor. *European journal of immunology* 42: 1833-1842.

56. Mace, E. M., P. Dongre, H. T. Hsu, P. Sinha, A. M. James, S. S. Mann, L. R. Forbes, L. B. Watkin, and J. S. Orange. 2014. Cell biological steps and checkpoints in accessing NK cell cytotoxicity. *Immunology and cell biology* 92: 245-255.

57. Zhang, M., M. E. March, W. S. Lane, and E. O. Long. 2014. A signaling network stimulated by beta2 integrin promotes the polarization of lytic granules in cytotoxic cells. *Sci Signal* 7: ra96.

58. Naganuma, H., R. Kiessling, M. Patarroyo, M. Hansson, R. Handgretinger, and A. Gronberg. 1991. Increased susceptibility of IFN-gamma-treated neuroblastoma cells to lysis by lymphokine-activated killer cells: participation of ICAM-1 induction on target cells. *International journal of cancer. Journal international du cancer* 47: 527-532.

59. Wang, R., J. J. Jaw, N. C. Stutzman, Z. Zou, and P. D. Sun. 2012. Natural killer cell-produced IFN-gamma and TNF-alpha induce target cell cytolysis through up-regulation of ICAM-1. *Journal of leukocyte biology* 91: 299-309.

60. Somanchi, S. S., V. V. Senyukov, C. J. Denman, and D. A. Lee. 2011. Expansion, purification, and functional assessment of human peripheral blood NK cells. *Journal of visualized experiments : JoVE*.

61. Bendall, S. C., E. F. Simonds, P. Qiu, A. D. Amir el, P. O. Krutzik, R. Finck, R. V. Bruggner, R. Melamed, A. Trejo, O. I. Ornatsky, R. S. Balderas, S. K. Plevritis, K. Sachs, D. Pe'er, S. D. Tanner, and G. P. Nolan. 2011. Single-cell mass cytometry of differential immune and drug responses across a human hematopoietic continuum. *Science* 332: 687-696.

62. Kotecha, N., P. O. Krutzik, and J. M. Irish. 2010. Web-based analysis and publication of flow cytometry experiments. *Current protocols in cytometry / editorial board, J. Paul Robinson, managing editor ... [et al.]* Chapter 10: Unit10 17.

63. Qiu, P., E. F. Simonds, S. C. Bendall, K. D. Gibbs, Jr., R. V. Bruggner, M. D. Linderman, K. Sachs, G. P. Nolan, and S. K. Plevritis. 2011. Extracting a cellular hierarchy from high-dimensional cytometry data with SPADE. *Nature biotechnology* 29: 886-891.

64. Burshtyn, D. N., J. Shin, C. Stebbins, and E. O. Long. 2000. Adhesion to target cells is disrupted by the killer cell inhibitory receptor. *Current biology : CB* 10: 777-780.

65. Romain, G., V. Senyukov, N. Rey-Villamizar, A. Merouane, W. Kelton, I. Liadi, A. Mahendra, W. Charab, G. Georgiou, B. Roysam, D. A. Lee, and N. Varadarajan. 2014. Antibody Fc engineering improves frequency and promotes kinetic boosting of serial killing mediated by NK cells. *Blood* 124: 3241-3249.

66. Nattermann, J., H. D. Nischalke, V. Hofmeister, G. Ahlenstiel, H. Zimmermann, L. Leifeld, E. H. Weiss, T. Sauerbruch, and U. Spengler. 2005. The HLA-A2 restricted T cell epitope HCV core 35-44 stabilizes HLA-E expression and inhibits cytolysis mediated by natural killer cells. *The American journal of pathology* 166: 443-453.

67. Aquino-López, A., V. V. Senyukov, Z. Vlasic, E. S. Kleinerman, and D. A. Lee. 2017. Interferon Gamma Induces Changes in Natural Killer (NK) Cell Ligand Expression and Alters NK Cell-Mediated Lysis of Pediatric Cancer Cell Lines. *Frontiers in immunology* 8: 391.

68. Lee, S. J., B. C. Jang, S. W. Lee, Y. I. Yang, S. I. Suh, Y. M. Park, S. Oh, J. G. Shin, S. Yao, L. Chen, and I. H. Choi. 2006. Interferon regulatory factor-1 is prerequisite to the constitutive expression and IFN-gamma-induced upregulation of B7-H1 (CD274). *FEBS letters* 580: 755-762.

69. Dong, H., S. E. Strome, D. R. Salomao, H. Tamura, F. Hirano, D. B. Flies, P. C. Roche, J. Lu, G. Zhu, K. Tamada, V. A. Lennon, E. Celis, and L. Chen. 2002. Tumor-associated B7-H1 promotes T-cell apoptosis: a potential mechanism of immune evasion. *Nature medicine* 8: 793-800.

70. Steimle, V., C. A. Siegrist, A. Mottet, B. Lisowska-Grospierre, and B. Mach. 1994. Regulation of MHC class II expression by interferon-gamma mediated by the transactivator gene CIITA. *Science* 265: 106-109.

71. Propper, D. J., D. Chao, J. P. Braybrooke, P. Bahl, P. Thavasu, F. Balkwill, H. Turley, N. Dobbs, K. Gatter, D. C. Talbot, A. L. Harris, and T. S. Ganesan. 2003. Low-dose IFN-gamma induces tumor MHC expression in metastatic malignant melanoma. *Clinical cancer research : an official journal of the American Association for Cancer Research* 9: 84-92.

72. Munker, R., and M. Andreeff. 1996. Induction of death (CD95/FAS), activation and adhesion (CD54) molecules on blast cells of acute myelogenous leukemias by TNF-alpha and IFN-gamma. *Cytokines and molecular therapy* 2: 147-159.

73. Li, J. H., M. S. Kluger, L. A. Madge, L. Zheng, A. L. Bothwell, and J. S. Pober. 2002. Interferon-gamma augments CD95(APO-1/Fas) and pro-caspase-8 expression and sensitizes human vascular endothelial cells to CD95-mediated apoptosis. *The American journal of pathology* 161: 1485-1495.

74. del Rio, M. L., C. L. Lucas, L. Buhler, G. Rayat, and J. I. Rodriguez-Barbosa. 2010. HVEM/LIGHT/BTLA/CD160 cosignaling pathways as targets for immune regulation. *Journal of leukocyte biology* 87: 223-235.

75. Renkvist, N., C. Castelli, P. F. Robbins, and G. Parmiani. 2001. A listing of human tumor antigens recognized by T cells. *Cancer immunology, immunotherapy : CII* 50: 3-15.

76. Horowitz, A., D. M. Strauss-Albee, M. Leipold, J. Kubo, N. Nemat-Gorgani, O. C. Dogan, C. L. Dekker, S. Mackey, H. Maecker, G. E. Swan, M. M. Davis, P. J. Norman, L. A. Guethlein, M. Desai, P. Parham, and C. A. Blish. 2013. Genetic and environmental determinants of human NK cell diversity revealed by mass cytometry. *Science translational medicine* 5: 208ra145.

77. Bernardini, G., F. Antonangeli, V. Bonanni, and A. Santoni. 2016. Dysregulation of Chemokine/Chemokine Receptor Axes and NK Cell Tissue Localization during Diseases. *Frontiers in immunology* 7: 402.

78. Mock, U., L. Nickolay, B. Philip, G. W. Cheung, H. Zhan, I. C. Johnston, A. D. Kaiser, K. Peggs, M. Pule, A. J. Thrasher, and W. Qasim. 2016. Automated manufacturing of chimeric antigen receptor T cells for adoptive immunotherapy using CliniMACS prodigy. *Cytotherapy* 18: 1002-1011.

79. Granzin, M., S. Soltenborn, S. Muller, J. Kollet, M. Berg, A. Cerwenka, R. W. Childs, and V. Huppert. 2015. Fully automated expansion and activation of

clinical-grade natural killer cells for adoptive immunotherapy. *Cytotherapy* 17: 621-632.

80. Safinia, N., C. Scotta, T. Vaikunthanathan, R. I. Lechler, and G. Lombardi. 2015. Regulatory T Cells: Serious Contenders in the Promise for Immunological Tolerance in Transplantation. *Frontiers in immunology* 6: 438.

81. Wang, W., A. K. Erbe, J. A. Hank, Z. S. Morris, and P. M. Sondel. 2015. NK Cell-Mediated Antibody-Dependent Cellular Cytotoxicity in Cancer Immunotherapy. *Frontiers in immunology* 6: 368.

82. Dobrenkov, K., and N. K. Cheung. 2014. GD2-targeted immunotherapy and radioimmunotherapy. *Semin Oncol* 41: 589-612.

83. Shochat, S. J., A. B. Abt, and C. L. Schengrund. 1977. VCN-releasable sialic acid and gangliosides in human neuroblastomas. *J Pediatr Surg* 12: 413-418.

84. Liu, Y., H. W. Wu, M. A. Sheard, R. Sposto, S. S. Somanchi, L. J. Cooper, D. A. Lee, and R. C. Seeger. 2013. Growth and activation of natural killer cells ex vivo from children with neuroblastoma for adoptive cell therapy. *Clinical cancer research : an official journal of the American Association for Cancer Research* 19: 2132-2143.

85. Freeman, G. J., A. J. Long, Y. Iwai, K. Bourque, T. Chernova, H. Nishimura, L. J. Fitz, N. Malenkovich, T. Okazaki, M. C. Byrne, H. F. Horton, L. Fouser, L. Carter, V. Ling, M. R. Bowman, B. M. Carreno, M. Collins, C. R. Wood, and T. Honjo. 2000. Engagement of the PD-1 immunoinhibitory receptor by a novel B7 family

member leads to negative regulation of lymphocyte activation. *The Journal of experimental medicine* 192: 1027-1034.

86. Li, Y., F. Li, F. Jiang, X. Lv, R. Zhang, A. Lu, and G. Zhang. 2016. A Mini-Review for Cancer Immunotherapy: Molecular Understanding of PD-1/PD-L1 Pathway & Translational Blockade of Immune Checkpoints. *Int J Mol Sci* 17.

87. Kim, E. S. 2017. Avelumab: First Global Approval. *Drugs* 77: 929-937.

88. Brugmann, W. B., A. Laureano, C. Denman, H. Singh, H. Huls, Z. Wafik, D. Sandberg, S. Khatua, D. Lee, L. Cooper, and V. Gopalakrishnan. 2014. Abstract B80: NK therapy for pediatric brain tumors of the posterior fossa. *Cancer research* 74: B80-B80.

Vita

Arianexys Aquino-López was born in Arecibo, Puerto Rico on October 18, 1988, the daughter of Doris López-López and Ediberto Aquino-Borrero. After completing her coursework at the Domingo Aponte Collazo High School in Lares, Puerto Rico, she was admitted to the University of Puerto Rico-Río Piedras Campus (UPR-RP) in 2006. At the UPR she completed the degree of Bachelor of Science with a major in Chemistry in May, 2010. She was then admitted to the U54 MD/Ph Program, a partnership between the University of Puerto Rico Medical Sciences Campus and The MD Anderson Cancer Center UTHealth Graduate School. She completed three years of medical training at the University of Puerto Rico Medical Sciences Campus, from 2010-2013. In August of 2013, she entered The University of Texas MD Anderson Cancer Center UTHealth Graduate School of Biomedical Sciences to complete her PhD degree in Clinical & Translational Sciences. She joined the Department of Pediatrics under the guidance of Dr. Dean A. Lee and Dr. Eugenie S. Kleinerman to carry out her dissertation work focused on adoptive NK cell therapy for pediatric malignancies. Thus far, her work has resulted in multiple publications such as co-authorship of a review article in *Blood Reviews* (*Blood Rev*. 2017 Mar;31(2):1-10), a co-author publication at *Frontiers in Immunology* (*Frontiers in Immunology*. **2016**; 7: 521) and the publication of her first author manuscript at *Frontiers in immunology* (*Frontiers in immunology* 2017, 8:391).

.